

**CHEMICAL AND PHYSICAL MODIFICATION OF**  
**DIAMOND SURFACES**

**Thesis submitted to the University of Glasgow in fulfilment of the  
requirement of the degree of Doctor of Philosophy**

**By**

**Christopher P. Kealey BSc.**

**Department of Chemistry, University of Glasgow**

**September 1999**

**© Christopher P. Kealey 1999**

ProQuest Number: 13834090

All rights reserved

INFORMATION TO ALL USERS

The quality of this reproduction is dependent upon the quality of the copy submitted.

In the unlikely event that the author did not send a complete manuscript and there are missing pages, these will be noted. Also, if material had to be removed, a note will indicate the deletion.



ProQuest 13834090

Published by ProQuest LLC (2019). Copyright of the Dissertation is held by the Author.

All rights reserved.

This work is protected against unauthorized copying under Title 17, United States Code  
Microform Edition © ProQuest LLC.

ProQuest LLC.  
789 East Eisenhower Parkway  
P.O. Box 1346  
Ann Arbor, MI 48106 – 1346

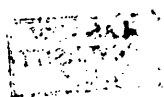
GLASGOW  
UNIVERSITY  
LIBRARY

11765 (copy 1)

## ACKNOWLEDGEMENTS

I would like to thank my supervisors, Professor John M. Winfield and Professor Tom Klapotke for their continued support throughout this work. Many thanks go to my industrial supervisor, Mr Max Robertson, for his help and expertise in the polishing experiments. I am indebted to Dr David McComb and Dr Sam McFadzean for their assistance with the electron microscopy studies and to Dr McComb for performing the EFTEM analysis and acting as a sounding board for ideas. Thanks are also due to Yongchang Fan for collecting the XPS data and to Professor Sandy Fitzgerald (University of Dundee) for kindly allowing use of the XPS instrument. Thanks go to all the staff at the Biomedical imaging centre in Aberdeen where the radioisotope,  $^{18}\text{F}$ , was prepared. I would like to thank all the technical staff at the University of Glasgow, without whom much of this work would not have been possible. To all my friends in the chemistry department I offer my sincere thanks for providing such enjoyable experiences during the course of this work. Special thanks go to Chris Barclay, Phil Landon and Robert Marshall who acted as fine role models, particularly on social occasions, where they showed great restraint.

None of this would have been possible without the tremendous support of my family and of my girlfriend Claire; my greatest thanks go to them.



## SUMMARY

In recent years it has become possible to grow a film of diamond, on substrates such as silicon, at low temperature and pressure by a process called chemical vapour deposition or CVD. These films have been found to exhibit properties comparable to those of natural diamond. As a result there has been a surge of interest in the use of the material as an alternative to natural, or HPHT (High Pressure High Temperature) synthetic diamond, in optical and microelectronic applications. Unlike natural or HPHT diamond, which are monocrystalline, these films are polycrystalline and have a rough surface. For many of the potential uses, such as a heat sink in microelectronic devices, smooth surfaces on the nanometre scale are required.

Polishing is seen to be one way of smoothing the rough surface of a CVD diamond film, however traditional methods, using harsh mechanical conditions have proved unsatisfactory often resulting in a damaged film. The development of a chemomechanical polishing process, involving chemical reaction at the diamond surface and subsequent removal of surface species formed, is one possible alternative to the traditional mechanical methods.

The first step in the development of a chemomechanical polishing process involves a detailed study of the chemistry possible on diamond and in particular those reactions, which may involve etching of the diamond surface.

In this work the behaviour of various fluorine compounds towards diamond films and powders has been determined. Reactions of  $F_2$  or  $ClF_3$  with hydrogen-pretreated diamond at ambient temperature led to the removal of hydrogen as HF or HCl. DRIFTS (Diffuse Reflectance Infrared Fourier Transform Spectroscopy) of powder samples has shown the loss of C-H and its replacement with C-F. When the reaction temperature is increased to 673 K, analysis of the gas phase using FTIR spectroscopy showed the presence of a fluorocarbon mixture and DRIFTS analysis of the diamond surface showed bands corresponding to CF,  $CF_2$  and  $CF_3$  moieties. Etching of  $CF_2$  from the diamond surface and the subsequent reactions of the former is believed to be responsible for the fluorocarbon mixture. However, SEM (Scanning Electron Microscopy) analysis of film samples following reaction at 673 K revealed that a massive etching reaction had not occurred, since the gross morphology of the film surface was maintained. EFTEM (Energy-Filtered Transmission Electron Microscopy) analysis on the nanometre scale was more informative, this technique allowed the density of  $sp^2/sp^3$  bonding character in the sample to be determined. The carbon environment at grain boundaries and grain edges was shown to be predominately  $sp^2$  prior to reaction with  $ClF_3$  and  $sp^3$  after reaction with  $ClF_3$ . This indicated a propensity for reaction at grain boundaries or crystal edges and these are expected to be the likely sites for etching of carbon.

XPS (X-ray Photoelectron Spectroscopy) allowed quantitative analysis of the fluorinated diamond surface; carbon to fluorine ratios could be calculated. The key feature of this part of the work was evidence for a subsurface reaction at 523 K,

resulting in the formation of a fluorinated layer, with a greater than monolayer thickness.

A model for the structure of this layer was provided by comparison with the related compound, graphite fluoride (CF)<sub>n</sub>. Fluorinated diamond surfaces have been shown to be stable to further reaction with F<sub>2</sub> or ClF<sub>3</sub>, a feature in common with many carbon-fluorine compounds. This indicates the presence of a kinetic barrier to extensive reaction, which accounts for the absence of a gross change in the morphology of fluorine-treated film surfaces.

The interaction of [<sup>18</sup>F]-HF ([<sup>18</sup>F] t<sub>1/2</sub> 110 min, β<sup>+</sup>-emitter) has been used to probe the extent and type of interactions that are possible between HF and a variety of diamond surfaces. Standard pretreatments were hydrogenation (99% H<sub>2</sub>, 1173 K, 1 h) or oxygenation (hydrogenation + 20% O<sub>2</sub>/ Ar, 673 K, 1 h). Fluorinations were performed with F<sub>2</sub>, ClF<sub>3</sub> or HF at ambient temperature or at 673 K with F<sub>2</sub> or ClF<sub>3</sub> and 573 K with HF. The extent of [<sup>18</sup>F] uptake on the surface was readily detected in all cases, even when H<sup>18</sup>F treatment was at ambient temperature. It has been established that the fluorine laid down on the surface is labile and is subject to hydrolysis upon exposure to moist air. Fluorine exchange reactions and DRIFTS analysis were used. These facts are not consistent with C-F termination of the surface in the reaction with HF, and this suggests a very different behaviour when compared with the reaction of F<sub>2</sub> with diamond.

Studies in the polishing behaviour of fluorine-treated diamond surfaces by traditional methods and the use of fluorine containing reagents in solution, such as [HF<sub>2</sub>]<sup>-</sup>, had limited success. The outcome of the experiments could be rationalised in terms of

the limited fluorination using  $F_2$  or  $ClF_3$  and the lack of interaction between HF and diamond surfaces in an aqueous environment. The knowledge gained in the study of diamond surface chemistry had an important role in the development of a promising process for the polishing of diamond film.

<b>CONTENTS</b>	<b>PAGE</b>
SUMMARY	I
CHAPTER 1 INTRODUCTION	1
1.1 Diamond: Structure, physical and chemical properties	1
1.2 Diamond growth methods	4
1.3 Polishing of diamond film	11
1.3.1 Polishing concepts	11
1.3.2 Methods for polishing CVD-grown diamond film	15
1.4 Aims of the current work	22
1.5 Diamond surface chemistry	23
1.5.1 Introductory remarks	23
1.5.2 Hydrogen chemisorption	24
1.5.3 Oxygen chemisorption	28
1.5.4 Fluorine chemisorption	30
CHAPTER 2 EXPERIMENTAL	37
2.1 Chemical modification of diamond surfaces	37
2.1.1 Nature of diamond powder and film samples	38
2.1.2 Hydrogenation/Oxygenation procedure	38
2.1.3 Vacuum systems	39
2.1.4 Calibration of vacuum systems	40

2.1.5	Reaction vessels	41
2.1.6	Passivation and leak testing of vacuum systems and reaction vessels	42
2.1.7	Purification of reagents	43
2.1.8	Preparation of anhydrous [ $^{18}\text{F}$ ]-HF	43
2.1.9	Reactions of diamond surfaces with halogen- containing reagents	45
2.1.10	Fourier Transform Infrared Spectroscopy (FTIR)	46
2.1.11	Characterisation and analysis of diamond surfaces following reaction with halogen-containing reagents	47
2.2	Physical modification of diamond surfaces	63
2.2.1	Polishing experiments	64
2.2.2	Analysis of diamond surface after polishing	65
CHAPTER 3 RESULTS: Physical modification of diamond surfaces		67
3.0	Introduction	67
3.1	Abrasive polishing of chemically oxidised diamond film	70
3.2	Abrasive polishing of chemically oxidised diamond film with the addition of aqueous potassium hydrogen difluoride solution	72
3.3	Abrasive polishing of diamond film in the	74

	presence of an electrical potential and a nucleophilic species	
3.3.1	Interaction of $[\text{HF}_2]^-_{(\text{aq})}$ with diamond film in the presence of an electrical potential	77
3.3.2	Interaction of $[\text{OH}]^-_{(\text{aq})}$ with diamond film In the presence of an electrical potential	78
3.3.3	Further investigation into the polishing of diamond film in the presence of an electrical potential	80
CHAPTER 4	RESULTS: Chemical modification of diamond surfaces	93
4.0	Introduction	93
4.1	FTIR spectroscopic investigation of diamond reaction chemistry	94
4.1.1	Reaction of hydrogenated diamond powder and film with difluorine ( $\text{F}_2$ ) and/or chlorine trifluoride ( $\text{ClF}_3$ )	94
4.1.2	Surface area analysis of diamond powder	98
4.2	Diamond surface structure analysis following fluorination	100
4.2.1	Diffuse Reflectance Infrared Fourier Transform Spectroscopy, DRIFTS	100
4.2.2	Scanning Electron Microscopy, SEM	103

4.2.3	Energy Filtered Transmission Electron Microscopy, EFTEM	106
4.2.4	X-ray Photoelectron Spectroscopy, XPS	108
4.2.5	The reaction of various diamond powders with anhydrous fluorine-18 radiolabelled hydrogen fluoride vapour, $\text{H}^{18}\text{F}$ , under a range of conditions	118
4.2.5.1	Handling of fluorine-18 raw counting data	118
4.2.5.2	Hydrogen-terminated diamond powder surfaces	122
4.2.5.3	Oxygen-terminated diamond powder surfaces	124
4.2.5.4	Fluorine-terminated diamond powder surfaces	125
4.2.5.5	Room temperature fluorine exchange reactions between $^{18}\text{F}$ -radiolabelled diamond powder surfaces and non-labelled anhydrous HF vapour	128
4.2.5.6	Fluorine exchange reactions between anhydrous $\text{H}^{18}\text{F}$ vapour and diamond powder surfaces pretreated with non-labelled HF vapour and determination of the f-factor	132
4.2.5.7	Specific activity determination following the reaction between highly fluorinated diamond surfaces and anhydrous $\text{H}^{18}\text{F}$ vapour	140
4.2.5.8	DRIFTS analysis of diamond powder surfaces following exposure to HF vapour	141

CHAPTER 5	DISCUSSION	144
5.0	Introduction	144
5.1	The reaction of $F_2$ or $ClF_3$ with polycrystalline diamond powder and film surfaces	145
5.2	The reaction of hydrogen fluoride, HF, with polycrystalline diamond powder surfaces	157
5.3	Polishing success	167

## REFERENCES

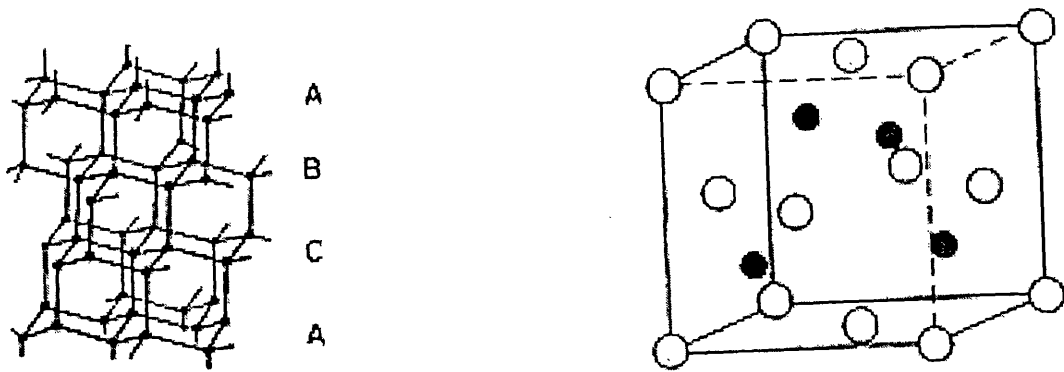
# CHAPTER 1 INTRODUCTION

## 1.1 Diamond: Structure, physical and chemical properties

Diamond is a crystalline allotrope of carbon; other commonly known crystalline forms are graphite, Buckminsterfullerene ( $C_{60}$ ),  $C_{70}$  and nanotubes. In its purest form diamond contains nothing but carbon, Lavoisier who observed the products of heat destruction, established this in 1792. The perfect diamond crystal can be described as a three-dimensional, aliphatic carbon polymer (1). Each carbon atom in the crystal is tetrahedrally co-ordinated to its four neighbour atoms by means of  $sp^3$  hybridised bonds 1.544 angstroms in length (2). The carbon atoms close pack in either a cubic or hexagonal array (figure 1.1) (3-5). The cubic form is the most common and accounts for almost all naturally occurring diamond. In the cubic structure the carbon-carbon bonds have a staggered arrangement which is more stable than the eclipsed arrangement which occurs in the hexagonal structure. The hexagonal form, known as lonsdaleite, can be synthesised from well-crystallised hexagonal graphite ( $>1273$  K, 130 kbar) and has been found in meteorite fragments in the U.S (6).

The face centred cubic structure places carbon atoms at the corners and in the faces of a cube. In addition, half of the available tetrahedral sites in the cube are occupied. For diamond, these sites are structurally identical (filled spheres figure 1.1 (a)). All Group IV elements (C, Si, Ge, Sn and Pb) and well-known compounds such as zinc blende (ZnS) and gallium arsenide (GaAs) share the diamond structure.

(a) Cubic diamond and unit cell



(b) Hexagonal diamond and unit cell

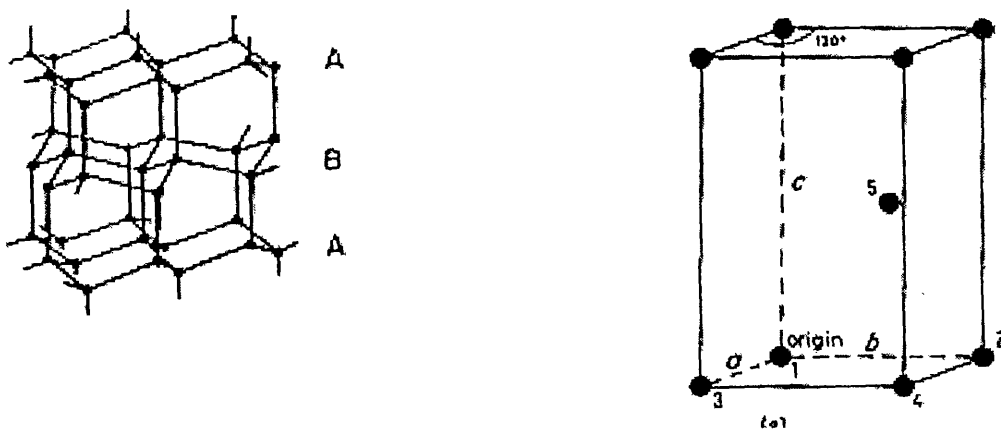


Figure 1.1 Crystal structures of diamond (3-5)

Diamond has a number of remarkable and extreme properties that are due to the crystal structure described. For this reason diamond is of great interest to scientists who seek to utilise its properties for industrial application. The exceptional properties of diamond and the potential uses for the material are summarised in table 1.1.

**Table 1.1** Properties and potential applications of diamond (7-12)

Property	Application
Extremely hard layers, mechanical hardness (90 GPa)	Hard coatings, Abrasives
High optical clarity, transparent from deep UV to far IR	Optical, X-ray and IR windows
Very high thermal conductivity ( $2 \times 10^3 \text{ Wm}^{-1}\text{K}^{-1}$ at 298 K)	Heat sink
Very low thermal expansion coefficient ( $0.8 \times 10^{-6} \text{ K}^{-1}$ )	
High friction resistance	Micromachine parts
Good insulator (resistivity $10^{16} \text{ } \Omega \text{ cm}$ at 298 K)	Electrical insulation
Chemically resistant	Protective coatings
Doping capacity (yielding resistivity range $10\text{-}10^6 \text{ } \Omega \text{ cm}$ )	Electronics, semiconductor (band gap + 5.4 eV)

Currently, natural diamond finds use in a number of areas, which include:

1. A gem stone for decorative jewellery, attractive due to its light refracting properties
2. Heat sinks, where diamond is effective due to its high thermal conductivity
3. An abrasive for polishing, e.g. stainless steels and wear-resistant coatings for cutting tools such as mining drills.

Diamond is the hardest material known with a value of 10 on the Mohs scale devised by Friedrich Mohs in 1812 for classifying minerals in order of hardness (13). The Mohs scale and some comparisons of diamond with other well-known substances are given in table 1.2.

Chemically, diamond is considered to be very inert. The high C-C bond strength of  $337 \text{ kJ mol}^{-1}$  (5) and the very low molar entropy of  $2.4 \text{ J mol}^{-1} \text{ K}^{-1}$  (14) mean that the diamond crystal structure is highly ordered and very stable. Therefore, spontaneous chemical reactions involving breakage of C-C bonds and disruption of the crystal lattice must overcome a highly unfavourable lattice parameter. Reactions may occur if sufficiently exothermic or if performed at high temperature. However, chemical reactions on the crystal surfaces without lattice disruption are much more feasible and will be considered later in this chapter (section 1.5).

**Table 1.2** Mohs scale of minerals (13)

Mohs value	Mineral	Other substances
1	Talc	
2	Gypsum	
2.5		Fingernail
3	Calcite	
3.5		Copper coin
4	Fluorite	
5	Apatite	
5.5		Steel blade
5.75		Glass
6	Orthoclase	
7	Quartz	Steel file
8	Topaz	
9	Corundum	
10	Diamond	

Note: The scale is not linear since diamond is 90 times harder than corundum.

## 1.2 Diamond growth methods

Naturally occurring diamond has been mined for more than 150 years. The most important mines, dating from 1867, can be found in South Africa where diamonds occur within extinct volcanic pipes (1). In recent times an explosion in the demand for diamond has resulted in an increase in the price of the mineral due to its scarcity. With many new applications envisaged for the material (table 1.1) there has been great interest in the development of synthetic methods.

According to the phase diagram for carbon, a schematic of which is shown in figure 1.2 (3,15), graphite is the stable form at ambient temperature and pressure. However, under high temperature and high pressure conditions, diamond becomes the favoured form. Once formed, diamond is kinetically stable or metastable

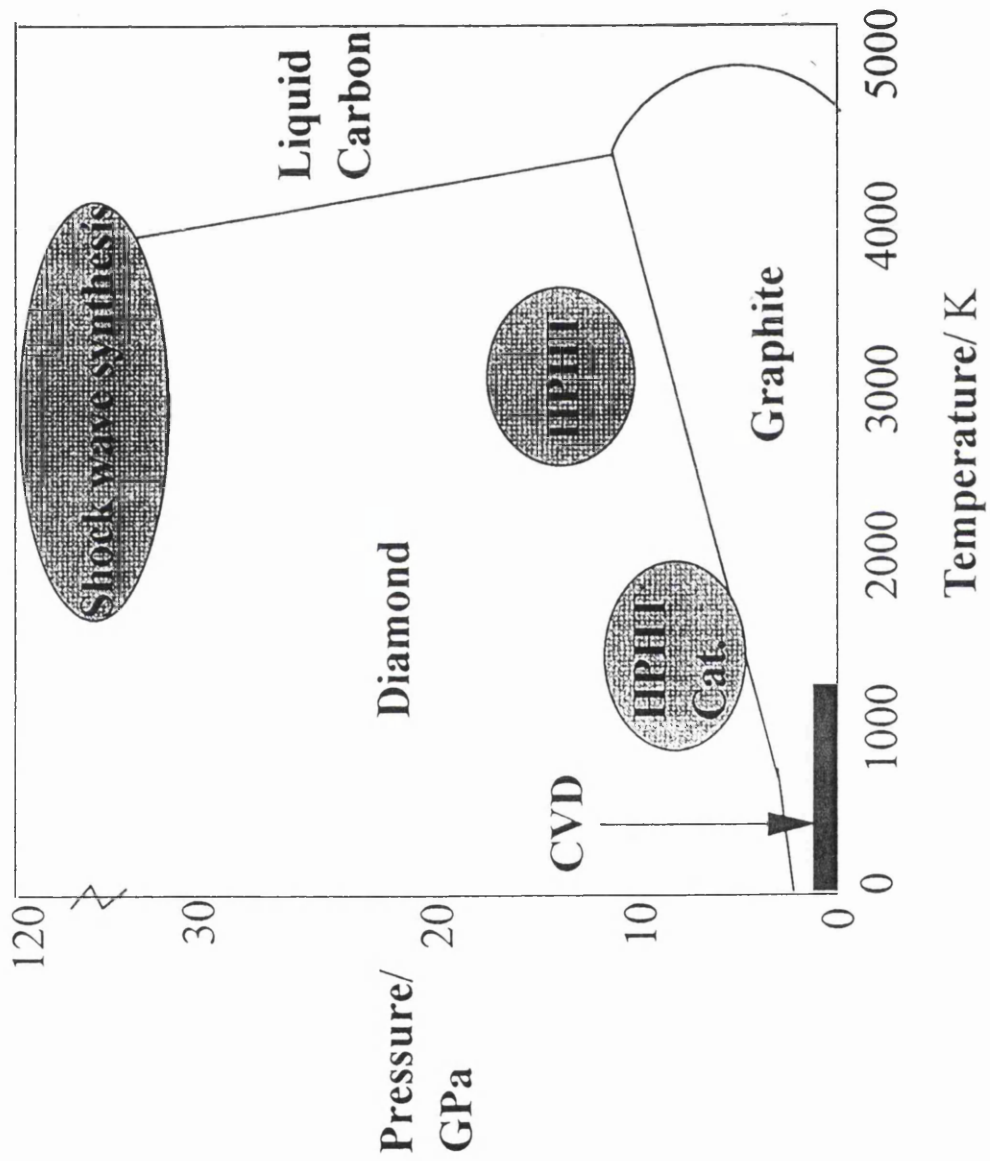


Figure 1.2 Phase diagram for carbon and methods of diamond growth

under ambient conditions and conversion to graphite, the thermodynamically favoured form, does not occur. For this reason, the synthesis of diamond from graphite at high temperature and pressure was attempted.

The General Electric Company conducted the first successful experiments in 1954 using a belt apparatus capable of maintaining a pressure of 200,000 atm at 5273 K (1). The introduction of a solvating metal catalyst (Fe, Ni) to the system made synthesis possible under more reasonable conditions (50-100 kbar, 1800-2300 K) thereby reducing the costs associated with the method (16,17). The catalyst works by dissolving graphite and reducing the energy required to break and reform C-C bonds to yield diamond. Crystals of 5 mm and greater in size could be produced readily at a growth rate of 1 mm per day (18). These experiments formed the basis of the HPHT (High Pressure High Temperature) method which accounts for most of the synthetic single crystal diamond available today.

As shown in figure 1.2 diamond can be synthesised by two other methods. These are shock wave synthesis and chemical vapour deposition or CVD.

As the name suggests, shock-wave syntheses involve exposing a carbon sample, usually graphite, to a high-energy shock wave (300 kbar). The shock wave is generated close to the sample by the controlled detonation of high explosive or by the impact of a metal plate at high velocity. The original method was pioneered by DeCarli in 1961 (19) and modified later by other workers (18,20). The crystals formed were small, 10  $\mu\text{m}$  across at best, and constituted only 1-9% of the original sample. Development in the experimental methods allowed the yield to

be increased, as high as 75%, but the crystals formed were still small. Despite advantages such as very high growth rates, failure to increase the crystal size has meant that shock wave synthesis is not a viable alternative to HPHT methods.

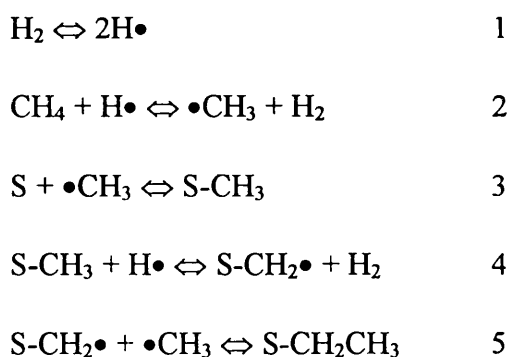
Growth of diamond at low pressure, where graphite is favoured from a thermodynamic standpoint, was thought to be impossible. However, the first successful synthesis of diamond at low pressure (0.001-1 atm) actually preceded the first HPHT synthesis at General Electric. In 1952, W.G.Eversole grew diamond at low pressure on diamond seed crystals (21). The basic concept of his work was the decomposition of a carbon-containing gas by heat to form carbon which, in the presence of diamond seeds, grows further diamond. Since this method did not involve a phase transformation from graphite to diamond, which is subject to a large activation energy barrier ( $> 720 \text{ kJ mol}^{-1}$ ) and the process was governed by surface free energies instead of bulk free energies, the phase diagram constraints could be overcome. Unfortunately, early in the process, spontaneous graphitisation of the diamond surface occurred to form a graphite coat (18,22,23). The graphite could be removed by controlled heating in oxygen and the diamond seeds measured for an increase in mass. The seeds were found to have increased very slightly in weight, corresponding to a diamond growth rate of  $0.1 \mu\text{m h}^{-1}$ , which is equivalent to 1 mm per year. Such low growth rates meant that low-pressure methods were not a viable alternative to HPHT diamond synthesis.

Nevertheless, the work formed the basis of the modern low-pressure method called chemical vapour deposition or CVD. Not surprisingly, this involves the deposition from a chemical vapour on to a substrate to grow diamond. There are a number of reactor designs (24-26) all of which work on the same fundamental

principles. A gas phase, which consists principally of dihydrogen (98-99%) and a few percent of a hydrocarbon, is introduced into the reactor. The hydrocarbon is normally methane but studies involving ethane and organic compounds such as methanol or acetaldehyde have been performed (27-29). The gas phase is then exposed to a high-energy source of some description, which produces atomic hydrogen from the dissociation of  $H_2$ . The source can be a hot filament, plasma or direct current, which provides the energy required to break the H-H bond. Atomic hydrogen is critical to the success of the method for at least three reasons:

1. Carbon-containing radicals are formed by H-atom abstraction to reform  $H_2$ .
2. The  $sp^3$  structure of the growing fragments is preserved since  $sp^2$  carbon is preferentially etched by atomic hydrogen (30). Graphitisation is prevented.
3. Surface hydrogen is abstracted to produce  $H_2$  thereby ensuring a concentration of local vacant sites for the adsorption of carbon radical (24).

The carbon-containing radicals diffuse to the substrate, which is normally silicon or molybdenum and form a bond. The substrate is maintained at a temperature of approximately 1273 K and heteroepitaxial growth of a diamond film occurs. The mechanism is complex and not fully understood, however, a number of key reaction equilibria have been identified (figure 1.3).



S = Substrate

**Figure 1.3** Some key reaction equilibria in the growth of diamond by CVD  
(24)

Figure 1.3 illustrates some of the early steps involved in the growth of diamond from a methane/hydrogen mixture. The exact nature of the carbon radical species seems to be dependent on the CVD method employed. Methyl radicals, as shown, have been identified in non-thermal methods (31-34) whereas more common products of methane decomposition, such as acetylene or methylene, are thought to occur when thermal methods are used (35). Adsorption of the radical species on the substrate surface occurs to form a carbide layer saturated with hydrogen (step 3). Since the H-H bond is stronger than the C-H bond there is always a concentration of radical sites as a result of H-atom abstraction to form H<sub>2</sub> (step 4). These radical sites can either be hydrogenated or react with incoming carbon radicals to form new C-C bonds and initiate diamond growth (step 5). The C-H bond is stronger than the C-C bond therefore hydrogenation is the favoured process and C-C bond formation only occurs to a small extent. Consequently, growth of a diamond film is a slow process with rates varying from 0.1 to 1000 μm h<sup>-1</sup>. It should be noted that growth at the higher end of this scale is generally

accompanied by a decrease in film quality when compared to the high quality film grown at lower rates. Film quality is a measure of the C-C to C-H and diamond to non-diamond ratios and the crystallinity (26). Laser Raman spectroscopy is the technique used to determine film quality since diamond and non-diamond carbon forms, such as graphite, are easily distinguished. High quality films can be grown at around  $10 \mu\text{m h}^{-1}$ , which is too slow for full exploitation of the potential market for CVD diamond. Improving the growth rate without compromising the film quality is one of the major challenges of current CVD research. Some recent developments include the periodic addition of oxygen to the feed gas mixture with improvements in growth rate as much as 500% reported (36,37). The atomic oxygen formed in the reactor is thought to have two key roles:

1. Etching non-diamond carbon.
2. Providing a higher density of sites for diamond growth as a result of surface etching.

Other workers have investigated pre-abrasion of the substrate surface using diamond grit. This produces surface defects where nucleation for diamond growth can occur in addition to growth on diamond particles left on the surface as a result of the abrasion process. Improved growth rates have been reported here also but the quality of the resulting films was questionable (26).

Another factor effecting the use of CVD diamond film commercially is the crystalline morphology. The films are polycrystalline and have surfaces such as that shown in figure 1.4. This is a result of random nucleation for crystallite

growth. The surface is rough or jagged and there are grain boundaries where individual crystallites meet. The crystallites grow in three main directions described by the {100}, {110} and {111} Miller planes (3). The films have been shown to have comparable properties to natural diamond such as extreme hardness and high thermal conductivity (38). Whilst they find application as hard coatings, these films are unsuitable for use as heat sinks in microelectronics or as optical windows, two of the most exciting applications, since very smooth surfaces are required. These surfaces are often described as sub-nanometre, which means there are no peak to trough distances greater than 1 nm. A typical CVD diamond surface has peaks, which are 10's-100's of microns in height.

There are two potential approaches to solving this problem:

1. Finding a way to grow smooth films and ultimately single crystals.
2. Smoothing or polishing of the surface following deposition.

In a recent review paper, Ashfold *et al.* (26) discussed the effects of varying growth parameters such as the methane/hydrogen ratio or the substrate temperature on the diamond film morphology. It was shown that the orientation of the growing crystallites was highly sensitive to the conditions employed. This is a result of the fact that different crystallographic faces grow at different rates, which depend on the availability of carbon species for addition to different crystal planes (24,39). By carefully controlling the methane/hydrogen ratio and the substrate temperature, it has been possible to grow diamond films with uniform crystal orientation (40). It was found that at high methane concentration (>1%)



**Figure 1.4** Surface morphology of a CVD-grown diamond film (used in the present work)

and high substrate temperature crystallites grew, almost exclusively, in the {100} direction. However, at lower methane concentrations and lower substrate temperatures crystallites grew in the {111} direction. Whilst these films are much smoother, they would still require post-growth polishing before use as a heat sink, for example, could be realised.

Highly oriented diamond film can also be grown by homoepitaxial methods, growing diamond on diamond. However, this involves a process of carefully aligning seed crystals such that the film grows in a particular direction (41). This is a laborious process and still results in a film requiring polishing for certain applications.

### **1.3 Polishing of diamond film**

Until a method of growing diamond film, which is smooth on the nanometre scale, is found there will be enormous research effort in the development of methods for polishing CVD diamond film with the ultimate goal of meeting the requirements for use in the fields of electronics and optics.

#### **1.3.1 Polishing concepts**

The science of polishing is well established and is defined as the production of a plane specular surface, which is free of defects and artifacts (42). A high quality polish is obtained by the gradual removal of material from a substrate surface

under tightly controlled conditions. A high degree of control is required, since the properties of a solid material are often dependent upon factors such as its shape and the nature of its surface.

Polishing processes can be categorised in three ways:

1. Abrasive or mechanical polishing
2. Chemical polishing or etching
3. Chemomechanical polishing

Abrasive polishing involves the use of abrasive particles, normally in the form of slurry, which are added across a rotating polishing plate thereby grinding the surface to the required finish. The choice of the abrasive depends on the substrate to be polished and, in particular, its hardness. In order to remove material from the substrate surface, the abrasive particles must be of equal or greater hardness (Table 1.2). The rate at which polishing proceeds is dependent upon a number of important parameters:

1. Abrasive particle size
2. The rate at which the abrasive is delivered to the polishing plate
3. The rotational speed of the polishing plate
4. Applied load or pressure on the sample
5. Temperature

In general, if each of these parameters is increased, the result is an increase in the amount of material removed from the surface and hence a higher polishing rate. However, as the polishing conditions become more aggressive, there is a greater chance that the substrate will be damaged. Types of damage include loss of shape, pitting and cracks or dislocations; all of these effect the properties of the substrate, which have consequences for its usefulness following the polishing procedure. Therefore, a compromise between achieving a reasonable polishing rate and avoiding damage must be found if the method is to be effective.

In chemical polishing the substrate surface is first modified by a chemical reaction and the modified species is dissolved away with an improvement in the surface finish. Chemical polishing is a diffusion-controlled process, which depends on the rate of reagent delivery to the surface. Typically, the substrate is dipped into a chemical solution and a stirring action used to effect polishing. Chemical polishing is often used to remove any defects from the surface of semiconductor materials like Si or GaAs which might have occurred as a result of the wafer cutting process. It can also be used to model the chemical reactions that occur at a substrate surface with a view to developing a chemomechanical polishing process (43).

Chemomechanical polishing is a hybrid of the previous processes, a chemical reaction and a rotating polishing plate respectively modify and remove surface material. A chemical reagent is delivered to the rotating polishing plate, reaction occurs at the surface and the modified material is wiped away under the action of

the plate. Since the new surface species is invariably easier to polish when compared to the parent substrate, mild mechanical conditions, e.g. low applied pressures, can be employed. This gives chemomechanical polishing an advantage over abrasive polishing because the risk of damaging the substrate is much reduced. For this reason it is the method of choice within the semiconductor/electronics industry where damaged substrates are unacceptable.

In her PhD thesis (44) and published work (45), Nicol proposed a general model for chemomechanical polishing with the following features:

1. Oxidation of the substrate surface by the chemical etchant or reagent.
2. Hydration/solvation of the initial reaction products by the diluent component of the etchant solution.
3. Removal of these secondary products from the substrate surface, with the aid of polishing pad and abrasive (passivation)

The model was used to explain the successful chemomechanical polishing of compound semiconductors such as GaAs by halogen-containing reagents such as aqueous sodium hypochlorite solution (NaOCl). In that instance, gallium and arsenic chlorides were identified as the initial reaction products, hydration of the chlorides produced oxide/hydroxide species whose solubility in the diluent solution varied according to pH. This feature was found to have a marked effect on the rate at which polishing would proceed and was ascribed to be a consequence of the amount of insoluble product present on the surface. When present at a high level, the insoluble product prevents access of the reagent to the

substrate surface and hence slows polishing. However, at the correct level, the insoluble species can assist polishing by depositing in the valleys and encouraging chemical reaction at the peaks followed by removal of surface species by the polishing pad. The latter case is described as passivation.

Generally, polishing processes are preceded by a lapping step, which is used to remove gross surface features and alters the shape of the material in preparation for polishing. Lapping is distinct from polishing and tends to involve the use of large grain abrasive particles that are allowed to rotate between the plate and the sample thereby removing large amounts of material.

### **1.3.2 Methods for polishing CVD-grown diamond film**

The success of a polishing regime is measured by the rate at which polishing proceeds, the quality of the polished surface and the running costs. The polishing rate is the rate at which material is removed from the substrate surface to produce a polished finish; it is normally defined in terms of microns removed per hour ( $\mu\text{m h}^{-1}$ ). The terms etch rate and stock removal rate are often used but do not always define the polishing process since large amounts of material can be removed from a surface without resulting in a fine polished finish. For example, a chemical etching reaction to form a pit is not polishing despite the removal of surface material. The quality of the polished surface is a measure of its smoothness; microscopy and surface profilometry are the methods employed for the determination of polished surfaces. Microscopy allows visual inspection of the polished surface and profilometry measures the average peak to valley distance

(Ra) (section 2.2.2). In addition to polishing rates and surface quality, the running costs must be considered if the method is to be economically viable.

Conventionally, abrasive polishing has been the method of choice for polishing CVD diamond film. The diamond film is contacted with a rotating polishing plate, typically made of cast-iron and diamond grit or powder added as an abrasive. Due to the extreme hardness of diamond, the film sample is normally placed under a very high load in order to increase the area in contact with the plate and effect polishing. This has been the method employed by Logitech Ltd. without much success. In order to achieve a reasonable surface finish ( $< 10$  nm Ra) on a sample area of  $1.25 \text{ cm}^2$ , a polishing time of 1-week (168 h) and an applied load of up to  $5 \text{ Kg cm}^{-2}$  were required. In addition to very long polishing times, the high loads made process conditions difficult and often induced damage to the film. Also the large amount of diamond powder used was costly. Clearly significant improvements were required if the method was to be economically viable.

Alternatives to abrasive polishing as methods for modifying the surface morphology of CVD diamond film are thermomechanical polishing, reactive ion etching and smoothing, plasma etching and laser ablation.

Dissolving carbon in metal at high temperature ( $>1173 \text{ K}$ ) is the basis for thermomechanical polishing. Metals such as iron or manganese are able to dissolve appreciable amounts of carbon (2 wt%) at high temperature to form solid solutions with a carbide phase (3). The solvation of carbon by iron, important in

the production of steel alloys, has been known for some time. More recently it has been shown that molten lanthanide metals like lanthanum and cerium can dissolve high amounts (up to 25 at%) of carbon at temperatures in excess of 1173 K (46). All thermomechanical polishing methods involve contacting the diamond film with a metal surface, which may be a rotating plate or a static foil or block, at temperatures ranging from 773 to 1273 K. The choice of metal and other polishing parameters such as atmosphere and the applied load on the film sample have been varied. It is generally accepted that diffusion of carbon from the diamond film into the hot metal occurs under applied loads of several thousand pounds per square inch (psi) (47, 48). The result is substantial thinning of the sample, up to 50% has been reported (47) and the surface roughness is reduced. However, due to the high loads and temperatures, damage to the film sample can occur. This problem has been combated in two ways:

1. Polishing in a dihydrogen atmosphere (49)
2. Using low melting metals or metal alloys (50,51)

A dihydrogen atmosphere is believed to aid polishing by reacting with diffused carbon to produce methane, this helps to maintain a fresh metal surface for further diffusion and hence polishing.

Metals such as lanthanum and cerium or metal alloys like lanthanum/nickel eutectics have much lower melting points when compared with iron (table 1.3). This means that the temperature at which thermomechanical polishing is performed can be significantly reduced. Metal alloys have been most successful

in this regard allowing polishing temperatures to be reduced from 1173 K to 773-873 K (50, 51). Higher diffusivity of carbon in the metal alloy, which is in the liquid phase, is believed to account for the observed improvements over the iron system. The rate at which material is removed from the surface is high, an etch rate of  $215 \mu\text{m h}^{-1}$  has been reported (50), but the resulting surfaces exhibit residual roughness and require further polishing, usually by abrasive methods. In addition, the process can be non-uniform, which has implications for the control of sample shape.

**Table 1.3** Melting point data for some metals and metal alloys used in thermomechanical polishing processes (3, 46, 50, 51)

Metal/ Metal alloy	Melting point/ °C
Iron	1514
Lanthanum (La)	918
Cerium (Ce)	798
La/Ni (88:12) eutectic	480
Ce/Ni (89:11) eutectic	477

Thermomechanical methods are effective for massive thinning of CVD diamond films, however, the running costs promise to be high and improving the quality of the surface finish must be addressed.

Reactive ion etching has been investigated as a method for removing non-diamond components from as grown CVD film, patterning the film for potential application in microelectronics and smoothing the rough surfaces (52-57). Reactive ions can be generated by exposing gases and gas mixtures to a source of high energy such as a microwave generator (55), radiofrequency (53) or ECR (electron cyclotron resonance) (54). Typical gases include dioxygen, dioxygen/fluorocarbon mixtures (53, 56), dihydrogen (57) and the noble gases (52, 54). The diamond film is normally placed under a negative bias voltage and the reactive positively charged ions accelerated towards it.

Substantial smoothing of the characteristic, faceted CVD film surface has been accomplished at modest rates. A reduction in peak to valley surface roughness from 3  $\mu\text{m}$  to 0.5  $\mu\text{m}$  in 8 hours has been reported (54). However such surfaces are far from the nanometre scale of roughness and further polishing using abrasive methods is required. The etching mechanism is believed to involve a local phase transformation from diamond to non-diamond forms followed by removal of the non-diamond carbon in the ion beam.

Reactive ion methods can be used to produce defined etch features on the diamond surface, channels and columnar structures hundreds of nanometres in depth have been fabricated (52, 53, 55, 57). Etching proceeds at grain boundaries leading, in some cases, to a porous structure. This has generated a recent surge of interest in using the method for patterning diamond, which is important for microelectronic application. In this regard Ramesham and co-workers (55) successfully patterned a CVD diamond film with an intricate university logo by

exposing the nickel-masked film to excited state atomic oxygen at 373 K. The process was fast with etch rates of  $12 \mu\text{m h}^{-1}$  and accompanied by a smoothing of the diamond surface, however the actual roughness of the film was not reported. Patterning of single crystal diamond, grown by HPHT methods, has also been accomplished (52, 53) and has the advantage of etching on to an already smooth surface.

Reactive ion etching has potential as a method for modifying the surface morphology of CVD-grown polycrystalline diamond film. However, smooth surfaces on the nanometre scale have yet to be reported and, until this is achieved, reactive ion etching is better placed as a technique for patterning single crystal diamond or diamond films polished by other means.

Laser polishing of diamond film uses pulsed laser radiation for the ablative etching of material from the diamond surface. It is accepted as the fastest way of reducing the surface roughness of a CVD-grown diamond film, which is a consequence of the high rate at which material can be removed from surface peaks and the ability to maintain a high laser pulse rate (58). Most studies involve excimer lasers (XeCl, KrF) which operate in the UV range or those operating in the visible and near IR range of the electromagnetic spectrum such as Nd:Yag lasers.

The most successful laser polishing experiments have used a scanning beam, which impacts the sample at a grazing angle, typically  $75\text{-}80^\circ$  thereby encouraging ablative etching from the surface peaks. Sublimation of carbon in the laser beam

is believed to occur. Using these conditions a reduction in surface roughness from 250  $\mu\text{m}$  to 3  $\mu\text{m}$  in 7 minutes, which is equivalent to  $\approx 2040 \mu\text{m h}^{-1}$ , for a sample area of 6  $\text{mm}^2$  has been reported (59). In that study, laser polishing was followed by a thermomechanical polishing step to produce a high quality surface finish. In order to achieve a surface roughness on the nanometre scale using laser polishing it is necessary to start with a film of decreased thickness where the diamond grains and hence surface roughness will be smaller. In this way surface finishes of 20-30 nm, on films with an initial roughness of 0.3-1  $\mu\text{m}$  and thickness on the micron scale, could be obtained (60, 61).

Laser polishing can be used to coarse-polish thick (0.7 mm) and rough (250  $\mu\text{m}$  Ra) diamond film at very high rates. However, achieving surfaces of high optical quality requires a further polishing step. In addition, the possibility of laser-induced defects evidenced by a reduction in the diamond Raman line intensity (62) following polishing could effect the use of the method for surface finishing in microelectronic applications.

#### **1.4 Aims of the current work**

In the absence of a process for polishing CVD-grown diamond film that offers vast improvement over conventional abrasive methods, there remains great value in the study of diamond polishing and a potential for high reward if a suitable process can be developed.

The aim of the current work was to investigate a process whereby diamond films could be polished rapidly to a good, continuous surface finish in the nanometre range. The limitations of current abrasive polishing methods, for example, slow polishing times and a propensity to damage the substrate were also to be addressed.

The investigation was to involve surface treatment of diamond with a range of strongly oxidising halogen-based reagents, followed by examination of the chemical and physical properties of the modified surface using various analytical techniques, for example, electron microscopy, radiotracers and spectroscopic methods. The behaviour of modified films with regard to conventional abrasive polishing systems would be studied.

Understanding the chemical reactions possible at the substrate surface has an integral role in the development of a chemomechanical polishing process. From this standpoint, an in depth study of diamond surface chemistry allows the potential for polishing diamond films by chemomechanical methods to be evaluated.

## **1.5 Diamond surface chemistry**

### **1.5.1 Introductory remarks**

Studies in diamond surface chemistry have relevance in understanding the mechanism for film growth by CVD, finding ways to alter advantageously the parameters of film growth and changing the chemical and physical properties of diamond film, thereby broadening the range of application.

Of particular interest is the chemisorption of hydrogen, oxygen and halogen atoms as well as hydrocarbons on diamond surfaces. Atomic hydrogen and hydrocarbons have a critical role in the CVD process for film growth (section 1.2). Atomic oxygen has been shown to influence film growth (section 1.2) and act as an etchant in reactive ion etching systems (section 1.3). Halocarbon/halogen/hydrogen CVD feed gas mixtures allow film growth at a substantially reduced substrate temperature when compared to conventional hydrogen/hydrocarbon systems (63, 64). This means that diamond coated plastics, for example, may be possible. Furthermore, halogenated diamond surfaces are expected to exhibit useful properties such as a low friction resistance. Fluorinated diamond has a reduced surface energy (65) making it ideal for use as a solid lubricant (66).

The reactions of diamond with fluorine-containing compounds and the influence of such reactions on the polishing behaviour of CVD-grown diamond film, in

abrasive and chemomechanical systems, is the focus of the current work. Therefore, studies on fluorine chemisorption are of greatest relevance here. Hydrogen and oxygen chemisorption are summarised also since both atoms can be found on the surfaces of CVD-grown diamond film and are, therefore, precursors to fluorination.

Most studies have involved single crystal or powder surfaces with a few examples using films.

### **1.5.2 Hydrogen chemisorption**

Hydrogen chemisorption on diamond has received considerable attention due to the integral role of atomic hydrogen in the growth of diamond from the vapour phase.

Numerous studies on single crystal surfaces have been performed and are well reviewed in a paper by Wei and Yates (67).

It has also been shown (67) that as-polished single crystal diamond surfaces are hydrogen terminated suggesting that surface C-H bond formation is more stable than the presence of dangling bonds. Investigations in diamond surface structure using XPS have shown that, upon heating, a new band appears as a shoulder on the low binding energy side of the bulk peak (68). This band has been attributed to the presence of surface dangling bonds resulting from the desorption of hydrogen atoms.

A typical single crystal experiment involves annealing the polished diamond crystal at a temperature in the range 1200-1500 K, exposing it atomic hydrogen at low pressure ( $10^{-5}$ -  $10^{-7}$  Torr) and reduced temperature, 973-1273 K mimicking CVD substrate temperatures, followed by further heating to a desired maximum. The experiment is performed in an ultra-high vacuum (UHV,  $10^{-9}$  Torr) chamber and the diamond surface structure is analysed at various stages during the experiment. Common methods of analysis include, low-energy electron diffraction (LEED), x-ray photoelectron spectroscopy (XPS), Auger electron spectroscopy (AES) and thermal and electron desorption methods (TPD, ESD). The theory and application of these methods can be found elsewhere (69), XPS has been used in this work, therefore a detailed explanation of the technique can be found in section 2.1.10. The diamond {111} and {100} surfaces have been studied most, since these are the dominant directions of crystal growth by CVD (26).

### *C{111} surface*

As a result of the annealing procedure the surface exhibits a change in LEED pattern from (1x1) to (2x1) which has been characterised by a  $\pi$ -bonded chain model (70). Desorption of surface species upon annealing produces dangling bonds, which then clip together forming a CC double bond. Treatment with atomic hydrogen, generated by thermal cracking of molecular hydrogen at 2000 K, causes the formation of a (1x1) LEED pattern (71, 72) consistent with the formation of C-H bonds at the diamond surface. In addition there is considerable

evidence for the formation of multiple hydride species such as  $\text{CH}_2$  and  $\text{CH}_3$  (72, 73) which have been detected as  $\text{CH}_x^+$  ( $x = 1-3$ ), in addition to  $\text{H}^+$ , using electron stimulated desorption methods (74). The mechanism for the formation of multiple hydride species is uncertain; multiple dangling bonds present at part (e.g. defects) or the entire annealed surface have been suggested (75). Thermal desorption experiments suggested that hydrogen was stable on the diamond surface up to approximately 1200 K where desorption begins to occur. The (1x1) LEED pattern is preserved up to nearly 1400 K and is only reduced to the (2x1) pattern when desorption is completed at 1420 K (72). This suggests that only a small amount of hydrogen is required to preserve the  $\text{sp}^3$  structure.

#### *C{100} surface*

As with the {111} surface a (2x1) LEED pattern is observed following annealing above 1300 K which is due to the presence of  $\pi$ -bonded dimer pairs at the surface (67). Upon exposure to atomic hydrogen, the formation firstly of  $\text{CH}$ , monohydride and then  $\text{CH}_2$ , dihydride would be predicted. In this case the monohydride structure would also exhibit a (2x1) LEED pattern whilst a (1x1) pattern is expected for the dihydride structure. The (2x1) LEED pattern is preserved following reaction with atomic hydrogen suggesting monohydride formation. The question of dihydride formation on the diamond {100} surface has yet to be resolved; studies in molecular mechanics (76) have indicated that the dihydride would suffer from severe steric repulsion between neighbouring hydrogen atoms making it unstable with respect to the monohydride. However,

the as-polished surface shows a sharp (1x1) LEED pattern (77) suggesting that the dihydride phase was present.

The chemisorption of hydrogen on powder surfaces, by thermal reaction with H<sub>2</sub>, has also been studied (78, 79). In a recent study (80), the hydrogenation of oxidised diamond powder was investigated. Surface species following hydrogenation at temperatures in the range 673-1373 K were identified using diffuse reflectance Fourier transform infrared spectroscopy (DRIFTS) and thermal desorption products measured by mass spectroscopy. Spectral features attributed to CH, CH<sub>2</sub> and CH<sub>3</sub> stretching vibrations were found to increase up to a treatment temperature of 1173 K after which their intensity began to decrease. The increase in (CH) band intensity was accompanied by a decrease in intensity for those bands attributable to surface oxygen (section 1.5.3). Desorption studies indicated the loss of CO and CO<sub>2</sub> above 563 K and H<sub>2</sub> above 1173 K; this led the authors to believe that the mechanism for hydrogenation involved chemisorption of hydrogen on surface radical sites created by the desorption of oxygen species.

In conjunction with the loss of hydrogen above 1173 K, the formation of graphite was identified using laser Raman spectroscopy confirming the importance of hydrogen for the preservation of the diamond structure. This could also be concluded from the single crystal studies on hydrogen chemisorption.

### 1.5.3 Oxygen chemisorption

The oxidation of diamond powder surfaces has been accomplished using hot acid mixtures (80) and reaction with molecular oxygen at various temperatures (78, 79, 81, 82). However, oxidation of annealed single crystal surfaces, {100} and {111} required the presence of atomic oxygen; molecular oxygen was found to be inactive unless mixed with atomic oxygen (83).

In a similar manner to hydrogen chemisorption on single crystal surfaces, reaction of atomic oxygen with the (2x1) reconstructed surface produced, as a result of the annealing procedure, a (1x1) LEED pattern. The process was shown to be reversible upon heating with CO and CO<sub>2</sub> identified as desorption products (83). Oxygen atoms interact with  $\pi$ -bonded species breaking them to form CO bonds and reforming the diamond structure. The nature of the oxygen interaction has been modelled using theoretical calculations (84) which suggest that both on-top and bridging configurations are stable, however such configurations do not account for the formation of CO<sub>2</sub> as a desorption product.

Studies using DRIFTS have proved useful in this regard, providing greater information as to the identity of the oxygen-containing surface species.

In their paper Ando *et al.* (81) studied the reaction of hydrogenated diamond powder with molecular oxygen over a range of temperatures (573-1073 K). They proposed a mechanism for oxidation with the following features:

1. Above 573 K dehydrogenation to form water accompanied by dissociative adsorption of oxygen to form C=O and C-O-C groupings occurred.
2. Further oxidation to form -COO- and -COOCO- groupings occurred between 573 and 673 K.
3. Desorption of CO and CO<sub>2</sub> occurred between 753 and 1073 K.

The study involved carefully monitoring the CO stretching region in the infrared (800-2000 cm<sup>-1</sup>) as a function of reaction temperature and correlating the observations with reference data for oxygen-containing compounds. As a result, desorption of CO<sub>2</sub> from oxidised diamond surfaces could be rationalised.

Given that CO and CO<sub>2</sub> can be desorbed from diamond surfaces, there has been an interest in the use of dioxygen as an etchant for diamond film. The use of oxygen in reactive ion etching processes has been discussed in section 1.3.2 and other workers (85) have investigated the effect of reaction in O<sub>2</sub> at high temperature (973 K). Under those conditions etching of diamond film to form a pitted surface is significant.

Studies in oxygen chemisorption have helped to explain the role of oxygen in CVD growth processes, provided a way of making diamond surfaces hydrophilic, and have led to the development of reactive ion etching processes for diamond film.

#### 1.5.4 Fluorine chemisorption

In recent years the chemisorption of halogens and, in particular, atoms of fluorine on a diamond surface has been investigated for the reasons outlined earlier (section 1.5.1). In agreement with studies on hydrogen and oxygen chemisorption, the reaction of fluorine-containing compounds with single crystal, powder and, to a lesser extent, film surfaces have been investigated.

In single crystal studies, thermally annealed {111} and {100} surfaces have been exposed to atomic and molecular fluorine at low pressure (2 Torr). Atomic fluorine is generated *in-situ*, either by exposing F<sub>2</sub> to an electrical discharge (86, 87) or by the decomposition of molecules such as XeF<sub>2</sub> which, are unstable in the presence of some solid surfaces (72, 88). A carrier gas such as argon is normally added to produce a mixture with around 5% fluorine, which can flow through the UHV chamber. The surface structure following fluorine treatment is investigated using LEED and XPS, the latter technique being particularly useful for detecting changes in the C(1s) binding energy as a result of fluorine adsorption.

##### *C{100} surface (86)*

Prior to reaction with atomic fluorine, LEED and XPS analyses suggested that the annealed surface had not undergone a (2x1) reconstruction hence a high degree of hydrogen desorption to produce dangling bonds was expected. These

observations were consistent with those outlined earlier which indicated that the (1x1) surface could be maintained up to 1300 K despite the low concentration of surface hydrogen present at this temperature. The (1x1) LEED pattern collapsed upon fluorine addition suggesting, a somewhat disordered surface, which may have been induced by repulsion between surface fluorine atoms.

XPS analysis of the surface following exposure to atomic fluorine at temperatures in the 300-700 K range revealed the presence of a new peak on the high binding energy side of the bulk diamond peak. The size of the shift was 1.8 eV indicating the formation of a carbon-monofluoride surface species (this topic is discussed later in the thesis, see section 4.2.4, table 4.8). In addition, a remnant of the low energy surface state, present before reaction with F, suggested the presence of dangling bonds and incomplete fluorination. The authors estimated the fluorine coverage to be about three-quarters of a monolayer.

The reaction was believed to involve chemisorption of fluorine on dangling bonds as the major process with replacement of H for F occurring to a much lesser extent. The absence of more highly fluorinated species such as  $\text{CF}_2$  and  $\text{CF}_3$  was explained as being due to unfavourable steric interactions and an inability of F atoms to penetrate the diamond surface. It was also noted that molecular fluorine was less reactive when compared to atomic fluorine even at 700 K where appreciable dissociation would occur. This was taken to indicate further the dependence of the extent of reaction on the number of adsorption sites available.

### *C{111} surface (72, 87, 88)*

The results obtained on this surface were very similar to those described for the {100} surface. Freedman and Stinespring (87) observed an almost identical XPS spectrum when compared with their previous work on the {100} surface and therefore came to the same conclusion, that only a carbon-monofluoride moiety was present. They also observed using LEED, a conversion from (2x1) surface reconstruction before fluorination to a (1x1) pattern after fluorination consistent with breaking  $\pi$ -bonds to form CF. Other workers (88) have observed a similar result, which suggested that monofluorination was correct.

Thermal desorption analysis indicated fluorine atoms were the major desorption product, HF and  $\text{CF}_n$  ( $n=2-4$ ) species were not identified but their existence could not be ruled out. Repolishing of the diamond surface to produce a good LEED pattern was necessary after several fluorination/desorption cycles but significant etching of carbon was not expected.

Since the etching of diamond to produce  $\text{CF}_4$  would be highly exothermic ( $> 200 \text{ kJ mol}^{-1}$ ) kinetic barriers to extensive fluorination of diamond surfaces are inferred. The extremely tight lattice structure of diamond apparently prevents penetration of fluorine atoms, which is required to produce the simplest etch product,  $\text{CF}_2$ .

The fluorination diamond powder surfaces has also been investigated, most notably in the work of a Japanese group led by Ando (89-91). Those studies involved the reaction of hydrogen and oxygen terminated diamond surfaces with  $F_2$  (90, 91) or  $CF_4$  plasma (89) under various conditions. Analysis of the fluorine-treated surface was performed using DRIFTS and mass spectroscopy used to identify thermal desorption products.

In the reaction of hydrogen-terminated diamond surfaces with  $F_2$ , complete replacement of hydrogen for fluorine was observed at a reaction temperature of 263 K. Evidence for this was the loss of C-H stretching vibrations in the region 2800-2970  $cm^{-1}$  and the appearance of new bands in the region 1000-1400  $cm^{-1}$  where C-F stretching vibrations occur. As the reaction temperature was gradually increased up to a maximum of 773 K, the intensity of these bands was increased and shifting to a higher wavenumber occurred. At least three distinct bands were identified and assigned to CF,  $CF_2$  and  $CF_3$  functionalities. Further evidence to support the formation of highly fluorinated species was obtained by monitoring the sample weight as a function of reaction temperature. Weights were found to increase as the reaction temperature was increased and at 773 K corresponded to a coverage of two or three fluorine atoms per carbon. Thermal desorption analysis (91) above 873 K showed peaks at masses 19, 20 and 69 for F, HF and  $CF_3$  desorption products.

Oxygen-terminated diamond powder was found to fluorinate less easily when compared to hydrogen-terminated surfaces, presumably due to the greater C=O

bond strength. Fluorination could be accomplished, but even after reaction at 773 K traces of surface oxygen were still observed.

Studies in fluorine chemisorption on powder surfaces suggest a very different reactivity of fluorine towards diamond when compared with single crystal studies. In their work on diamond {111} and {100} surfaces, Freedman and Stinespring (86, 87) concluded that only mono-fluorination was possible, breakage of C-C back bonds did not occur and fluorination at room temperature was not possible using  $F_2$ .

In contrast, Ando et al. (89-91) suggest that breakage of C-C back bonds to form  $CF_2$  and  $CF_3$  groups is possible and that  $F_2$  can fluorinate diamond at 263 K. This apparent difference in reactivity may be a function of the experimental conditions, whilst the reaction temperatures are similar in both cases, the work on powder surfaces involved a much higher fluorine concentration (1 atm, 100 %  $F_2$ ) when compared to the single crystal work (2 Torr, 5 %  $F_2$  / bal. Ar). The chemical nature of the diamond surface before reaction with fluorine varied also. Single crystal studies were performed on annealed surfaces, which were close to or completely free of adsorbed hydrogen or oxygen, whilst the powder surfaces were covered with hydrogen or oxygen. The presence of surface hydrogen, for example, may effect the reactivity of fluorine towards diamond. The problem is compounded by the fact that neither group attempted to identify etch products, during the reaction. Instead, the nature of the diamond surface after reaction was the major focus. Freedman and Stinespring suggest that there is not enough room on diamond surfaces to accommodate more than one fluorine atom per carbon. If

this is correct, in order to produce the  $\text{CF}_2$  and  $\text{CF}_3$  groups as observed on powder surfaces, etching of carbon to make room for additional fluorine seems likely.

The growth of diamond film from fluorinated precursors, for example  $\text{CF}_4$ , has been achieved and the resulting films shown, in some cases, to be contaminated with surface fluorine (92, 93). Since atomic hydrogen was also present in these growth systems, removal of surface F to form HF occurred. In addition, desorption of F at the substrate temperatures employed was expected. However, upon the termination of the growth process, chemisorption of small amounts of F can apparently occur. XPS studies of the film surface suggested that only a carbon monofluoride species was present.

The reaction of CVD diamond films with fluorine-containing reagents has received very little attention. However, attempts to etch diamond film, using  $\text{CF}_4$  or  $\text{SF}_6$  plasmas, have been made (94). The etching rate, determined by monitoring the production of  $\text{CF}_3^+$  using mass spectroscopy, was found to be very slow. In addition, XPS of the resulting diamond film showed a single high-energy shifted (+1.8 eV) feature in exact agreement with single crystal studies suggesting that the fluorination was limited to a monolayer of single-phase carbon monofluoride. It should also be noted that the etching conditions were similar to those used in single crystal studies and the diamond sample was exposed to very low pressures (50 mTorr) of the active reagent and reaction was performed at room temperature.

Studies in the chemisorption of H, O and F have great value with regard to understanding the mechanisms of diamond growth by CVD methods and for

modifying the surface properties of diamond. However, the chemisorption of fluorine on diamond, for example, is not yet fully understood with apparently conflicting results observed on powder and single crystal surfaces. In this work the development of a process for modifying the surface of diamond films to make polishing easier involves further investigation of diamond surface chemistry and addressing questions such as the extent of fluorination possible by reaction with a range of reagents.

## CHAPTER 2 EXPERIMENTAL

### 2.1 Chemical modification of diamond surfaces

To exclude air and moisture all reactions were performed under vacuum ( $10^{-4}$  Torr) and samples were handled in a dry atmosphere box ( $H_2O < 5$  ppm). The reagents employed (Table 2.1) in this work are all corrosive gases. Because of this all vacuum equipment and reaction vessels were constructed from Monel. Monel is an alloy of nickel and copper and is resistant to chemical corrosion.

**Table 2.1** Reagents employed and supplier

Reagent	Supplier
$F_2$	MG Gas Products
HF	Air Products
$ClF_3$	Fluorochem Limited

A procedure for purifying  $F_2$  and  $ClF_3$  is discussed in section 2.1.7, with emphasis on the removal of HF contamination.

### **2.1.1 Nature of the diamond powder and film samples**

Diamond powder and film samples were available for use in this part of the work. For the most part, powder samples were used since they were cheaper, more readily available than films and offered greater surface area for reaction.

All diamond samples were obtained from Logitech Ltd. Powder samples were available in a range of particle sizes (1-90  $\mu\text{m}$ ). However most of the work was performed using 1  $\mu\text{m}$  diamond powder. Film samples (1  $\text{cm}^2$  typically), grown by the CVD method (GEC) were used. These were generally available unsupported i.e., with the silicon substrate (ref. section 1.2) removed, presumably by oxidation in an acid media.

### **2.1.2 Hydrogenation/Oxygenation procedure**

The diamond samples used in this work were hydrogenated or oxygenated before reaction with any of the reagents listed above (table 2.1). Hydrogenation and/or oxygenation of the diamond surface has been shown to affect the reactivity towards halogenation (80, 81, 89, 90). A simple flow rig (Figure 2.1) was constructed for this purpose. A quantity of diamond powder or a piece of polycrystalline diamond film was loaded into a small boat fashioned from nickel foil. The boat was then loaded into a 1-inch o.d. Monel tube reactor that could be attached to the flow line via Monel couplings (Swagelok). A wrap-round furnace was used to heat the reaction vessel to the desired temperature, which could be monitored using a thermocouple wire and multimeter. The conditions employed for hydrogenation or oxygenation are shown in table 2.2.

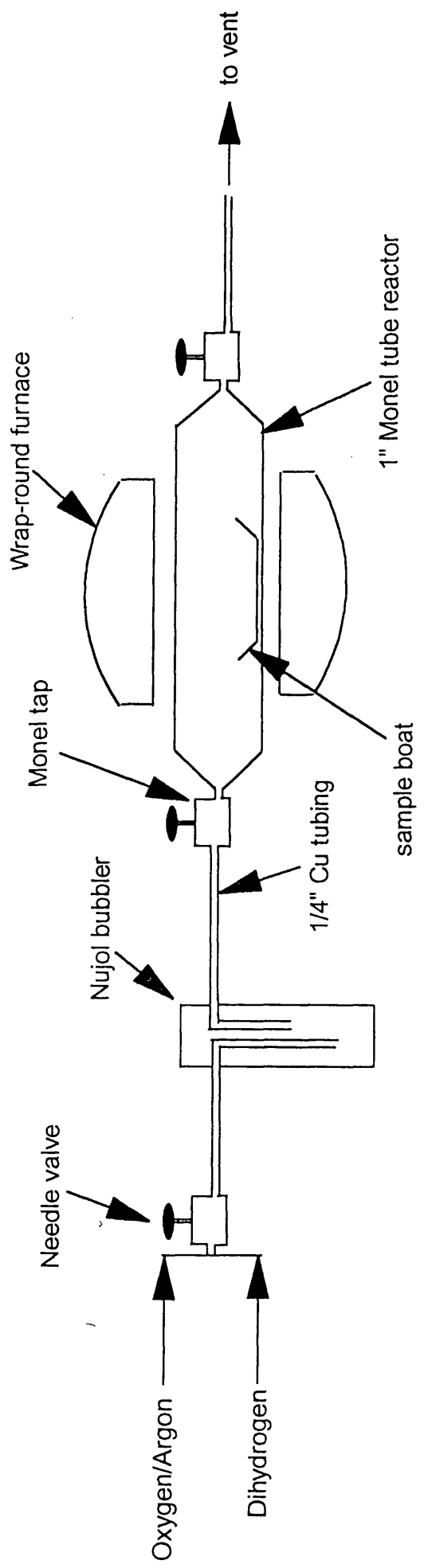


Figure 2.1 Flow line for hydrogenation/oxygenation of diamond samples

**Table 2.2** Conditions for hydrogenation or oxygenation of diamond samples

Procedure	Reagent	Flow rate/ cm <sup>3</sup> min <sup>-1</sup>	Temperature/ K	Time/ h
Hydrogenation	H <sub>2</sub> (99.9%)	30	1173	1
Oxygenation	O <sub>2</sub> :Ar = 20:80	30	673	1

It should be noted that oxygenated samples were prepared from samples which had already received a hydrogenation treatment. This could be achieved readily by allowing the reaction vessel to cool to 673 K in a flow of hydrogen and then switching to a flow of oxygen. In both cases, hydrogenation and oxygenation, the vessel was allowed to cool to ambient temperature in a gas flow before removal to the dry atmosphere box where the sample was stored.

### 2.1.3 Vacuum Systems

Three Monel metal vacuum systems were used for handling HF, ClF<sub>3</sub> and F<sub>2</sub> respectively; a vacuum (10<sup>-4</sup> Torr) was achieved using a rotary pump (Edwards or Genevac). Pyrex waste traps cooled under liq. N<sub>2</sub> (77 K) protected the pump from any residual volatile in the system. The pump and waste traps could be isolated from the remainder of the system. The pressure of reagent gases introduced to the vacuum system was measured using a gauge (Air Products or Budenberg). The systems used for handling ClF<sub>3</sub> and HF were constructed from, 2/5-inch o.d Monel tubing and had a similar design (Figure 2.2). A series of Monel valves (Autoclave Engineers) allowed connection of Monel reaction

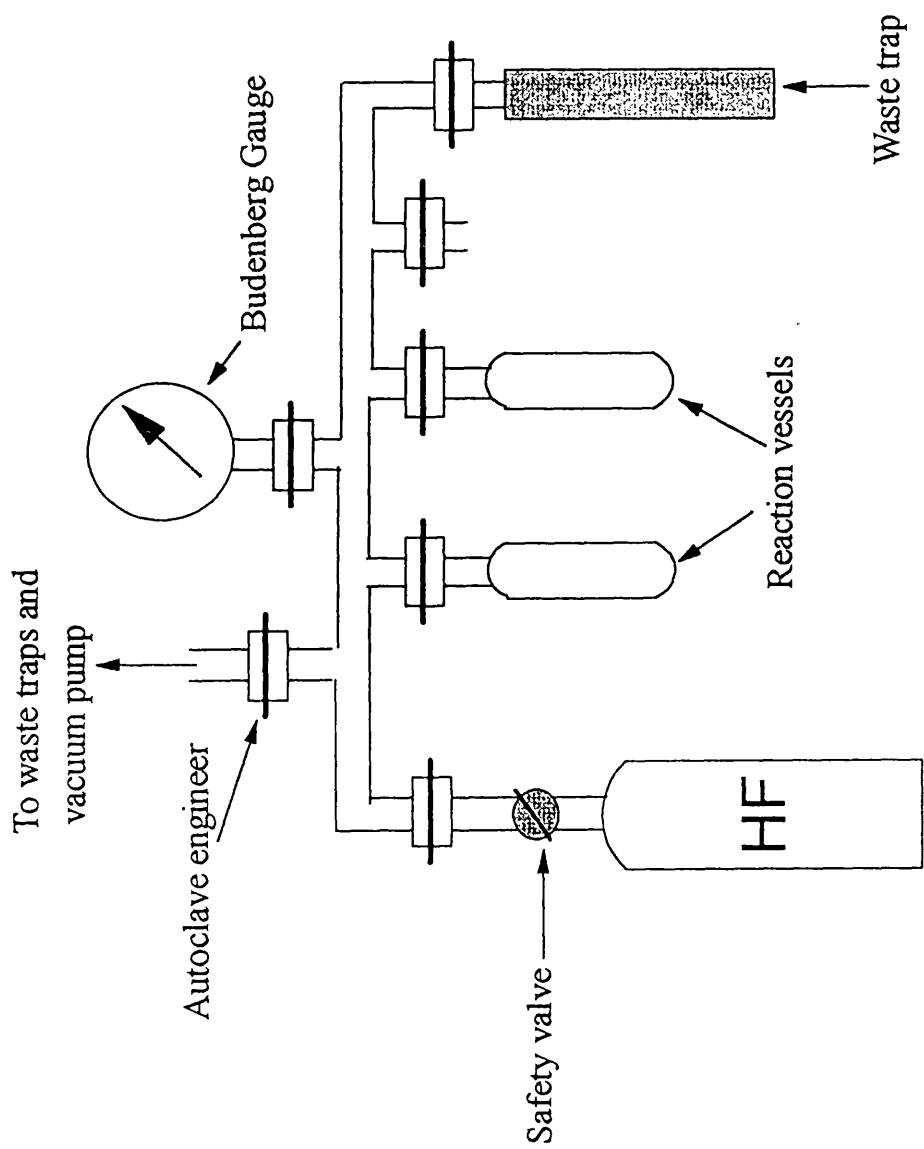


Figure 2.2 Monel vacuum line for handling anhydrous hydrogen fluoride

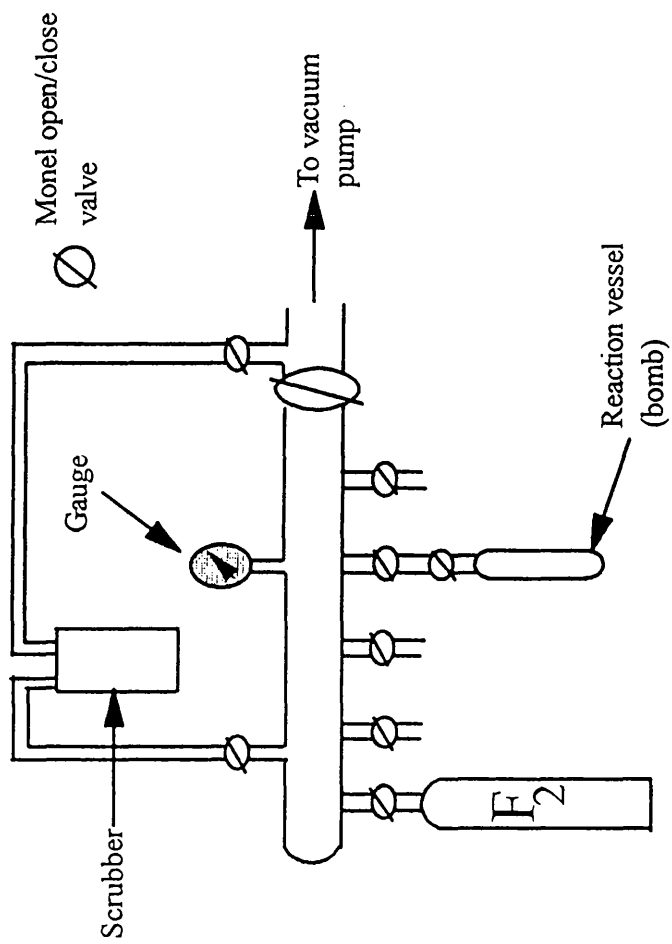


Figure 2.3 Monel vacuum line for handling difluorine

vessels or bombs via nipple and collar screw couplings. In a similar manner a cylinder or lecture bottle of the desired reagent was attached to the line on a permanent basis. A Monel waste trap was also present and cooled under liq. N<sub>2</sub> while the system was in use, any unused reagent could be removed here. The system used for handling F<sub>2</sub> was of a simpler design (Figure 2.3) a length of Monel tubing 3/4-inch o.d equipped with five Monel valves (Whitey) formed the manifold for gas handling. A cylinder of F<sub>2</sub> was attached to the system using a length of 1/4-inch o.d Monel tubing and Monel couplings (Swagelok). Unused reagent was removed via a sodalime scrubber, which could then be evacuated.

#### **2.1.4 Calibration of vacuum systems**

Calibration of a vacuum system is the determination of the total volume of that system. If the volume of the system is known then it is possible to determine the quantity of any ideal gas used in that system according to the ideal gas law as shown in equation 2.1.

A Pyrex bulb of known volume was attached to the system, evacuated and then isolated from the rest of the system, which was filled to atmospheric pressure with air. The decrease in pressure upon opening the bulb was measured and the volume of the system calculated using equation 2.2. The procedure was repeated several times and a mean value obtained.

$$PV = nRT \dots\dots\dots 2.1$$

In equation 2.1, P = pressure (atm); V = volume (L); n = number of moles; R = gas constant (0.08206 L atm mol<sup>-1</sup> K<sup>-1</sup>).

$$P_1V_1 = P_2V_2 \dots\dots\dots 2.2$$

In equation 2.2,

P<sub>1</sub> = Pressure in vacuum system (1 atm), P<sub>2</sub> = Pressure in vacuum system + bulb (atm), V<sub>1</sub> = Volume of vacuum system, x (L), V<sub>2</sub> = x + volume of bulb (L).

The use of a vacuum system of known volume made it possible to determine the volume of reaction vessels in a similar manner. Determination of vacuum line volume allowed the quantity of any ideal gas expanded into the reaction vessel to be expressed in moles.

### 2.1.5 Reaction vessels

Two types of Monel reaction vessel were used in this work; these were a tube vessel, identical to that described in 2.1.2 and high pressure bombs (Hoke). Both types of vessel were equipped with Monel open/close valves (Whitey) and could be attached to a vacuum system via Monel couplings (Swagelok). The choice of vessel depended upon the experimental conditions employed and the physical form of the diamond sample, for example, reactions involving diamond film were performed in the tube reactor, offering easier sample handling.

### 2.1.6 Passivation and leak testing of vacuum systems and reaction vessels

Passivation involved the formation of an inert fluoride layer on the inner surface of the Monel vacuum systems and reaction vessels. This renders the metal resistant to corrosive attack from the reagent. The vacuum systems used in this work were already passivated and it was standard practice to leave the system in an atmosphere of HF or F<sub>2</sub> when not in use. The reaction vessels were constructed from virgin Monel and passivation was necessary before any experiments could be performed. A typical passivation procedure involved heating the reaction vessel using a wrap-round furnace to 473 K in an atmosphere of F<sub>2</sub> or HF for 24 h. Following the passivation treatment the inner surface of the vessel was inspected visually and the quality of the surface confirmed.

Since the reagents used in this work are a potential health hazard, it was imperative that all vacuum systems and reaction vessels were leak tested before any experiments could be performed. If a vacuum system or reaction vessel could hold a vacuum for a period of 24 h it was assumed to be leak tight. The presence of air due to a leak could be determined by changes on a pressure gauge or more sensitively by examining the electrical discharge from isolated parts of the system. If air was present, a pink discharge was observed due to the excitation and decay back to ground state of nitrogen molecules in the air. The procedure, best performed in subdued light, involved contacting a Tesla coil with the Pyrex section of the system and sequentially opening the valves of the system manifold and reaction vessels. In this way the faulty part could be found

and replaced. If the system or vessel was leak tight a discharge was not detected.

### 2.1.7 Purification of reagents

It is common for reagents such as F<sub>2</sub> or ClF<sub>3</sub> to be contaminated with HF, it was important in this study that HF be removed from the starting material since it was a predicted reaction product. A Monel vessel containing activated NaF (Aldrich, 10g heated to 423 K for 24 h) was used for this purpose. An aliquot (~6 mmol) of F<sub>2</sub> or ClF<sub>3</sub> was condensed on to the NaF under liq. N<sub>2</sub> and allowed to interact at room temperature for several hours, HF is removed as NaHF<sub>2</sub> according to equation 2.3. A gas sample (5-10 Torr) was analysed using infrared spectroscopy to confirm the absence of HF. The infrared spectrum of HF contains a diagnostic peak, at 4000 cm<sup>-1</sup>, that exhibits rotational fine structure (95).



If HF was evident, the procedure was repeated until HF could no longer be detected.

### 2.1.8 Preparation of anhydrous [<sup>18</sup>F]-HF

Considerable work on the interaction between HF and diamond surfaces has been conducted. The radioisotope <sup>18</sup>F (β<sup>+</sup>-emitter, t<sub>1/2</sub> 110 min.) is a useful probe in such reactions.

### ***Preparation of the radioisotope $^{18}\text{F}$***

The  $^{18}\text{F}$  used in this work was prepared (PET centre, Aberdeen hospital, Foresterhill, Aberdeen) by the deuteron irradiation (15 MeV, cyclotron generated) of neon according to equation 2.4. A schematic of the apparatus used is shown in figure 2.4. The target was charged with a mixture of gases ( $\text{Ne}:\text{F}_2 = 99.7:0.3$ ), via taps 1-7, until a pressure of 12 bar was reached. The target was then irradiated with deuterons to form  $^{18}\text{F}$ , which undergoes an exchange reaction with  $\text{F}_2$  to form  $^{18}\text{F}_2$  *in-situ*. With tap 4 closed and taps 5-8 open, the radiolabelled gas was bubbled into a vessel of water contained in the hot cell (Figure 2.4). The total radioactivity of the resulting  $^{18}\text{F}^-$  solution was measured and an aliquot (50 MBq, ~2-3 ml) was dispensed into a glass vial, which could be placed in a lead pot for transportation back to Glasgow.



### ***Preparation of anhydrous [ $^{18}\text{F}$ ]-HF vapour***

Anhydrous [ $^{18}\text{F}$ ]-HF vapour was prepared via a fluorine exchange reaction between [ $^{18}\text{F}$ ]-CsF and anhydrous HF (Equation 2.5). Solid [ $^{18}\text{F}$ ]-CsF was prepared as follows. Solid CsOH (3 g, Aldrich Chemical Co.) was dissolved in tap water (10 cm<sup>3</sup>), to this was added a solution of  $^{18}\text{F}^-$  (2-3 ml) and aqueous HF (4 cm<sup>3</sup>, Fisher Scientific 40% assay) facilitating the neutralisation reaction. The mixture, contained in a Pyrex crystallising dish, was heated to dryness on a hotplate and white crystalline [ $^{18}\text{F}$ ]-CsF powder ( $\approx 3\text{g}$ ) loaded into a Monel

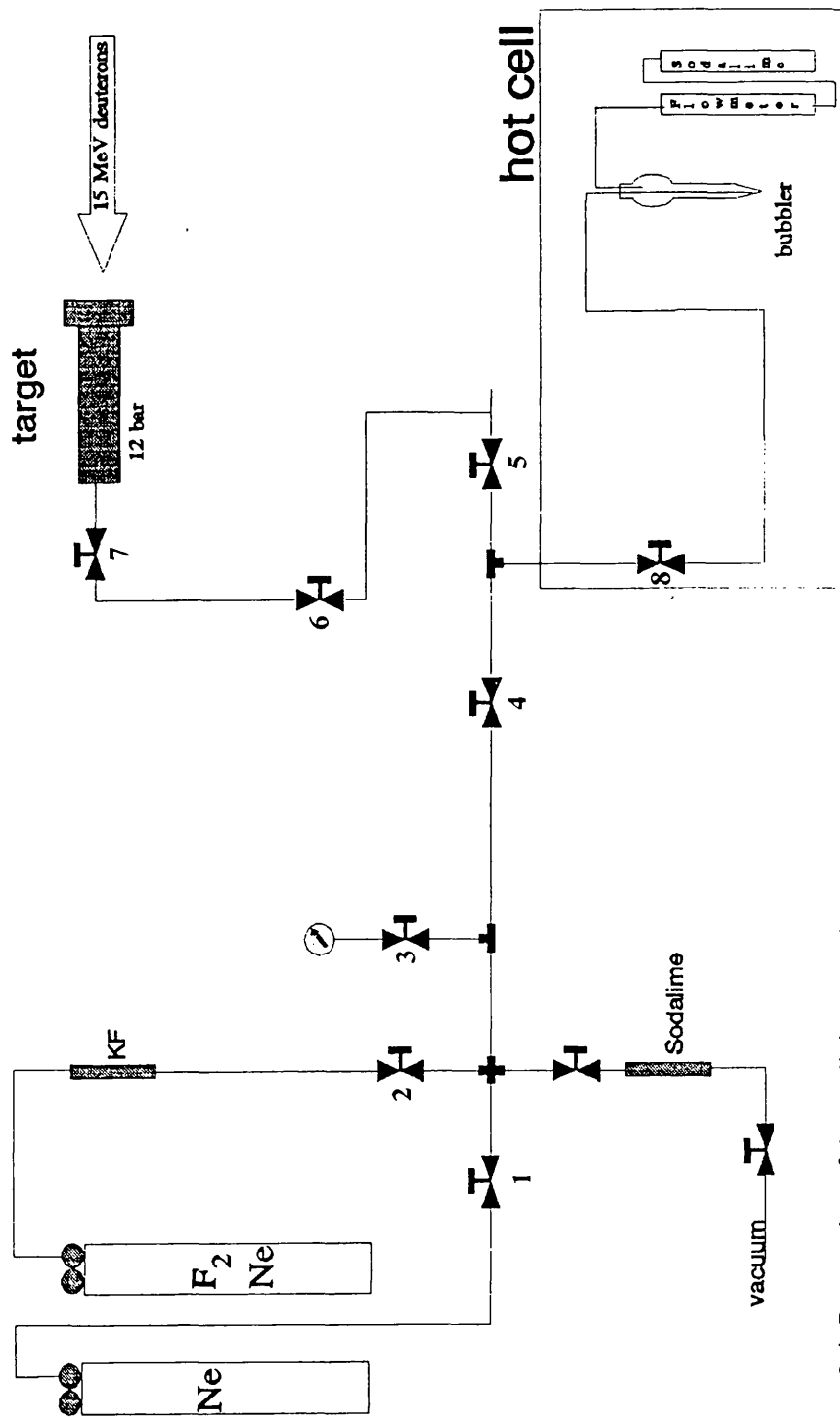
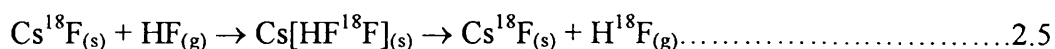


Figure 2.4 Preparation of the Radioisotope Fluorine-18

bomb. The sealed bomb was then transferred to the Monel vacuum system for handling of anhydrous HF. In a closed system HF (20 mmol) was condensed under liq. N<sub>2</sub> into the bomb which was then sealed and heated to 523 K using a wrap-round furnace. This condition was maintained for 45-60 minutes after which [<sup>18</sup>F]-HF was removed to a Monel storage bomb from where it could be dispensed conveniently in subsequent reactions.



### 2.1.9 Reactions of diamond surfaces with halogen-containing reagents

The chemical reaction of diamond with a range of halogen-containing gaseous reagents (Table 2.1) has been studied. The experimental conditions and methods of analysis that were employed are shown in table 2.3.

#### *General strategy*

A sample of diamond was loaded into a Monel reaction vessel; this procedure was generally performed in a dry atmosphere box. The box contained an analytical balance, which allowed powder samples to be weighed precisely in a dry inert atmosphere. The sealed reaction vessel was then removed to the appropriate vacuum system for gas handling. Following evacuation a pressure of gas (typically 1 atm) was admitted into the system and vessel. The reaction vessel was then isolated and the reagent remaining discarded. Alternatively, a pressure of gas was admitted to the vacuum system only and then condensed

**Table 2.3** Experimental conditions employed in the reaction of diamond with a range of halogen-containing reagents

Diamond sample	Reagent	Reaction temperature	Methods of analysis
Hydrogenated diamond powder	F <sub>2</sub>	Ambient, 300-400°C	Gas phase FTIR, DRIFTS, SEM
	ClF <sub>3</sub> HF		Gas phase FTIR, <sup>18</sup> F-radiotracer <sup>18</sup> F-radiotracer, DRIFTS
Oxygenated diamond powder	F <sub>2</sub>		Gas phase FTIR
	HF		<sup>18</sup> F-radiotracer, DRIFTS
F <sub>2</sub> -treated diamond powder*	F <sub>2</sub>		Gas phase FTIR
	HF		<sup>18</sup> F-radiotracer
ClF <sub>3</sub> -treated diamond powder*	ClF <sub>3</sub>		Gas phase FTIR
HF-treated diamond powder*	HF		<sup>18</sup> F-radiotracer
Hydrogenated diamond film	F <sub>2</sub>		Gas phase FTIR, SEM, XPS
Virgin diamond film	ClF <sub>3</sub>		Energy filtered TEM

\* Applies to hydrogenated and oxygenated powder samples

completely into the vessel. The procedure employed was dependent upon the reaction for study and the vessel in use. Liquid nitrogen (77 K) was used for condensation purposes, waste traps or a soda-lime scrubber was used for discarding unused reagent. If desired, the reaction vessel could be heated using a wrap-round furnace and the temperature monitored using a thermocouple wire and multimeter. The reaction time was 24 h except for reactions involving the radioisotope  $^{18}\text{F}$ , which due to its short half-life must be used within one working day. Analysis was performed during and after reaction using a range of techniques as outlined in table 2.3. Before analysis of the gas phase the reactor was allowed to cool to room temperature. Analysis of the solid surfaces was not always accompanied by prior analysis of the gas phase.

#### **2.1.10 Fourier Transform Infrared Spectroscopy (FTIR)**

FTIR spectroscopy was used extensively in this work for gas phase analysis following reaction between diamond and various reagents. Infrared spectroscopy is simply used and, since there are large libraries of literature spectra, product identification is possible. However, there are a number of problems associated with the use of the technique in this work; halides are susceptible to hydrolysis which may lead to ambiguous results and determination of reaction stoichiometry by this means is difficult. To exclude moisture, all samples were handled in a dry atmosphere box ( $\text{H}_2\text{O} < 5\text{ppm}$ ) and all reaction vessels were passivated as discussed in section 2.1.6. All analyses were performed in absorbance mode and identical conditions were used before and

after reaction, in this way a semi-quantitative comparison could be made providing some information as to the nature of the reaction.

An aliquot of the reaction gas phase (5-10 Torr) was sampled in an infrared cell and a spectrum collected using a Paragon 1000 FTIR spectrometer (Perkin Elmer). Initial experiments were performed using a Pyrex cell, however this was found to be subject to chemical etching, which led to unwanted peaks in the spectrum. The problem was remedied by the construction of a Monel infrared cell (Figure 2.5). Spectra were accumulated for 4 scans in the 5000-400  $\text{cm}^{-1}$  region. The key absorptions for the IR active reagents used in this work are shown in table 2.4 (95, 96).

**Table 2.4** Key infrared absorptions for the reagents used in this work (95, 96)

Reagent	$\nu_{\text{max}} / \text{cm}^{-1}$	Assignment
HF	4000.6	HF str
ClF <sub>3</sub>	761	$\nu_1(\text{ClF}) \text{ClF}_3$
	709	$\nu_2(\text{ClF}) \text{ClF}_3$

The information listed above was used to aid the assignment of bands in the infrared spectra recorded following reaction of the appropriate reagent with a diamond sample.

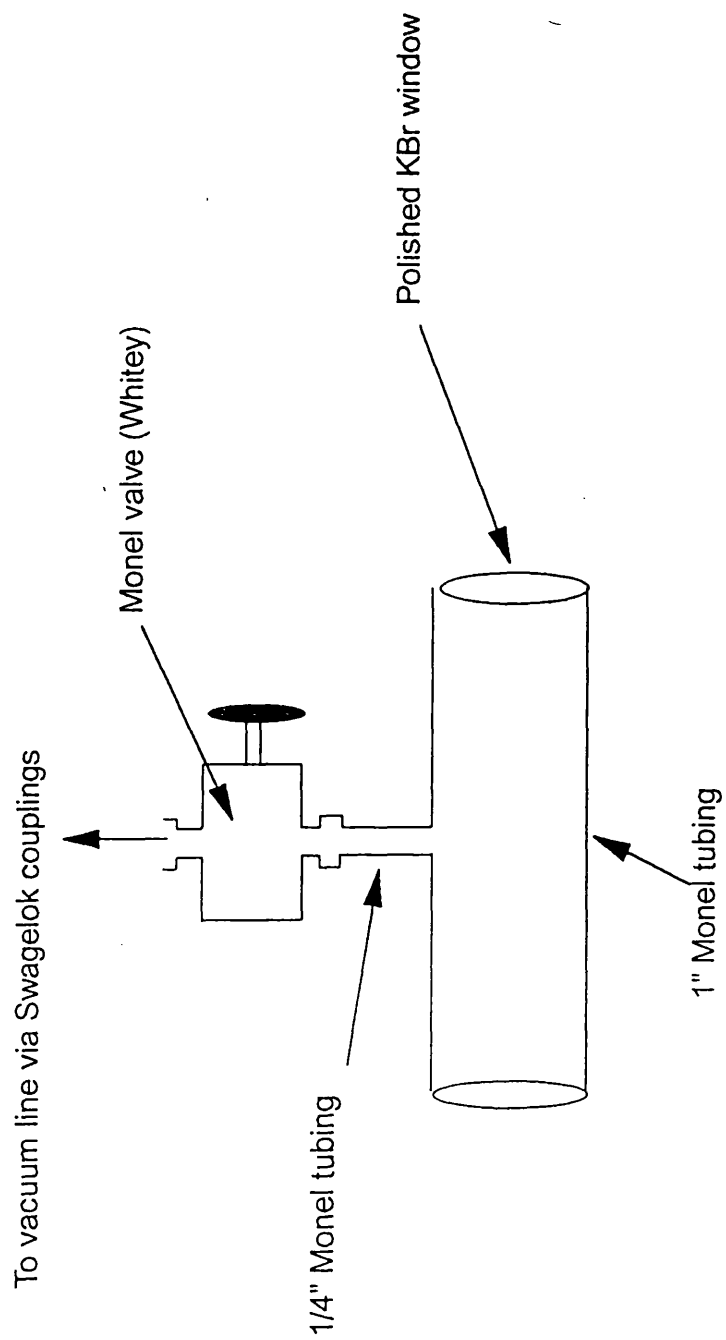


Figure 2.5 Monel infrared cell

### **2.1.11 Characterisation and analysis of diamond surfaces following reaction with halogen-containing reagents**

#### ***Diffuse Reflectance Infrared Fourier Transform Spectroscopy (DRIFTS)***

DRIFTS has been used to study the surfaces of a range of chemically treated diamond powders, proving to be a useful way of characterising the diamond surface before and after reaction with fluorine-containing compounds. The technique involves detection of scattered infrared radiation from a substrate surface (69) in contrast to transmission spectroscopy where the radiation passes through the sample. Scattered radiation is very diffuse and hence a very sensitive method of detection is required.

In this work DRIFT spectra were collected on a Magna 550 infrared spectrometer (Nicolet) equipped with an MCT (Mercury Cadmium Telluride) detector cooled in liq. N<sub>2</sub> to prevent burn out. The powder sample for analysis was loaded into a sample cup before placement on a mounting block contained within the beam compartment. Radiation that was reflected without penetrating the sample surface was prevented from reaching the collection mirror by a beam blocker B (figure 2.6). Spectra were accumulated from 60 scans in the 4000-400 cm<sup>-1</sup> region.

### *Surface area determination*

The B.E.T surface areas of selected diamond powder samples were determined. The diamond sample (0.1g) was predried in flowing N<sub>2</sub> (48 h, 383 K) and N<sub>2</sub> adsorption at 77 K measured using a Gemini 1275 analyser (Micrometrics). The saturation pressure, P<sub>0</sub>, was determined prior to each analysis. The free space (Figure 2.7) is determined by dosing the sample tube and a reference tube, of identical dimensions, with Ne and comparing the saturation volumes. This procedure minimises error. The raw data was processed by a computer program named Stardriver, which uses a transformation of the BET equation (97) to calculate the volume of N<sub>2</sub> adsorbed on the diamond surface at a range of relative pressures (equation 2.6). This yields an adsorption isotherm, which can be converted into a BET surface area plot from which the surface area of the sample can be calculated using equation 2.7. A typical surface area plot is shown in figure 2.8.

$$V_A = (P/P_0)/(1-P/P_0)(N_{ADS}) \dots\dots\dots 2.6$$

Where, V<sub>A</sub> is the volume of N<sub>2</sub> adsorbed per gram of sample (cm<sup>3</sup> g<sup>-1</sup>), P/P<sub>0</sub> is the relative pressure and N<sub>ADS</sub> is the amount of gas adsorbed (cm<sup>3</sup> STP).

$$SA_{BET} = CSA (6.023 \times 10^{23})/(22414 \text{ cm}^3 \text{ STP})(10^{18} \text{ nm}^2/\text{m}^2)(S + Y_{INT}) \dots\dots\dots 2.7$$

Where, CSA is the analysis gas molecular cross section (0.162 nm<sup>2</sup> for N<sub>2</sub>), S is the slope of the BET surface area plot (cm<sup>3</sup> g<sup>-1</sup>) and Y<sub>INT</sub> is the y-axis intercept.

It was also possible to measure pore surface area for selected powder samples. The desorption of adsorbed N<sub>2</sub> was monitored over a range of relative pressures. The radius of a pore is related to the relative pressure by the relationship given in equation 2.8, which was first developed by Kelvin (98). The Stardriver program uses a transformation of this equation, developed by Barrett, Joyner and Halenda (99) (BJH), which accounts for the adsorption of a layer of gas on the wall of the pore.

$$R_c = -A/(1 + F)\ln Pr \dots\dots\dots 2.8$$

Where, R<sub>c</sub> is the radius of the pore core, A is an adsorbate property factor (fixed value of 9.53 for N<sub>2</sub>), F is the fraction of pores open at both ends (assumed to be zero for desorption) and Pr is the relative pressure.

In a similar way to the BET calculation, the surface area of the pore could be calculated. The procedure was repeated over a range of relative pressures, which allowed a cumulative pore area to be obtained.

***Scanning Electron Microscopy (SEM)***

Scanning Electron Microscopy is a high-resolution technique, which can provide topographical information, making it a useful tool in the examination of rough surfaces. An electron beam (20 keV) is generated at the top of an evacuated column (10<sup>-5</sup>-10<sup>-6</sup> Torr) and focussed to a fine point on the sample by a series of condenser lenses. An electron beam interacts with matter in a number of ways

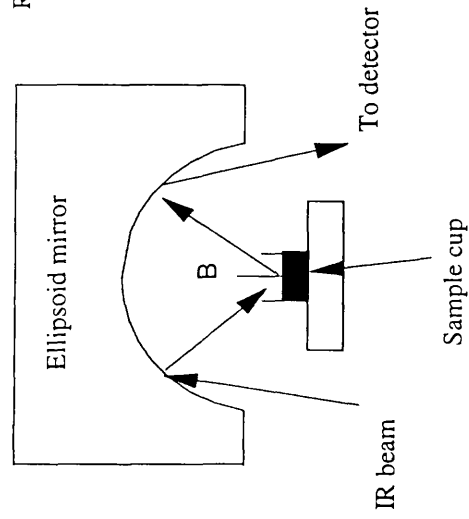


**Figure 2.6** DRIFTS analysis

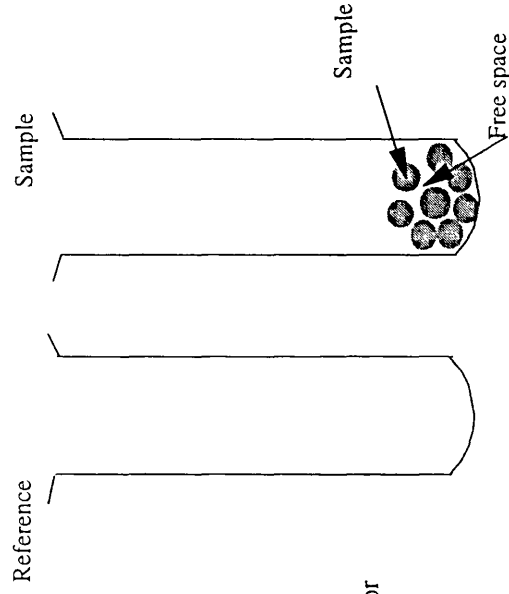


**Figure 2.7** Surface area analysis

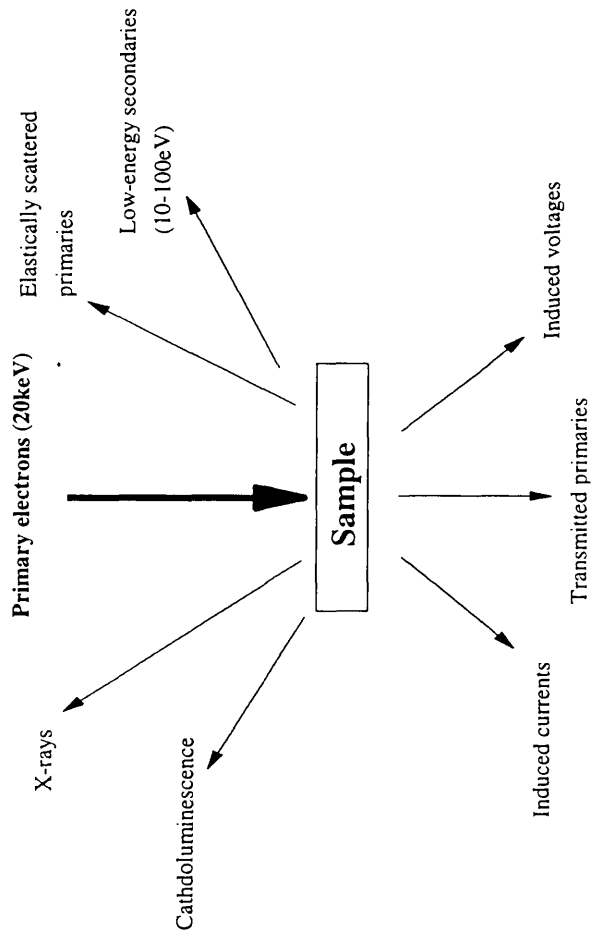


**Figure 2.9** Interactions of electrons with a solid surface

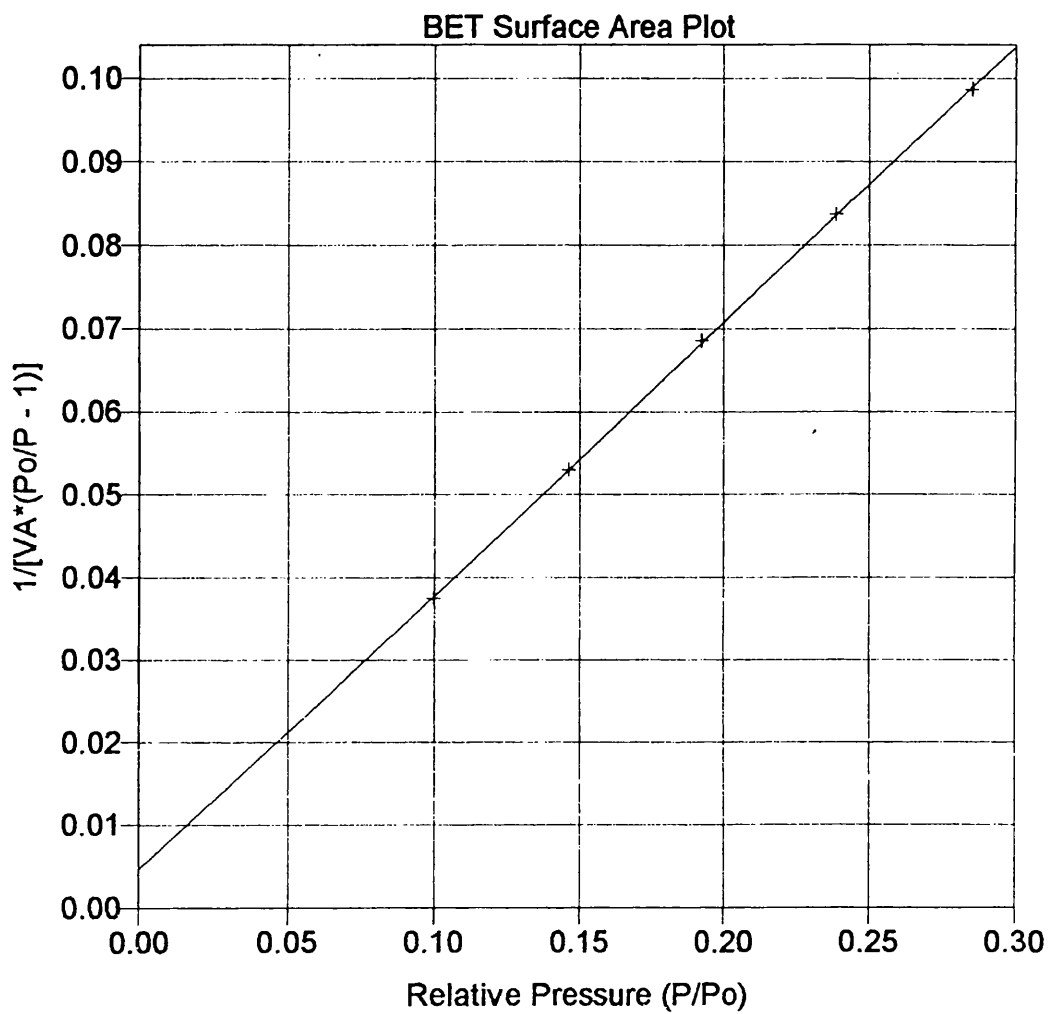


**Figure 2.8** BET adsorption isotherm obtained in the surface area determination of a diamond powder sample

(Figure 2.9) producing a range of signals (100). It is the low energy (10-100 eV) secondary electrons, which provide the topographical information of interest here. These electrons are subjected to a voltage bias, which attracts them towards a scintillation detector. The detected signal is then amplified to produce a cathode ray spot, which can be viewed on a TV monitor. To form an image of the sample the electron beam is swept or scanned across the surface in a rectangular array called a raster. A signal is recorded for each point in the array and the image formed. Since the cathode ray spot is considerably larger than the raster the image that appears on the screen is magnified. Varying the dimensions of the rectangular array that forms the raster can alter the magnification.

SEM has been used in this work to examine the surface morphology or topography of diamond film and powder before and after reaction with  $F_2$  at ambient and elevated temperatures (573- 673 K). Since diamond has insulating properties, charging of the sample in the electron beam can occur. To prevent this, the samples were coated with a thin layer of gold. The diamond sample was mounted on an aluminium stub using a piece of conductive carbon tape and then loaded into the vacuum chamber of the microscope (Phillips 515 SEM) for analysis.

### ***Electron Energy Loss Spectroscopy (EELS) and Energy Filtered Transmission Electron Microscopy (EFTEM)***

Conventional electron imaging and diffraction methods utilise elastically scattered electrons, which occur when the incident electron is attracted to the nucleus by coulombic forces. The collision between a high-energy electron and

a specimen may also result in inelastic scattering of the incident electron. Inelastic scattering can occur when the incident electron interacts with an atomic core level causing the excitation of a core electron to the lowest unoccupied state. This excitation or transition is only possible if the incident electron provides sufficient energy. Therefore, by measuring the energy of the incident electron following interaction with the specimen, the amount of energy lost can be determined. This forms the basis of electron energy loss spectroscopy or EELS. Core electrons are sensitive to the size of the nuclear charge and also to the bonding environment. The size of the nuclear charge varies with the atomic number of the scattering atom hence EELS provides information on the elemental composition of the specimen. In addition, the number of transitions possible will depend on the local bonding environment. In this work the specimen is diamond film and the electronic transitions of interest are given in equations 2.9 and 2.10.

$$C(1s) \rightarrow \sigma^* (sp^3 \text{ hybrid orbitals}) \dots\dots\dots 2.9$$

$$C(1s) \rightarrow \pi^* (sp^2 \text{ hybrid orbitals}) \dots\dots\dots 2.10$$

These transitions require energies of 300 eV and 280 eV respectively (101) and the potential to differentiate between diamond and graphite is quickly realised. Typical energy loss spectra for diamond and graphite are shown in figure 2.10, which illustrates the sensitivity of the technique to bonding environment. Electron energy loss spectroscopy has been used (102) successfully to determine the  $sp^3/sp^2$  ratio of hydrogenated diamond like carbon film (H-DLC) and hence the effectiveness of the hydrogenation treatment. If the inelastically scattered

electrons are used in a transmission electron microscopy experiment it becomes possible to form an image of the specimen which is directly related to the energy lost by the scattered electrons and hence the bonding levels present. An energy filter can be used to select a narrow energy range, typically 5 eV in width, making it possible to image specific regions of the energy loss spectrum and produce bonding level maps. This is the basis of energy filtered transmission electron microscopy (EFTEM). The technique has been used to study the carbon bonding at the carbon-silicon interface of CVD-grown diamond films supported on silicon in an attempt to understand the nucleation process (103). The study revealed that diamond nucleates on a thin layer of amorphous carbon less than 1nm thick.

In the present study it was of interest to examine diamond samples before and after chemical reaction to determine if a change in bonding was a feature of the reaction.

Data were acquired for two diamond film samples, an as-grown sample and a chemically treated ( $\text{ClF}_3$ , 623 K, 24 h) sample. Back ion milling in an  $\text{Ar}^+$  beam was used to reduce the sample thickness from 20  $\mu$  to 0.1  $\mu$  making them suitable for TEM. The images were collected using a CM20 FEG-TEM (200 keV accelerating voltage, Materials Technology Laboratory, NRCan, Ottawa) equipped with a gatan image filter or GIF. The window size was 5 eV and could be centred on 284 eV for mapping  $\text{sp}^2$  or 303 eV for mapping  $\text{sp}^3$  bonding as illustrated on figure 2.10. A high quality diamond film should be free of  $\text{sp}^2$  bonding except perhaps at surface defects such as grain boundaries. To

investigate this the images were acquired at a grain boundary and at the edge of a grain.

### *X-ray Photoelectron Spectroscopy (XPS)*

X-ray photoelectron spectroscopy is one of the most widely used surface analytical techniques involving the measurement of electrons. This is due to its sound theoretical basis and high information content. The technique involves the interaction of an X-ray photon with a specimen, which can have a number of outcomes, including emission of a photoelectron, Auger electron and X-ray emissions. It is the photoelectric effect, which is of interest here; this occurs when the total energy of the X-ray photon is transferred to a core electron causing it to be ejected into the vacuum level. The ejected electron is termed a photoelectron. This is the noteworthy difference between XPS and EELS where the core electron is excited to an unoccupied state but not as far as the vacuum level. The result of the XPS experiment is atomic ionisation, which requires a supplied energy greater than the binding energy ( $E_B$ ) of the core electron, which is given by equation 2.11 where,  $h\nu$  is the energy of the X-ray photon and KE is the kinetic energy of the photoelectron.

$$E_B = h\nu - KE \dots\dots\dots 2.11$$

In the XPS experiment KE is measured and  $h\nu$  is known, hence  $E_B$  is easily determined. The size of  $E_B$  is dependant upon both initial and final state effects. Initial state effects occur because the size of the nuclear charge and the chemical

environment of the atom in question influence the size of  $E_B$ . Consider a carbon atom and compare the  $C_{1s}$  binding energy when bonded to hydrogen with that when bonded to fluorine or oxygen as shown in table 2.5.

**Table 2.5**  $C_{1s}$  binding energies for C-H and C-F functional groups (69)

Functional group	$E_B$ (eV)
C-H	285.0
C-F	287.8
C=O	288

This difference in  $E_B$  is termed a binding energy or chemical shift and results from the fact that, for C-F when compared with C-H, there is an increased effective charge ( $Z_{eff}$ ) per electron in the  $C(1s)$  shell. These electrons are held more tightly to the nucleus and more energy is required for their ejection. The potential of XPS to monitor chemical changes as a result of fluorination reactions is quickly realised.

Processes which occur during and after the photoemission, can also affect the binding energy of the core electron; such effects are termed final state effects. The most important of these are relaxation and shake-up transitions. Relaxation occurs after the photoemission when electrons from neighbouring shells and atoms rearrange to shield the core hole, shake-up transitions result when the photoelectron loses some energy to a valence electron and causes it to be excited

into an unoccupied level e.g.  $\pi \rightarrow \pi^*$ . In this work initial state effects are of greatest importance but final state effects must be born in mind when performing data analysis.

It was stated earlier that XPS is a surface technique, this is because only electrons that have escaped from the specimen without any loss in energy contribute to the photoemission, bulk photoelectrons are absorbed by the material and never reach the detector. The average depth from which an electron of a given kinetic energy will escape without any loss in energy, due to inelastic collisions, is given by the inelastic mean free path (IMFP) (101) as shown in figure 2.11. It can be seen that the inelastic mean free path for an electron from the C(1s) shell is approximately 8 angstroms. Consequently, in the analysis of carbon-based materials, to a first approximation, the C(1s) photoemission peak represents information obtained from a sampling depth of at least 8 angstroms. It should be noted that the IMFP for an electron in matter and hence the XPS sampling depth, varies according to the energy of the electrons, the instrument used to perform the analysis and the nature of the sample. An estimate of the IMFP value can be obtained using the relationship given in equation 2.12 (104).

$$\text{IMFP} (\lambda) = 538\text{KE}^{-2} + 0.41(a\text{KE})^{0.5} \dots\dots\dots 2.12$$

Where, KE is the electron kinetic energy (eV) and a is the monolayer thickness (nm) of the material for analysis.

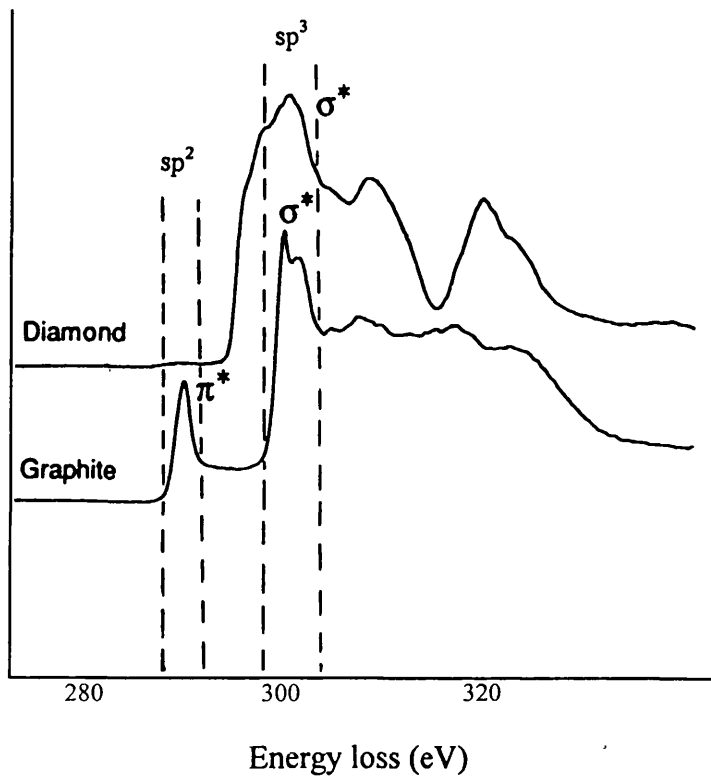


Figure 2.10 Carbon K-edges for diamond and graphite, illustrating regions for EFTEM

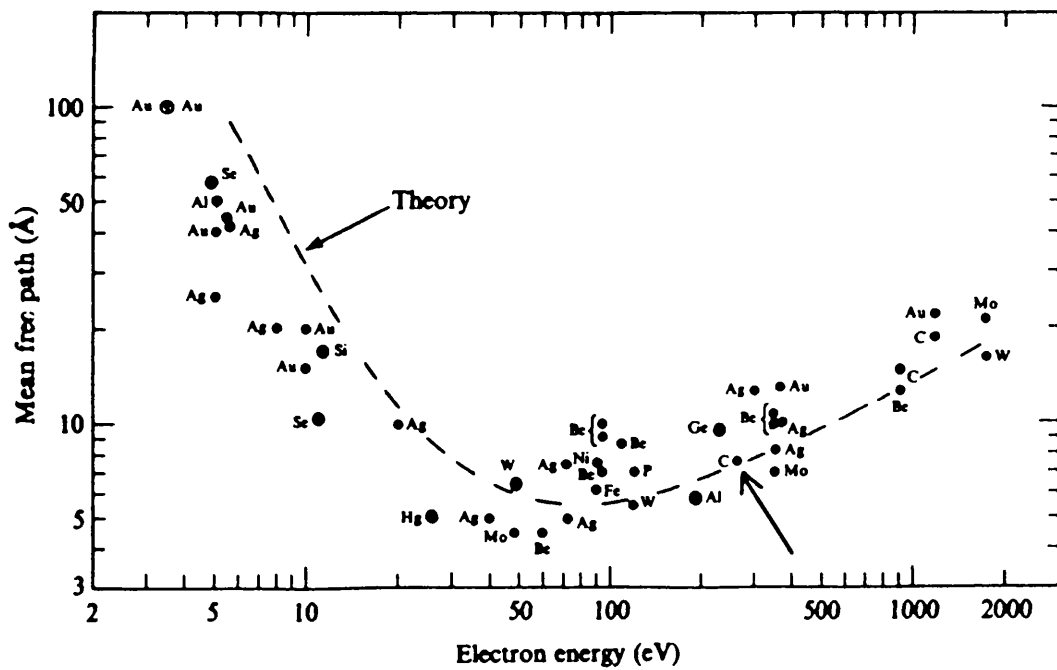


Figure 2.11 Inelastic mean free path (IMFP) of an electron in matter

In this work three diamond film samples, a reference (hydrogenated only) and two which had received a fluorination (1. F<sub>2</sub>, RT, 1 atm, 24 h & 2. F<sub>2</sub>, 523 K, 1 atm, 24 h), were studied using XPS. The fluorinations were performed in a vessel similar to that described in section 2.1.5, except that a Teflon sample boat was used. This was to ensure that contamination of the samples with NiF<sub>2</sub>, even at microscopic level, did not occur. The surface structure properties of the diamond samples were investigated using a VG HB 100 UHV SEM system equipped with XPS facilities (University of Dundee). The specimens were irradiated with an X-ray source (Mg K $\alpha$  line 1256.60 eV) and the ejected photoelectrons analysed by a hemispherical electron energy analyser. In order to calibrate the instrument, the specimens were flash coated with gold and the gold 4f<sub>7/2</sub> (83.8 eV) and 4f<sub>5/2</sub> (87.5 eV) photoelectron lines used as a reference.

In order to maximise the information extracted from the XPS spectrum, the area and binding energy ( $E_B$ ) of each subpeak for a given core electron must be determined. The raw data obtained in the XPS experiment represents information from a number of individual monolayers, which may be chemically or structurally distinct. The subpeaks are rarely completely resolved in the raw spectrum and peak fitting is required. In this work raw data were fitted using a peak fitting module, available with Origin data analysis and graphics packages (Microcal<sup>TM</sup> Software, Inc.). The important parameters in the peak fitting process are: peak shape, peak position, peak height and peak width. Initially, upon inspection of the raw data, these parameters are estimated and then refined using a least-squares, iterative fitting routine. In this work a gaussian peak shape

was used and the peaks were fitted to the same width, in accordance with other XPS studies of fluorinated carbon materials (105-109).

When a quality fit of the raw XPS data has been obtained, it is possible to quantify the amount of each element present in the XPS sampling region of the sample surface. The relationship used to do this is given by equation 2.13, a complete derivation of which can be found elsewhere (69).

$$\%n_i = (I_{ij}/\sigma_{ij}KE^{0.7})/\Sigma(I_{ij}/\sigma_{ij}KE^{0.7}) \times 100 \dots\dots\dots 2.13$$

Where,  $n_i$  is the concentration of element  $i$ ,  $I_{ij}$  is the intensity or area of peak  $j$  from element  $i$ ,  $\sigma_{ij}$  is the photoionisation cross-section of peak  $j$  from element  $i$  and  $KE$  is the kinetic energy of the photoelectron.

In this work the elements of interest are carbon and fluorine for which  $\sigma$  is 1 and 4.43 respectively (110). The factor of  $n$  on  $KE^n$  is termed the instrument factor and accounts for variations in the sensitivity of the electron detector for different instruments. A range of  $n$  values have been calculated for various instruments (111), in this work a VG 100 analyser was used, for which the appropriate  $n$  value is 0.7. The total area of the fitted subpeaks in the binding energy envelopes for C(1s) and F(1s) is obtained by integrating the area of each subpeak and calculating the summation. Integration of subpeaks is a routine analytical function available with the data-handling and graphics package used in this work.

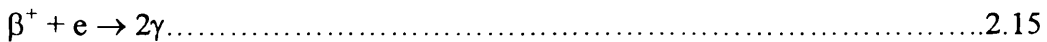
Using equation 2.13, a carbon/fluorine ratio on the surface zone of the sample can be obtained, providing information on the extent of fluorination. The method has been used to characterise the surface structure, in terms of fluorine content of many carbon-fluorine materials, such as fluoropolymers, graphite fluorides, fluorinated carbon fibres and fluorinated carbon black (105-109). In addition estimates of oxygen (112) or fluorine (113-117) on monocrystalline silicon or gallium arsenide surfaces have been made using this method.

### *Radiochemical studies*

Radioisotopes such as chlorine-36 ( $^{36}\text{Cl}$ ) and fluorine-18 ( $^{18}\text{F}$ ) have been used successfully to probe the interaction of halogenated compounds such as hydrogen chloride or fluoride with catalyst surfaces (118, 119). The information obtained has proved very useful in determining reaction pathways and in characterising catalyst surfaces with implications for catalyst activity. In this work the radioisotope  $^{18}\text{F}$ , prepared as outlined in section 2.1.8, has been used extensively to investigate the reaction of HF with diamond and study the effect, if any, of chemical changes on the diamond surface.

### *$\beta^+$ -Decay*

Fluorine-18 decays by the emission of  $\beta^+$ -radiation (equation 2.15) which undergoes annihilation with electrons to produce  $\gamma$ -radiation (equation 2.16) with an energy of 0.511 MeV and a half-life of  $109 \pm 0.6$  min (120).



***Scintillation counting (121)***

Gamma radiation is most effectively measured using a scintillation counter. The gamma ray photon interacts with a crystal of sodium iodide producing a photoelectron. As the photoelectron moves through the crystal lattice it causes ionisation and, in turn, the production of visible light photons or scintillations. When these scintillations converge on a photocathode, electrons are released, these electrons are then amplified by a factor of  $10^4$ - $10^7$  and a voltage pulse is produced at the anode. A scalar ratemeter records the voltage pulse with a magnitude proportional to the energy of the initiating photon or  $\gamma$ -radiation. Radiochemical counts were accumulated using a NaI/Tl (0.1-0.2% Tl) crystal scintillation counter housed in a lead well and wired to a scalar ratemeter. The ideal operating voltage for the ratemeter was determined by monitoring counts from a  $\text{Cs}^{137}$  sample whilst varying the applied voltage. The resulting  $\gamma$ -ray spectrum with a maximum at 541 V is shown in figure 2.12. The operating voltage was accordingly set at 541 V and this condition was maintained for all radiochemical-counting experiments.

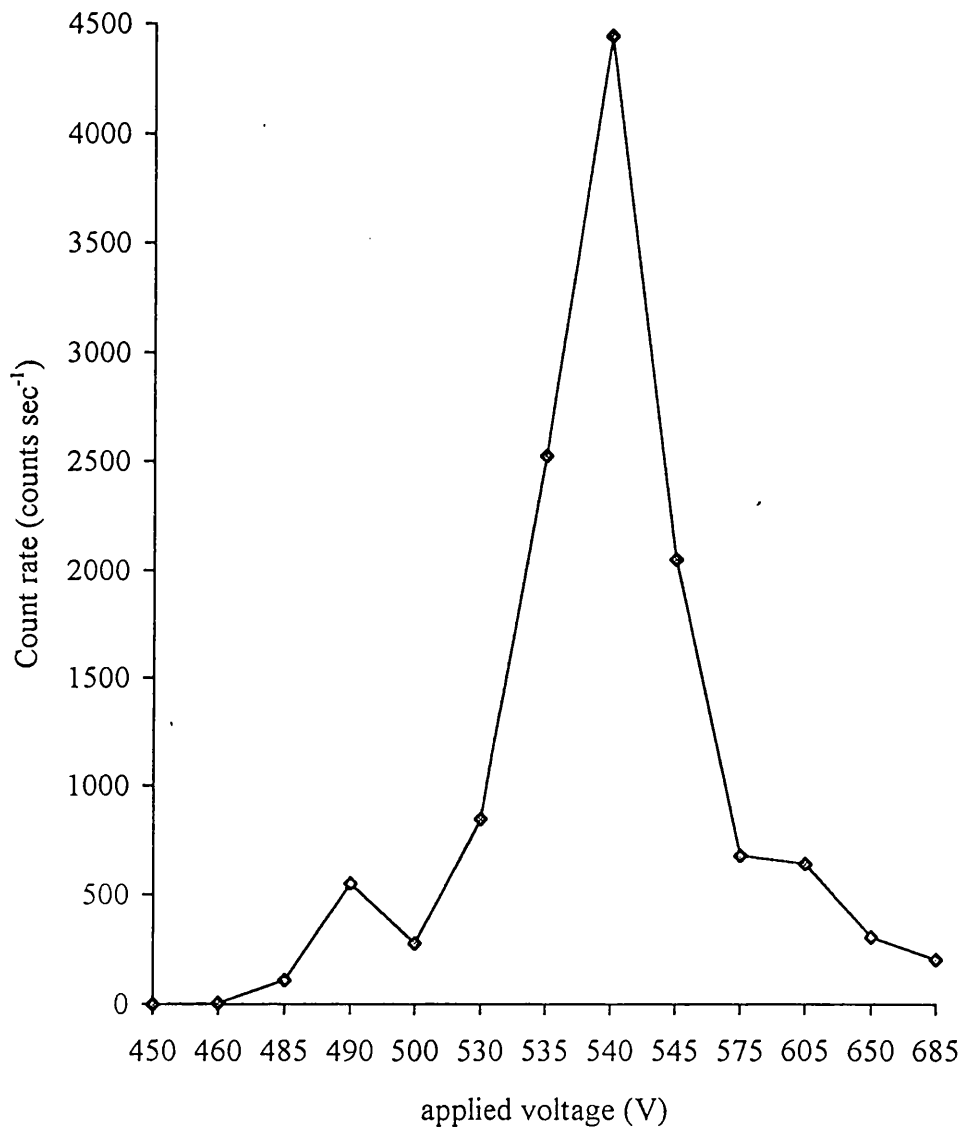


Figure 2.12  $\gamma$ -ray spectrum for Cs<sup>18</sup>F

### *Specific Activity*

This is the measured activity of a known quantity (e.g. 1 mmol) of radiolabelled material and is expressed as a count rate per millimole ( $\text{count sec}^{-1} \text{mmol}^{-1}$ ). The specific activity of as prepared  $\text{H}^{18}\text{F}$  was determined by absorbing a measured quantity of the vapour on to a solid sample of caesium fluoride. Caesium bifluoride is formed according to equation 2.5 and the resulting radiolabelled solid can be counted more efficiently than a liquid or gas.

Caesium fluoride (0.5 g) was loaded into a PTFE/FEP tube vessel (figure 2.13) which was evacuated overnight following attachment to the vacuum system for handling HF. A measured pressure of HF (142 torr, 1 mmol) was condensed on to the CsF under liq  $\text{N}_2$ . After warming to room temperature, the vessel was removed to the well counter where the solid was counted for a given time (60 sec). The procedure was repeated several times during the experimental day to ensure reproducible measurement. Typically, a specific activity of 500-1000  $\text{count sec}^{-1} \text{mmol}^{-1}$  was obtained. Determination of  $\text{H}^{18}\text{F}$  specific activity before reaction allows quantitative measurement of the radiochemical uptake on the diamond surface and provides information about the reaction stoichiometry.

### *Experimental procedure for the reaction of $\text{H}^{18}\text{F}$ with diamond powder*

In a dry atmosphere box, diamond powder (1 g, 1  $\mu\text{m}$ ) was loaded into a Monel bomb and removed to the Monel vacuum line for handling HF. Following evacuation and in a closed system  $\text{H}^{18}\text{F}$  (500 Torr, 3.5 mmol) was condensed

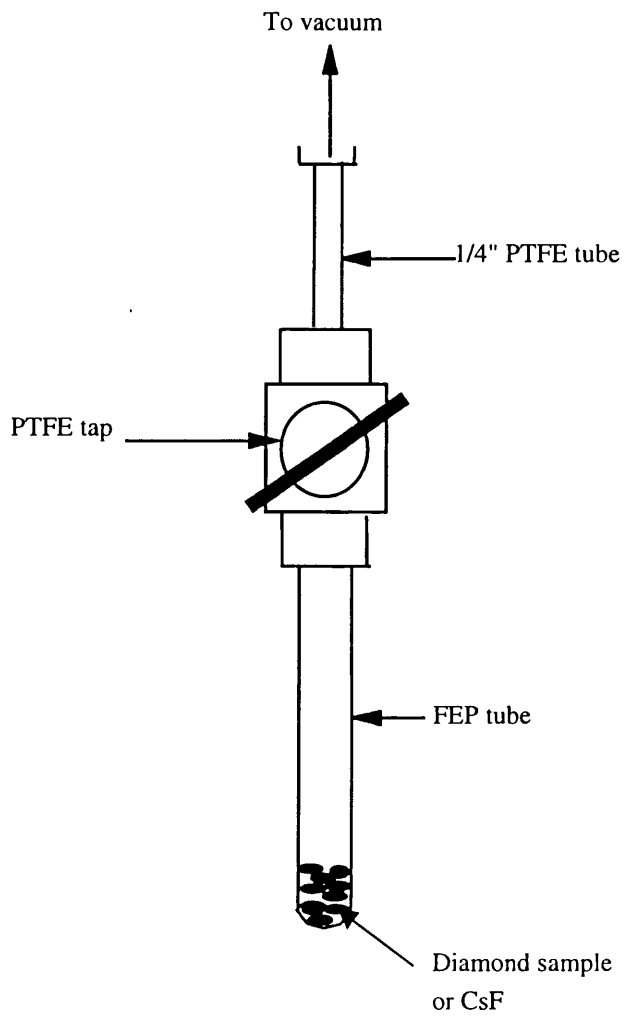


**Figure 2.13** PTFE/FEP tube vessel for measurement of  $\text{H}^{18}\text{F}$  specific activity and the  $^{18}\text{F}$  activity of diamond samples after exposure to  $\text{H}^{18}\text{F}$

onto the diamond sample and the sealed bomb allowed to warm to room temperature. Using a wrap-around furnace the bomb could be heated and the temperature monitored using a thermocouple wire and multimeter. The reaction was studied at ambient temperature and 573 K for a range of diamond samples as outlined in table 2.3. The reaction time was 45 minutes allowing 4-6 experiments to be performed in a working day before the activity of the  $H^{18}F$  was reduced to unusable levels. Following removal of unreacted  $H^{18}F$  to a waste bomb under static vacuum, the reaction vessel was removed from the vacuum line and the powder sample tipped into a weighed FEP tube which could be reattached to the PTFE part (figure 2.13) and conveniently placed in the well counter. Radiochemical counts were accumulated over a period of 60 s or until 10,000 counts had registered. The FEP tube could be reweighed easily allowing the sample weight to be determined. All counts were corrected for background and radioactive decay.

***Decay correction and statistical error***

As a consequence of the relatively short half-life ( $t_{1/2} \approx 110\text{min}$ ) of fluorine-18 all experimental count rates were corrected for radioactive decay using equation 2.17.

$$A_t = A_0 e^{-\lambda t} \dots\dots\dots 2.17$$

Where,  $\lambda = \ln 2/t_{1/2}$ ,  $t$  is the decay time,  $A_t$  is the activity at time  $t$  and  $A_0$  is the activity at time zero. Time zero is the time at which the first radiochemical count of the experimental day was measured, i.e. the specific activity measurement.

Radioactive decay is a random process; this means that the number of radioactive disintegrations in a given time is not constant. The standard deviation on a radiochemical count is described by equation 2.18 (122), where  $n$  is the number of counts.

$$\sigma_{s,D} = \pm\sqrt{n} \dots\dots\dots 2.18$$

## 2.2 Physical modification of diamond surfaces

This section outlines the general experimental procedures that were used in the investigation of polishing of CVD-grown, polycrystalline diamond film. As will be discussed further in the next chapter, the experimental procedures were subject to continual development to cope with process problems or to improve the efficiency of the process. The techniques used in the analysis of the diamond surface, following polishing, were not subject to change and these are described here.

### 2.2.1 Polishing experiments

Before a polishing experiment it was necessary to mount the diamond sample on a flat metal puck for use on the polishing machine. Two types of bond were used, these were a soft wax or an epoxy resin. Often the epoxy resin was used when the soft wax bond had been compromised during the experiment. In both cases the diamond sample was fixed and pressed on to the puck and the bond heat cured on a hotplate. The diameter of the sample puck used was dependent on the complexity of the experiment that was to be performed. Large pucks could be placed directly on to the polishing machine. However, if more precise control over the sample height and loading was required a smaller puck, which could be fixed to a polishing jig (figure 3.6) was used. When using a polishing jig the diamond sample/ puck assembly was mounted on the vacuum chuck face of the jig, which could then be raised or lowered. This offered variation in the position of the sample relative to the plate, which has proved important in the success of lapping or polishing methods for semiconducting materials such as GaAs.

Polishing of the diamond film samples was investigated on Logitech polishing equipment. Two machines were used in this work; these were the LP40 and CP3000. Both machines were of similar design, consisting of a polishing plate, which could be revolved at speeds varying from 0-300 rpm. Most of this work was performed on the LP40 machine (figure 3.7), however the CP3000, which was constructed from plastic components, was used when corrosive reagents were involved. The LP40 was equipped with an autofeed cylinder, which could

be used to deliver the abrasive mixture to the plate, whilst for experiments using the CP3000, the reagents were normally added via a plastic dropping funnel.

A range of polishing plate materials were available for use in this work, traditional lapping or polishing processes for diamond film use a cast iron plate, which, when used with diamond grit as abrasive, develops a diamond skin which removes material from the sample surface.

There are a number of variables available in a polishing experiment and a balance, which offers good process condition and high polishing rate, is normally required. As described in section 1.3.1, for abrasive polishing methods these are, the abrasive particle size, the rate at which the abrasive is delivered, the plate speed, the applied load or pressure on the sample and the temperature. In this work variations in these parameters were investigated when it was deemed necessary to improve the process conditions in an attempt to improve the polishing rate.

### **2.2.2 Analysis of the diamond surface after polishing**

After a polishing experiment the morphology of the diamond surface was investigated for evidence of smoothing using a Zeiss optical Nomarski microscope. The microscope was used in normal light reflectance mode for the detection of polished peaks or pits on the diamond surface. A polaroid camera which could be placed at the top of the microscope, was used to record images when an interesting effect was observed.

Profilometry techniques (123) were used to evaluate the roughness of the diamond surface. The method involves measuring the vertical displacement of a diamond stylus tip as it moves across the sample surface; a picture of the surface topography emerges. In the course of this work two profilometers were used, these were the Rank Hobson Taylor talystep, precision  $\pm 10\%$  and the Dektak surface profiler, precision  $\pm 5\%$ . Both instruments used a stylus tip with a diameter of  $12\ \mu\text{m}$ . The average surface roughness  $R_a$ , which is the root mean square of the sizes of peaks and troughs over a certain distance of the surface, was evaluated. The magnification of the instrument could be varied, allowing examination of larger or smaller features. The information that is obtained is not an absolute measurement of the surface roughness, because the diameter of the stylus tip usually exceeds the peak to valley distances, except when the surfaces are very rough. This limitation is especially true for surfaces believed to be smooth on the nanometre scale. For this reason the values obtained are usually used for comparative purposes only, where they are a good indication of the effectiveness of a particular polishing regime.

## CHAPTER 3 RESULTS

### Physical modification of diamond surfaces

#### 3.0 Introduction

A study into the polishing of CVD grown diamond film has been undertaken; the results that were obtained are described in this chapter. In accordance with the aims of this work (chapter 1.4) the starting point was to investigate the polishing of diamond film by traditional abrasive methods and assess the effects of surface modification, by chemical means, prior to polishing. The potential for polishing diamond film by chemomechanical processes, which are desirable alternatives to abrasive methods, could then be evaluated.

It was always recognised that the development of a commercially viable, chemomechanical polishing process for diamond film was a great challenge and possibly outwith the scope of this project. When compared with silicon and gallium arsenide, which can be polished successfully by chemomechanical methods (43-45), diamond is known to be much less reactive. Therefore developing a chemical process for modifying the diamond surface, which is effective under polishing conditions, is inherently difficult. Instead, this study, which was conducted in tandem with an investigation of diamond surface chemistry (chapter 4), focussed on broadening our understanding of diamond polishing and chemistry and examining the use of chemical reagents in polishing

situations. This represents the first step in the development of a new process and is therefore of great value.

The polishing studies performed in this work followed a general cycle, which is shown in figure 3.1.

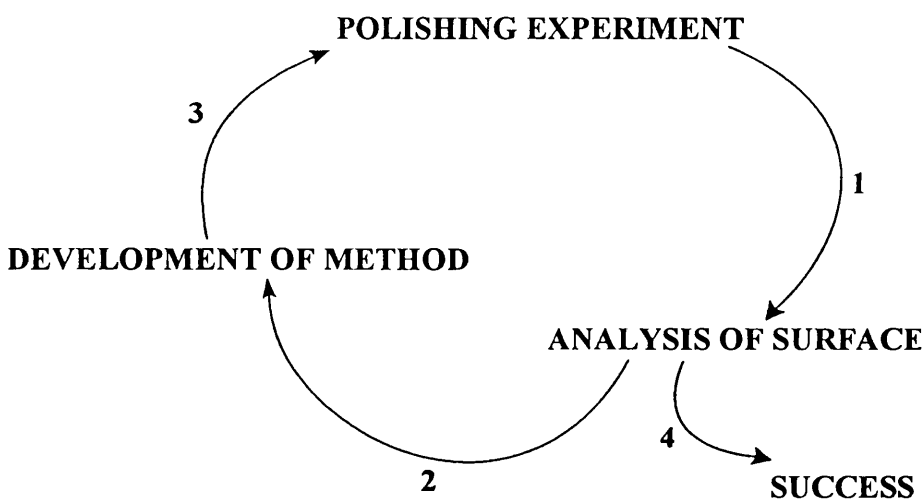


**Figure 3.1** The polishing cycle

Following a short (45-60 min) polishing experiment (step 1) the diamond surface was examined for significant polishing effects such as a local brightening of the surface and/or a reduction in surface roughness. The analyses (step 2) were performed using the microscopy and profilometry techniques described in chapter 2 (section 2.2). In the event of a negative result, the parameters of the experiment were altered (step 3) and the process of polishing and analysis repeated. The range of variable parameters has also been described in chapter 2 (section 2.2).

If there was evidence that the experiment had been successful the method was pursued with a number of possible outcomes:

1. The polishing effect could be repeated to produce a completely polished sample.
2. The polishing effect could be repeated to a limited extent producing a sample that contained polished areas.
3. The polishing effect could not be repeated.

Point 1 would lead to the development of a process which, depending on other factors such as running costs, could be commercially viable. As mentioned already, achieving this was thought to be beyond the scope of this project.

It was more likely that point 2 or 3 would occur; in either case the implication was a new development phase which might be followed by further examination of the process.

The results of polishing experiments using a range of methods are presented below, as already indicated, development of the methods employed was an integral part of this study; the key developmental steps taken and the reasons behind them are also discussed.

Initial experiments were performed on the non-growth or substrate side of the diamond sample; this allowed the surface roughness before and after the experiment to be measured using profilometry. If a successful regime could be

found a progression to experiments on the rougher, growth side of the sample was envisaged.

### 3.1 Abrasive polishing of chemically oxidised diamond film

This was the starting point of the study, designed to assess the effect of surface modification, by aggressive chemical reaction, prior to polishing by traditional abrasive methods. The experimental procedures involved for both chemical pretreatment and abrasive polishing have been described in chapter 2, sections 2.1 and 2.2 respectively. Typical profilometry results after 60 minutes abrasive polishing for a number of diamond samples (approximate dimensions: 1.25 cm x 1.25 cm x 0.5 mm) are given in table 3.1; in addition the observations made using the light microscope are described.

**Table 3.1** Surface profilometry data for a number of diamond film samples polished using a traditional abrasive method

Sample number/ Pretreatment conditions	Mean surface roughness* (Ra)/ nm	
	Before polishing expt.	After polishing expt.
1/ H <sub>2</sub> only (reference)	441.7 ± 44	291.0 ± 29
2/ H <sub>2</sub> + F <sub>2</sub> (RT, 24 h)	448.4 ± 45	343.8 ± 34
3/ H <sub>2</sub> + ClF <sub>3</sub> (673 K, 24 h)	320.4 ± 32	320.5 ± 32
4/ H <sub>2</sub> + ClF <sub>3</sub> (673 K, 24 h)	503.6 ± 50	395.2 ± 40

\* Recorded using a Talystep instrument, 2000 data points averaged over a sampling distance of 250 microns with an accuracy of  $\pm 10\%$  (section 2.2)

After 60 minutes polishing there has been a reduction in surface roughness for each sample except sample 3, with no evidence for enhancement as a result of chemical pretreatment using mild or aggressive conditions ( $F_2/RT$  or  $ClF_3/673\text{ K}$ ). The apparent lack of polishing on the surface of sample 3 was believed to be a spurious result. The surface profiles obtained using the Talystep instrument, before and after polishing of the reference sample, are shown in figure 3.2. This figure illustrates the non-uniformly sized, peak and valley features, which are characteristic of a CVD-grown diamond film surface. The surface profile after the polishing experiment showed a general reduction in peak heights for a given area of the sample, accounting for non-uniformity and the mean surface roughness ( $R_a$ ) decreased from 441 nm to 291 nm. The results obtained for the chemically treated samples suggested behaviour similar to that of the reference sample.

Light microscopy after the polishing experiments revealed that the grey, unreflective and lapped surface, that was present before polishing, had been preserved.

In all cases, analysis of the diamond surface after the experiment produced results that were typical of the early stages of polishing by a purely abrasive mechanism, which was known to proceed at a very slow rate.

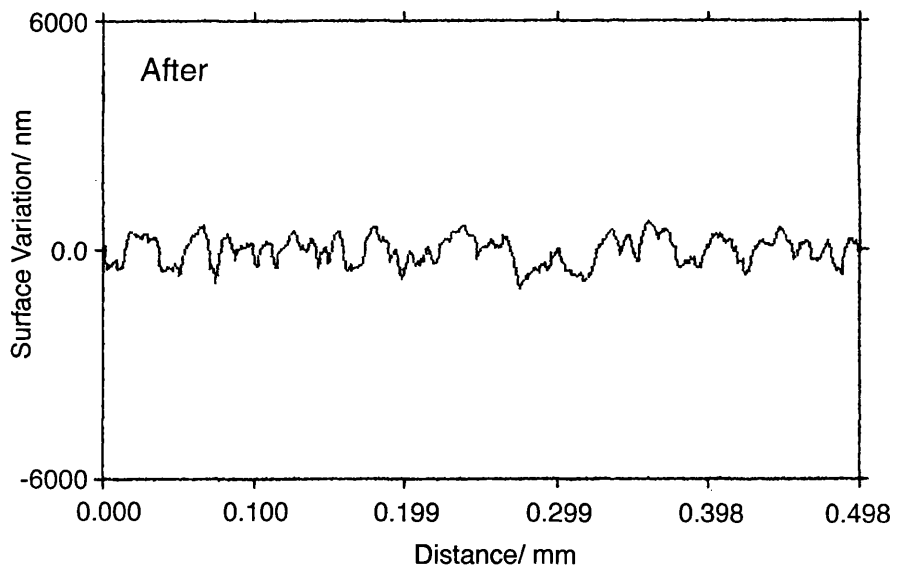
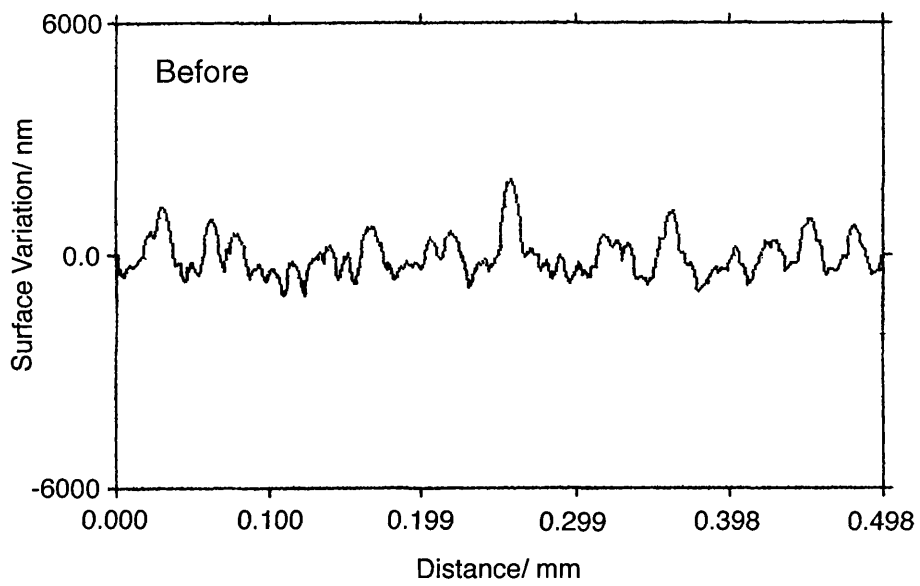


**Figure 3.2** Talystep profiles obtained before and after 45 minutes abrasive polishing (reference sample)

Since purely abrasive processes had been shown by Logitech to be inadequate (chapter 1, section 1.3.2), the experiments which followed represented an attempt to introduce a chemical reaction at the diamond surface during the polishing process thereby aiding the action of the abrasive and improving the polishing rate.

### **3.2 Abrasive polishing of chemically oxidised diamond film with the addition of aqueous potassium hydrogen difluoride solution**

Aqueous hydrogen difluoride ion,  $[\text{HF}_2]^-$  has been shown to have a crucial role in the chemomechanical polishing of silica surfaces using the highly acidic Pilkington reagent (43). Silicon is etched from the surface as the sparingly soluble hexafluorosilicate,  $\text{K}_2\text{SiF}_6$ , which can act as a passivating compound thereby aiding the polishing of the substrate surface (chapter 1, section 1.3.1). The interaction of aqueous hydrogen difluoride with diamond film (dimensions as 3.1) in a polishing situation has been studied, with and without the addition of  $3\mu$  diamond grit as an abrasive. In all cases cerium(IV) oxide powder (Logitech Ltd.) was added on to the polishing plate during the experiment, this helps to produce a polishing slurry which aids sample rotation, making the polishing process more efficient. The apparatus used for polishing experiments involving corrosive reagents, CP3000, has also been described in chapter 2, section 2.2.

Acidic  $[\text{HF}_2]^-$  solution was prepared by dissolving potassium hydrogen difluoride (270 g, 99%, Aldrich Chemical Co.) in dilute hydrochloric acid (120  $\text{cm}^3$  conc. HCl, 36% w/w, M&B Ltd. + 400  $\text{cm}^3$  distilled water) and adding

sucrose (450 g, Fisher Scientific) with stirring. Due to the corrosive nature of the reagent, plastic apparatus was used. The pH of the solution was measured using a digital pH meter, which had been calibrated using pH 4 and 7 buffer solutions. Following a polishing experiment, the effluent was neutralised by the careful addition of aqueous sodium carbonate solution ( $100 \text{ g dm}^{-3} \text{ Na}_2\text{CO}_3$ , BDH, Analar).

Table 3.2 summarises the surface roughness measurements obtained for a number of diamond film samples before and after the 60 minute polishing experiments.

Examination of the data given in table 3.2 reveals that, in general, the interaction of  $[\text{HF}_2]^-$  with diamond film had minimal effect on the surface roughness, but a small reduction was observed, even in the absence of abrasive. Interestingly, on two occasions (samples 3 and 5) the measurements indicated a roughening of the diamond surface following interaction with the hydrogen difluoride solution.

Analysis of sample 3 under the light microscope after the polishing experiment yielded an unexpected result; holes were visible on the surface. A micrograph was recorded and is shown in figure 3.3. For some time this result was thought to be indicative of an etching reaction which may have begun during the pretreatment with  $\text{ClF}_3$  and been continued by  $[\text{HF}_2]^-$  during the polishing experiment. However the effect could not be repeated. A routine analysis of a virgin diamond film, at Logitech, revealed the presence of similar holes. These holes, which are present only on the substrate or non-growth side of the film, are

**Table 3.2** Surface profilometry data obtained in a study of the interaction of aqueous potassium hydrogen difluoride solution with diamond film surfaces in a polishing situation

Sample number/ Pretreatment conditions	Polishing conditions	Ra/ nm	
		Before	After
<b>1/</b> (Table 3.1)	$\text{KHF}_{2(\text{aq})}$ (pH < 1) + $\text{CeO}_2$ powder	291.0 ± 29	247.7 ± 25
	$\text{KHF}_{2(\text{aq})}$ (pH < 1) + $\text{CeO}_2$ + 3 $\mu$ diamond grit	247.7 ± 25	234.1 ± 23
	$\text{KHF}_{2(\text{aq})}$ (pH < 1) + $\text{CeO}_2$ powder	343.8 ± 34	262.7 ± 26
	$\text{KHF}_{2(\text{aq})}$ (pH < 1) + $\text{CeO}_2$ + 3 $\mu$ diamond grit	262.7 ± 26	214.5 ± 21
<b>3/</b> (Table 3.1)	$\text{KHF}_{2(\text{aq})}$ (pH < 1) + $\text{CeO}_2$ powder	320.4 ± 32	404.1 ± 40
	$\text{KHF}_{2(\text{aq})}$ (pH < 1) + $\text{CeO}_2$ + 3 $\mu$ diamond grit	404.1 ± 40	338.6 ± 34
<b>5/</b> $\text{H}_2$ only (reference)	$\text{KHF}_{2(\text{aq})}$ (pH < 1) + $\text{CeO}_2$ powder	252.9 ± 25	419.4 ± 42
<b>6/</b> $\text{H}_2$ + $\text{F}_2$ (RT, 24 h)	$\text{KHF}_{2(\text{aq})}$ (pH < 1) + $\text{CeO}_2$ powder	540.5 ± 54	406.4 ± 41
<b>7/</b> $\text{H}_2$ + $\text{ClF}_3$ (673 K, 24 h)	$\text{KHF}_{2(\text{aq})}$ (pH < 1) + $\text{CeO}_2$ powder	545.4 ± 55	527.9 ± 53

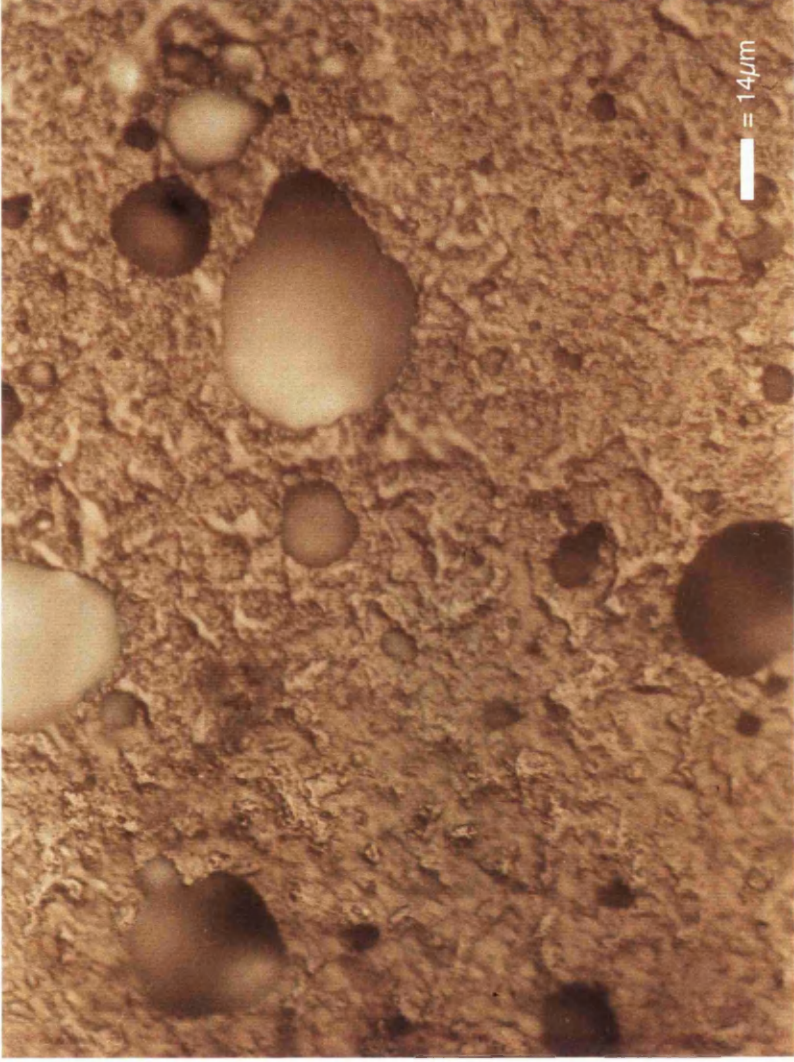


**Figure 3.3** Light micrograph illustrating holes on the non-growth side of the diamond surface.

believed to occur, on occasion, during the CVD growth process (chapter 1, section 1.2), perhaps as the film grows round an area which had been poorly seeded. In general, the diamond films used in this study did not have holes on the surface. The interaction of chemical reagents with such artifacts could not be ruled out, but it seemed clear that chemical reaction was not the initial cause of hole formation.

In light of the minimal effect which had been observed (table 3.2), a series of experiments was devised which attempted to maximise the interaction of nucleophilic species, such as  $[\text{HF}_2]^-$  or  $[\text{OH}]^-$ , with the diamond surface. These experiments involved creating an electrical potential between the diamond sample and the polishing plate.

### **3.3 Abrasive polishing of diamond film in the presence of an electrical potential and a nucleophilic species**

The basis for this part of the current work was a study in ionic polishing of diamond film by Yehoda and Cuomo (124). In their study a piece of diamond film ( $1 \text{ mm}^2$ ) was polished by superoxide ions ( $\text{O}_2^-$ ) at 663 K, this was made possible by the application of an electrical potential over a film of yttria-stabilised zirconia (YSZ) intimately contacted with the diamond sample. Superoxide anions, liberated from the YSZ film, were conducted towards the diamond film, which was the positive electrode and etching of carbon to produce carbon monoxide or carbon dioxide occurred. As a result, a polished surface with a roughness of less than 5 nm Ra could be produced at an etching rate of

650-1860 nm/min for current densities of 1.8-14.3 mA/cm<sup>2</sup> respectively. The initial roughness of the film was 40 nm Ra and the polished region had an area of approximately 6 μm<sup>2</sup>.

In the present study polishing experiments were performed on a much larger scale, in terms of sample area and initial surface roughness, when compared with the study described above. However, the study described and others mentioned earlier (chapter 1, section 1.3.2), have shown that etching of diamond can be achieved by reaction with ionic species.

A number of experiments using a modified apparatus, which has the facility for creating an electrical potential between the sample and the polishing plate, to be applied during polishes, have been performed. In addition to the variable parameters outlined in section 2.2, the size and direction of electrical current flow were considered.

The first experiments used a similar apparatus to that described in section 3.2; the electrical potential was formed between two electrodes, a small carbon brush contacted with the polishing plate and a brass block placed on top of the sample puck. Both electrodes were wired to a D.C. power supply and, depending on the wiring arrangement, the sample could be made the anode or the cathode. Initially, the sample was the anode since this would be the direction of travel for negatively charged nucleophiles. An ammeter was placed in the circuit, which allowed the size of the current at any time during the experiment to be measured.

It was, of course, recognized that diamond has insulating properties and does not conduct electricity. However, if the concentration of the nucleophilic species in the vicinity of the diamond sample could be increased, a greater interaction may occur. In addition, diamond film grown by the CVD method contains imperfections, such as cracks, grain boundaries and even holes on the non-growth side, where the concentration of graphitic carbon is likely to be high. It is therefore possible that conductive regions exist on the diamond surface and these could provide sites for increased interaction with a nucleophilic species.

The results obtained from a range of polishing experiments on diamond film samples, which had received no chemical treatment prior to polishing, are summarised in table 3.3. The chemical pretreatment process was abandoned at this stage for two reasons:

1. In the previous experiments there had been no obvious enhancement in polishing behaviour, gained from chemical pretreatment, compared with untreated samples.
2. Remote chemical pretreatment was inconvenient from a polishing process point of view and in light of point 1 was not considered worthwhile.

It can be seen from table 3.3 that the interaction of diamond film with nucleophilic reagents, in the presence of an electrical potential, has been studied under a wide range of polishing conditions. The chemical reagents, method of reagent delivery, polishing plate material and direction of current flow have all been varied in an attempt to find a regime that produced a positive effect.

**Table 3.3** Surface profilometry data obtained in a study of the interaction of  $[\text{HF}_2]^-$  or  $[\text{OH}]^-$ -containing reagents with diamond film, in the presence of an electrical potential and various process conditions

Sample number	Polishing conditions (reagent used and polishing plate material)	Ra/ nm	
		Before	After
8	Cerium oxide wet impregnated with $\text{KHF}_2$ , polyurethane plate*	215.8 ± 22	312.2 ± 31
	$\text{KHF}_2(\text{aq})$ (pH < 1), cast iron plate	312.2 ± 31	232.6 ± 23
	$\text{KHF}_2(\text{aq})$ (pH < 1), brass plate	232.6 ± 23	306.7 ± 31
	$\text{KHF}_2(\text{aq})$ (pH < 1)+ diamond grit (3 $\mu$ ), brass plate	306.7 ± 31	242.2 ± 24
9	$\text{BaOH}_2(\text{aq})$ (pH 13) + $\text{CeO}_2$ powder, brass plate	190.6 ± 19	171.1 ± 17
	$\text{BaOH}_2(\text{aq})$ (pH 13) + $\text{CeO}_2$ powder, polyurethane plate	171.1 ± 17	185.3 ± 19
	$\text{BaOH}_2(\text{aq})$ (pH 13) + $\text{CeO}_2$ powder, brass plate**	185.3 ± 19	150.1 ± 15
		34.46 ± 3	23.21 ± 2

\* Water was dripped on to the plate; this allowed gradual dissolution of the reagent, which facilitated current flow. Logitech were investigating the use of polyurethane as a replacement for cast-iron.

\*\* The direction of current flow was reversed such that the sample became the cathode; in addition the polishing time was extended with talystep analysis after 30, 90 and 210 minutes polishing.

In all cases aqueous conditions were required to facilitate current flow, which was controlled at up to 3 A for a maximum voltage of 24 V. This was normally achieved by using an aqueous reagent, which could be dripped on to the polishing plate. However, on one occasion, the method of reagent delivery was altered; a paste was prepared by heating (373 K) a solution of  $\text{KHF}_2$  and  $\text{CeO}_2$  until almost dry, this was then applied to a polyurethane plate that was covered with holes to contain the reagent. The addition of water to the plate was required to obtain a current, gradual release of the reagent from the plate into solution occurred.

### **3.3.1 Interaction of $[\text{HF}_2]^-$ (aq) with diamond film in the presence of an electrical potential**

The results obtained here were disappointing, as shown in table 3.3 (sample 8) the roughness of the diamond surface before and after four polishing experiments (215.8 nm and 242.2 nm respectively), accounting for error, is essentially unchanged. There was evidence of an interaction between  $[\text{HF}_2]^-$  and diamond, resulting in a worsened finish, which agrees with data, presented earlier (Table 3.2). However the effect was minimal and could be reversed by the addition of diamond powder or the use of a cast-iron plate, this was almost certainly due to the onset of abrasive polishing. At no time was improved polishing, as a result of chemical interaction, observed. In addition, the absence of any obvious effect upon examination of the sample under the light

microscope, suggested that; whilst an etching reaction seemed possible, it was not significant and did not improve the quality of the surface finish.

### **3.3.2 Interaction of $(\text{OH})^-_{(\text{aq})}$ with diamond film in the presence of an electrical potential**

Previous experiments under acidic conditions had proved unsuccessful, these experiments allowed polishing to be investigated at a highly alkaline pH.

An aqueous solution of barium hydroxide,  $\text{Ba}(\text{OH})_2$  ( $73.15 \text{ dm}^{-3}$ , BDH) with a pH of 13, provided the nucleophilic species.

As shown in table 3.3 (sample 9), there was little effect on the roughness of the diamond surface until the direction of current flow was reversed and the diamond sample made the cathode. The first indication of a significant effect was the appearance of shiny crystals, observed using the light microscope, after 30 minutes polishing. To investigate this further the experiment was continued and the mean surface roughness (Ra) measured intermittently. As shown in figure 3.4 the Ra value decreases in a non-linear fashion throughout the experiment. The greatest reduction occurred between 30 and 90 minutes polishing time, at which stage the effected area represented approximately 30% of the sample surface. Whilst a further reduction in Ra was observed after an additional 120 minutes (210 minutes in total) the size of the effected region, in terms of sample surface area, was unchanged.

Sample height measurements, accomplished using a Sylvac 80 instrument (chapter 2, section 2.2), prior to the polishing experiment, revealed the presence of a gradient from one side to the other, which meant that areas of contact and non-contact with the polishing plate were present. The polishing effect observed occurred at the high part of the sample, which would have been in contact with the polishing plate.

Variations in sample height or thickness are common for diamond film grown by the CVD method and are due to a non-uniform growth rate across the substrate surface.

Throughout the experiment a green colour was present on the polishing plate and upon removal of the sample for analysis, a brassy layer on the surface could be observed. This layer could be removed by gentle rubbing with emery paper before analysis.

A micrograph, recorded after 210 minutes and the Talystep surface profile in the effected region are shown in figure 3.5.

Using light microscopy it was possible to identify three distinct regions on the sample surface: a highly reflective area, a rougher lapped area which formed a corona around the reflective area and a completely non-reflective area to the outside of the sample which was rougher still. In contrast to the irregular profile, obtained at the start of the experiment, which was similar to the example

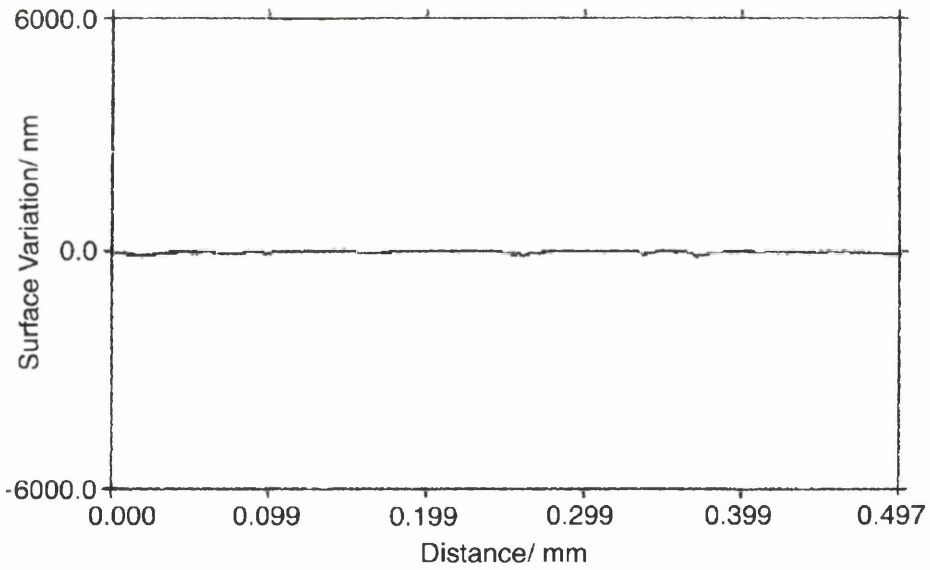
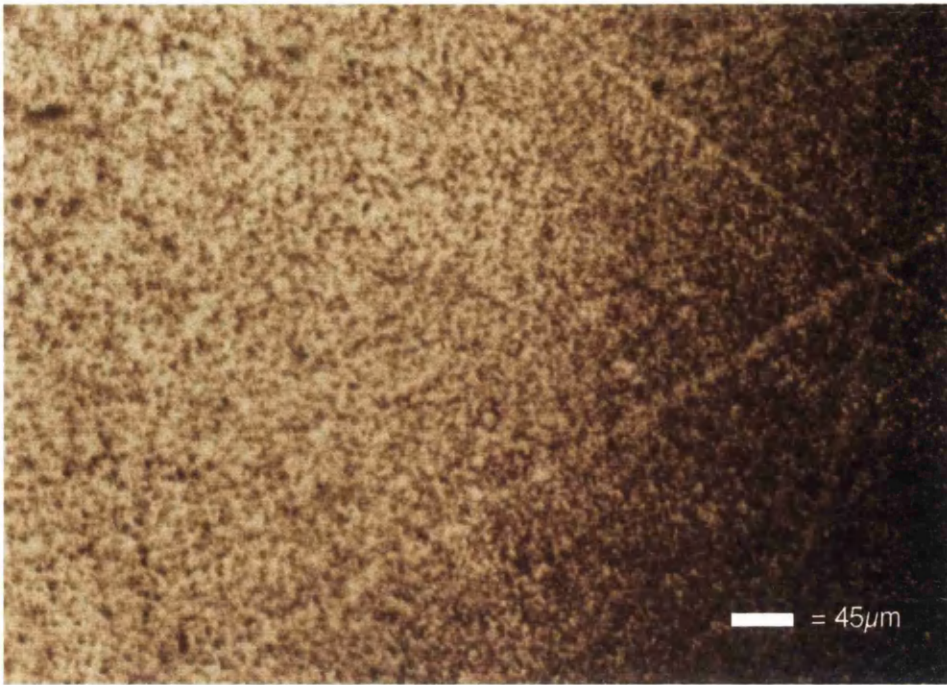


**Figure 3.5** Light micrograph and Talystep profile obtained in the polished region of the diamond sample surface.

given in figure 3.2, a flat line profile, corresponding to the reflective area of the sample surface was observed.

These results represented a landmark in this work since, for the very first time it was possible to produce a diamond surface with a finish of reasonable quality, in a reasonable time and without the addition of diamond grit or the use of high loads on the sample. However, the process was limited, apparently beginning the contact zone between the sample and the plate and extending to a maximum area of 30% after 90 minutes. This area could not be increased significantly, despite processing for a further 120 min.

At this time a number of hypotheses to explain these results were considered but it was of paramount importance to repeat the effect and establish the parameters which had a controlling influence.

### **3.3.3 Further investigation into the polishing of diamond film in the presence of an electrical potential**

The aim of this part of the work was to develop further the process described in section 3.3.2; preliminary experiments had shown promise but limitations were apparent.

## **Experimental considerations**

A number of key changes were made to the original experimental apparatus; these were designed to remove process problems that had been identified in the early experiments and to allow maximisation of the desired effect.

1. The diamond sample and puck assembly was attached to a polishing jig with a vacuum chuck face that could be raised or lowered. This allowed variation in the position of the sample relative to the plate. The process could be examined with the sample in or out of contact with the plate. Logitech had shown that precise control of the sample height, relative to the plate, greatly influences lapping and polishing processes (chapter 2, section 2.2). The polishing jig was similar to that shown in figure 3.6, however the jig design and in particular the nature of the driving were subject to change depending upon the process conditions. The driving affects the rotational properties of the jig on the polishing plate; efficient rotation has been shown to promote the removal of material in lapping or polishing processes.
2. The carbon brushes, which had been found to wear easily, were replaced by mercury contacts (figure 3.7).
3. The original power supply was replaced with one of much higher rating which allowed higher currents (10-50 A) to be used. In this way the current density across the sample could be increased. The current density was believed to be one of the factors that determined the extent to which material was removed from the diamond surface.
4. A number of failed experiments on non-metal plates, such as polyurethane, established that a chemical reaction was unlikely to be

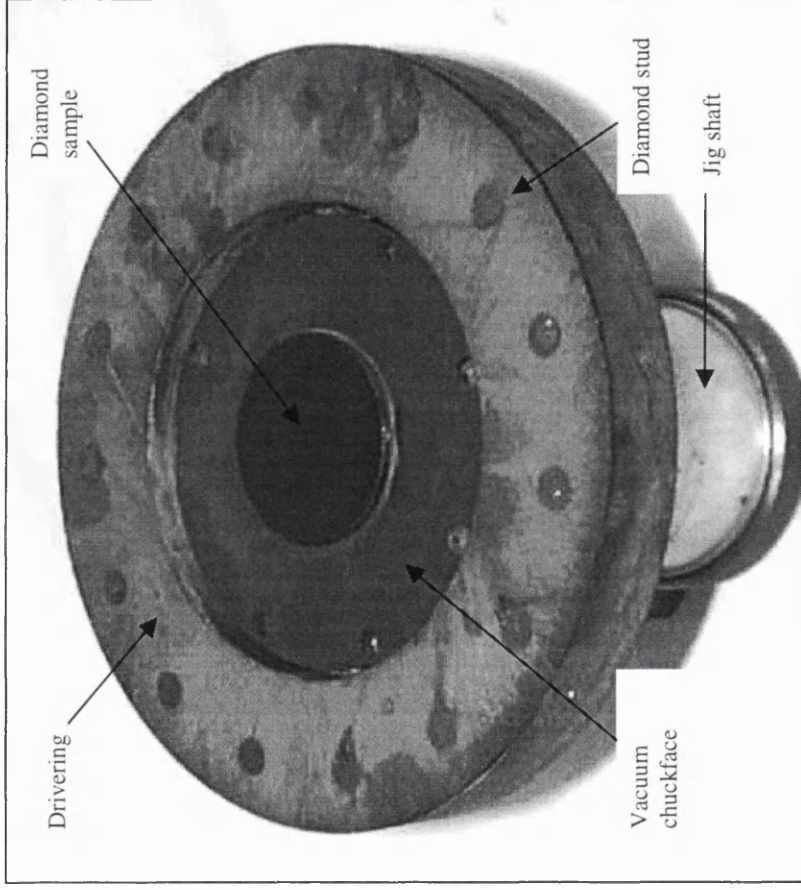


**Figure 3.6** Polishing jig with sample/puck assembly in place  
(shown in upturned position)

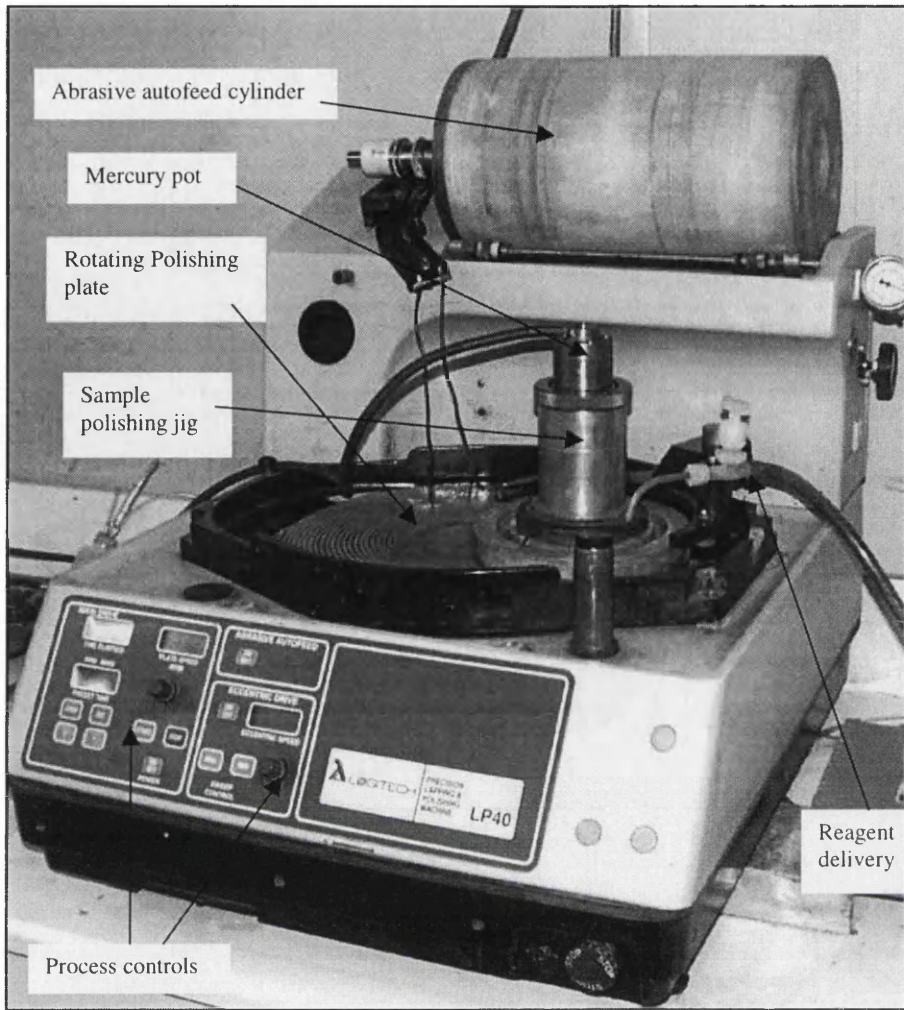


**Figure 3.7** Polishing apparatus used in the processing of samples 10 and 11 (note for sample 10 the reagent was dripped onto the polishing plate from a dropping funnel, whilst for sample 11 a recirculation system (see text) was used)

responsible for the observed effect. The likely role of the chemical reagent was to act as an electrolyte, facilitating current flow. For this purpose a simple salt (NaCl) solution would suffice.

The points listed above are only the key changes. As indicated previously (figure 3.1) the experimental parameters were often altered to cope with any problems encountered and to improve the process.

Two diamond film samples (GEC), denoted samples 10 and 11, were used in this part of the work. The samples were 2 inches in diameter and about 0.6 mm thick with a surface roughness on the growth side in the region of 100  $\mu\text{m}$  Ra.

Polishing on the growth side of the diamond surface was investigated; previous studies in this work had been restricted to the non-growth side, which was substantially smoother. In addition, for the following work, the samples were not lapped in order to evaluate the potential of the method for removing material from rough surfaces. A copper plate was chosen, since the metal deposited on the surface of sample 9 was almost certainly copper and it was desirable to investigate the effect on plates which were traditionally ineffective for lapping or polishing diamond.

The roughness of these samples was outside the range of the Talystep instrument. In order to determine if material was removed as a result of experiment, the vertical height or thickness of the sample/puck assembly was measured, before and after the experiment, using the Sylvac 80 instrument,

precision  $\pm 1$  micron. The accuracy of these measurements depends on an assumption that only the thickness of the sample is subject to change during the experiment. This was reasonable since, at all times, only the sample was in contact with the polishing plate, therefore, changes in the thickness of the puck were not expected. The alternative to this method would have been to dismount and remount the sample at each measurement stage, this would have caused enormous process inconvenience, largely due to the time taken (1-2 hours) to break and reform the epoxy bond.

The difference in sample height before and after an experiment is termed stock removal. High stock removal is desirable in lapping and polishing processes.

## **Results**

Table 3.4 summarises the observations made on sample 10 under a range of experimental conditions.

Vigorous sparking, a green colour and the evolution of gas were observed almost immediately, a popping sound suggested that ignition of the gas was occurring and, due to the risk of explosion, the experiment was terminated after 15 minutes.

Despite the short experiment time, a considerable effect on the diamond surface could be seen to have occurred upon examination of the sample under the light microscope. A light micrograph of the surface is shown in figure 3.8; it can be

**Table 3.4** Experimental observations made during the processing of diamond film sample 10 under a range of conditions

Experiment No.	Experimental conditions	Observations/Results
1	Copper plate, 4 mol dm <sup>-3</sup> NaCl solution dripped on to the plate, current was very high (> 50 A), alumina/water mixture added from the abrasive autofeed cylinder (figure 3.7)	Green colour present, sparking audible and visible, explosive gases were formed- the experiment was ceased after 15 minutes, no change in sample height but microscopy indicated removal of diamond from peaks (figure 3.8) and the sample was coppered
2	As 1 with reduced NaCl concentration (2.5 then 0.025 mol dm <sup>-3</sup> ), current 10-20 A. Jig modified to allow the gases formed to escape (figure 3.9) Effect of changes in sample height and plate speed investigated	As 1 with little change in the appearance of the sample under the microscope after 180 min. Black colour developed from the green as the experiment progressed
3	As 2 with 50μ diamond grit (10g dm <sup>-3</sup> ) added to the alumina/water mixture	Material removed in an annulus across the sample surface (figure 3.11), total stock removal in 300 min. was ≈ 300 μm. Microscopy revealed the presence of a lapped surface and the measured roughness was 43 ± 2 nm Ra. The colouration effects were as before and the sample was coppered.

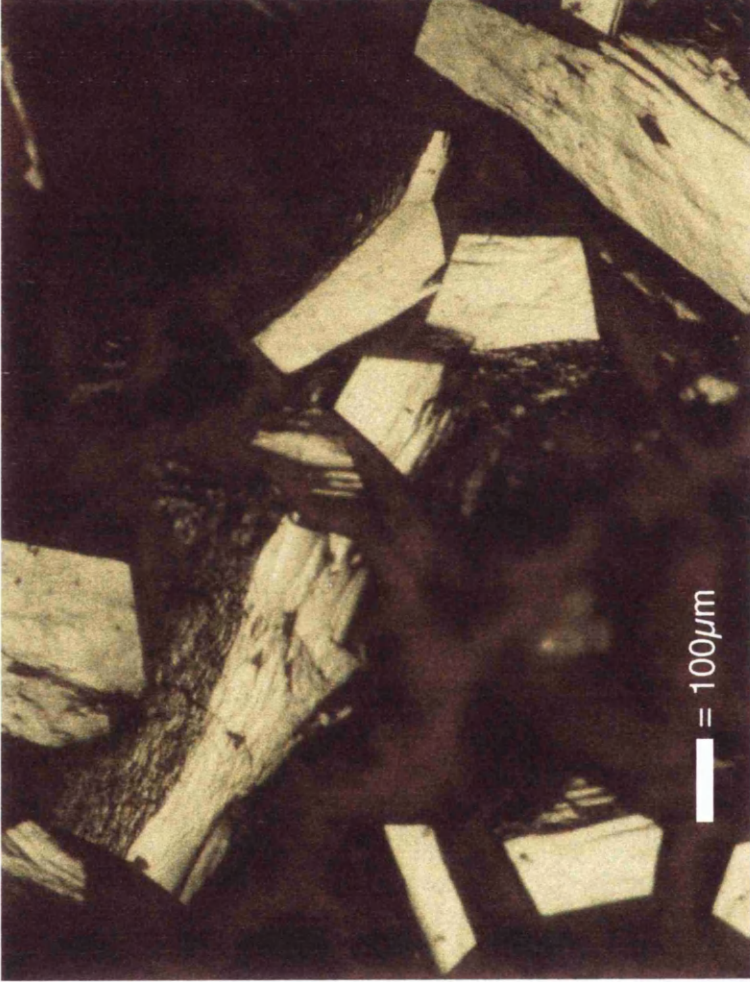


**Figure 3.8** Light micrograph illustrating eroded peaks and copper present at the interstices between peaks.

seen that peaks, which have been etched or eroded, are present. The nature of the erosion/etching was inconsistent with anything observed previously during lapping or polishing of diamond film. The observed effect could be suitably described as being a result of blasting material off the diamond peaks.

The presence of copper at the interstices between peaks on the surface can also be seen in figure 3.8, consistent with the coppering effect which had been observed previously on the surface of sample 9. Deposition of copper on the diamond surface was clearly an important feature of these experiments but its exact role was uncertain.

Measurement of the sample height following the initial 15-minute period suggested that essentially no stock removal had occurred, however significant stock removal in such a short time was not expected and since there was clear evidence for a positive effect the experiment was continued. Before this was possible a number of measures, aimed at reducing the potential hazards, were taken:

1. Considerable erosion was present on the exposed area of the sample puck surface, which suggested that much of the sparking had been occurring between the puck and the polishing plate. Whilst the puck surface under the diamond sample was unaffected, if erosion continued the accuracy of the sample height measurement would have been questionable. To prevent this, the puck was machined to the same diameter as the sample (2 inches), such that only the sample surface was presented to the plate.

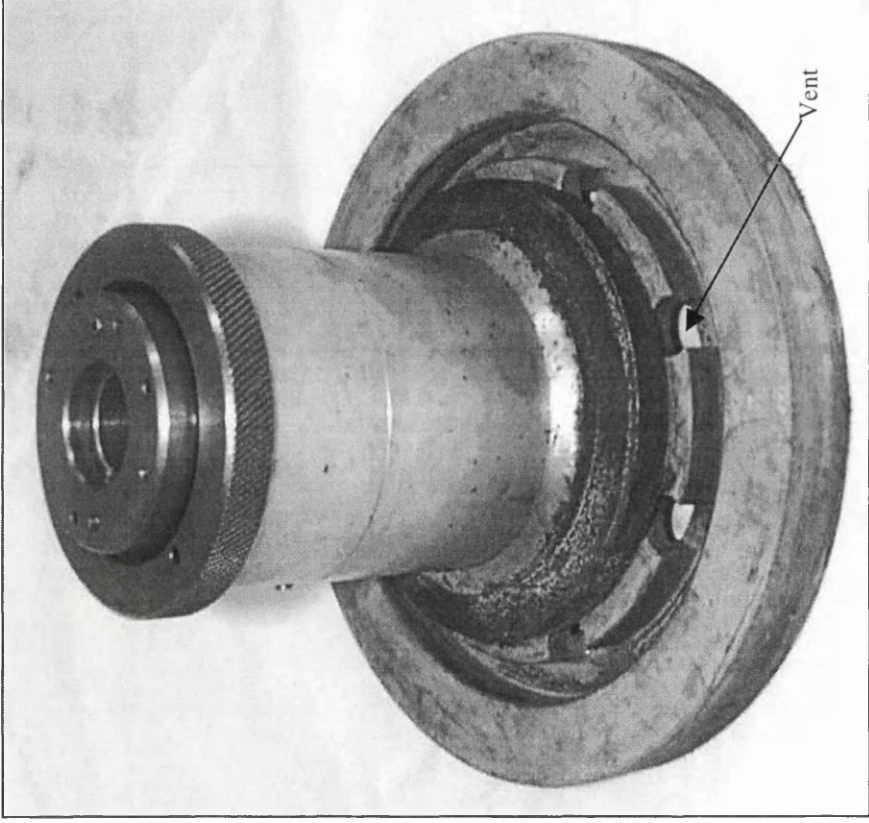


**Figure 3.9** Modified jig to allow venting of gases formed during processing of samples 10 and 11

2. Build up of explosive gases in a sparking environment was clearly undesirable. In order to alleviate this problem a series of holes were machined round the drivering allowing venting (figure 3.9) and a fan was used to remove the vented gas from the sparking area.
3. In addition to the changes described above, the concentration of the electrolyte (NaCl) solution could be easily reduced offering greater control over the size of the flowing current.

With the above measures in place the process could be further investigated (Expt. 2, table 3.4) under safe conditions. Sparking continued to a lesser extent and a green followed by black colour developed on the plate as the experiment progressed. The size of the current was found to be dependent on a number of factors: the concentration and rate of delivery of the electrolyte (NaCl) solution, the plate speed and the height of the sample relative to the plate. Table 3.5 illustrates how the current changed with each of the factors mentioned.

**Table 3.5** Dependence of current (I) on experimental parameters (↓ decrease, ↑ increase)

Parameter	I
NaCl concentration ↓	↓
Reagent delivery rate ↑	↑
Plate speed ↑	↓
Sample height above plate ↑	↓

Not surprisingly, as the concentration of NaCl in the electrolyte solution was decreased the current also decreased and if the rate at which the electrolyte solution was increased the current increased. Changes in the plate speed affect the length of time the electrolyte solution is present on the plate and hence the size of the current. It was also shown that as the sample was raised off the plate, under vacuum action, the current decreased and eventually reached zero where no contact between the sample and the plate occurred. The sample had to be in or close to contact with the plate to achieve current flow, proving that the process was not independent of the diamond sample.

The sample was examined for stock removal and changes in surface morphology at various stages during experiment 2, however after 180 minutes there was no increase in stock removal with some evidence for an increase in the concentration of eroded peaks. It was clear that some kind of erosion process was occurring but the amount of material removed was not significantly high and the overall roughness of the sample remained constant.

In an attempt to increase stock removal, 50  $\mu$  diamond grit ( $10 \text{ g dm}^{-3}$ ) was added to the alumina/water mixture and delivered to the plate from the abrasive autofeed cylinder (experiment 3, table 3.4). As a result, material was removed from the sample surface at an average stock removal rate of  $60 \mu\text{m h}^{-1}$  over a 5-hour period, 30 times faster than previously observed for lapping of diamond film. After 5 hours the mean surface roughness in the effected region (measured using the Dektak instrument, section 2.2) was  $43 \pm 2 \text{ nm Ra}$  and light



**Figure 3.10** Light micrograph illustrating the lapped surface of sample 10 after 300 minutes.

microscopy indicated a lapped/semi-polished surface as shown in figure 3.10. A marked distinction between this surface and that recorded after experiment 1 (figure 3.8) was obvious, the eroded peaks had now been completely removed and the resulting surface was considerably smoother.

The progression of the affected area across the sample surface is shown schematically in figure 3.11, which also illustrates the height gradients present on the sample at the start of the experiment. Material was removed initially at the high part of the sample, which during the experiment would have been closest to the plate and continued in an annulus across the surface until the effected area was  $4\text{cm}^2$ , which represented about 70% of the total sample area. At this point three distinct regions could be seen on the surface of the sample (figure 3.11), a semi-polished region ( $\approx 3\text{ cm}^2$ ), a lapped region ( $1\text{ cm}^2$ ) and an unaffected region. These observations were consistent with those obtained in the original experiment, described in section 3.3.2, except in this case the effect was occurring on a larger scale. However, as before, the process was found to be limited and despite several hours further processing the sample was unaffected with no additional stock removal.

Considerable progress had been made as a result of the work on sample 10 and it was felt that if the correct conditions could be found the method had considerable promise as an alternative to traditional lapping and polishing processes for diamond film. The obvious course of action was further experiments with additional investigation of the important process parameters. After more than 10 hours processing, sample 10 was beginning to breakup and

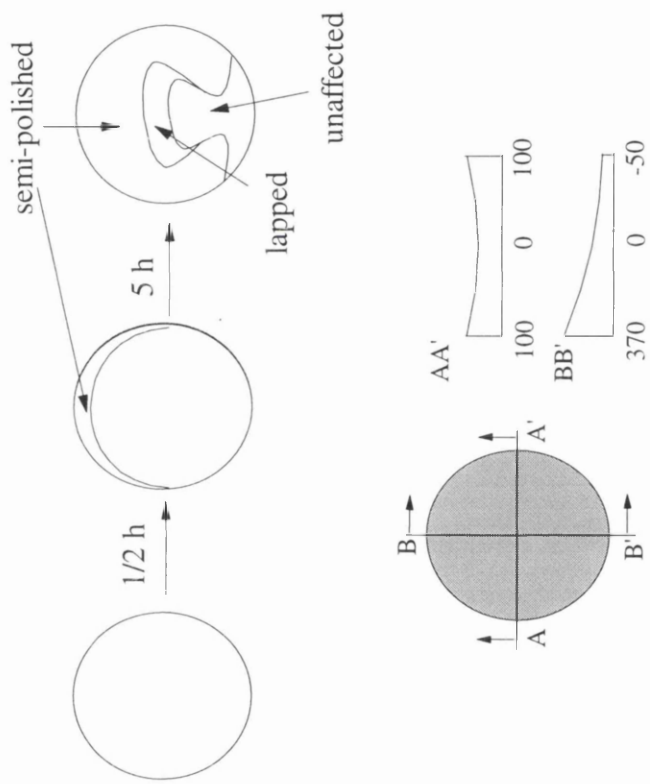


**Figure 3.11** Development of a semi-polished region on the surface of sample 10 and the height gradients (microns) across the sample surface

loose shape, therefore experiments were continued on a new sample, denoted sample 11.

The experimental apparatus was identical to that described previously (figure 3.7) with one alteration, the electrolyte solution was delivered to the plate via a recirculation system. This consisted of a small suction pump placed in a vessel containing the solution and with a length of tubing attached to allow flow of the solution on to the plate. The polishing effluent was flushed into the same vessel such that continual recirculation was possible. In addition, diamond grit could be added to the vessel containing the electrolyte solution, allowing it to be reused. This was far superior to the previous condition where used diamond grit and electrolyte solution was flushed into a waste container and required regular replacement. Replacement of the solution for recirculation was required due to the build up of scum, but only after several hours experiment which meant that the method was more efficient and less costly in terms of the diamond grit used.

The process data obtained after a range of experiments on sample 11 are shown in tables 3.6 and 3.7. Unless otherwise stated, each experiment was 30 minutes in duration, a copper polishing plate was used and the sample was placed under minimal loading. The sample height before and after each experiment was monitored at 10 points across the surface providing detailed information with regard to the extent and location of stock removal. The process involved a 5-point measurement horizontally from edge to edge across the sample surface, followed by a 90° rotation and a further 5-point measurement. Light microscopy

**Table 3.6** Ten-point height measurement during the processing of sample 11 under a range of conditions

Experiment No.	Process conditions	Sample height/ mm									
		1	2	3	4	5	6	7	8	9	10
	Before processing	11.341	11.245	11.234	11.243	11.288	11.276	11.235	11.235	11.232	11.249
1	Cu plate, I=10-30A	11.311	11.245	11.232	11.245	11.287	11.278	11.234	11.234	11.233	11.257
	Sample re-bonded	11.320	11.240	11.231	11.261	11.338	11.272	11.220	11.220	11.235	11.321
2	As 1	11.308	11.235	11.231	11.260	11.320	11.268	11.220	11.227	11.233	11.298
3	As 1	11.297	11.235	11.225	11.251	11.299	11.256	11.215	11.221	11.227	11.288
4	Electrical supply off	11.296	11.235	11.225	11.252	11.299	11.255	11.216	11.223	11.228	11.287
5	As 1	11.290	11.235	11.225	11.251	11.295	11.250	11.220	11.228	11.223	11.283
6	As 1, Load increased	11.285	11.239	11.228	11.246	11.294	11.249	11.232	11.224	11.234	11.278
7	As 1, Load decreased	11.283	11.238	11.227	11.246	11.293	11.253	11.224	11.225	11.228	11.268
8	As 6, cooling water added	11.271	11.244	11.229	11.249	11.286	11.246	11.224	11.222	11.228	11.261
9	As 8	11.270	11.244	11.228	11.250	11.280	11.247	11.224	11.233	11.240	11.272
	Sample re-bonded	11.270	11.243	11.222	11.232	11.254	11.245	11.215	11.219	11.218	11.237
10	As 1, cast-iron plate, I=20A	11.272	11.241	11.222	11.237	11.254	11.246	11.218	11.220	11.224	11.235
11	As 10, I=35A	11.270	11.241	11.222	11.237	11.254	11.246	11.218	11.220	11.224	11.235
12	As 1, no grit, 1 h	11.263	11.231	11.210	11.225	11.250	11.227	11.211	11.214	11.210	11.224

**Table 3.7** Stock removal across the surface of diamond sample 11 during processing under a range of conditions

Experiment No.	Stock removed in 30 min period/ $\mu\text{m}$									
	1	2	3	4	5	6	7	8	9	10
1	30	0	2	0	1	0	1	0	0	-9
2	12	5	0	1	18	4	0	1	2	23
3	11	0	6	9	21	12	5	6	6	10
4	1	0	0	-1	0	1	-1	-2	-1	1
5	6	0	0	1	4	5	-4	-5	5	4
6	5	-4	-3	5	1	1	-12	4	-11	5
7	2	1	1	0	1	-4	8	0	6	10
8	12	0	-2	-3	7	7	0	3	0	7
9	1	0	1	-1	6	-1	0	-11	-12	-11
10	-2	2	0	-5	0	-1	-3	-1	-6	2
11	2	0	0	0	0	0	0	0	0	0
12	7	10	12	12	4	19	7	6	14	11
Total*	89 $\pm$ 18	18 $\pm$ 8	22 $\pm$ 10	26 $\pm$ 12	63 $\pm$ 18	49 $\pm$ 14	21 $\pm$ 8	20 $\pm$ 10	33 $\pm$ 11	73 $\pm$ 18

\* Negative values not included in summation, these indicated no stock removal in the -1 to -5 range or lifting of the sample at greater than -5  
 The error on sample height measurements (table 3.6) is  $\pm 1$  micron; therefore the error on difference values is  $\pm 2$  microns and the error on the total stock removal is as shown above

and profilometry were used as before for evaluating the surface morphology and roughness as a result of experiment.

Analysis of the data presented in tables 3.6 and 3.7 revealed the following features:

1. The stock removal was greatest in the first 120 minutes of processing (table 3.7, expts 1-3) and occurred at the highest parts of the sample as indicated in table 3.6 (points 1, 5/6, 10).
2. The importance of an electrical current in the stock removal process is illustrated in experiment 4 where, in the absence of a current, no material was removed from the sample surface. Stock removal did occur at the high parts of the sample when the electrical supply was restored (expt 5).
3. The effect of altering the loading on the sample was investigated in experiments 6, 7 and 8. Traditionally, increasing the sample load results in polishing with low stock removal and reducing the sample load results in lapping with higher stock removal. The stock removal measurements in the high parts (point 1, 5/6 and 10) of the sample suggest that similar amounts of material can be removed under conditions of high and low load depending on the region of sample considered. However, the occurrence of a large negative stock removal (-11) at point 9 after experiment 6 suggested that sample lifting was beginning to occur and casts some doubt on the values obtained at point 10. If the values at point 1 only are considered the stock

removal was greatest under high load where, greater contact between the sample and the plate was encouraged.

4. Lifting of the sample was confirmed after experiment 9 with large negative stock removal values at points 8, 9 and 10. The temperature on the plate reached 323 K, which caused the sample bond to be compromised. Cold water was added to the plate to reduce the temperature of the surface but this seemed to be ineffective. After experiment 9 the sample was re-bonded.
5. The critical role of copper in the stock removal process was confirmed by experiments using a cast-iron plate (experiments 10, 11) where, despite high current levels no stock removal occurred.

The variation in stock removed with experiment number at point 1 on the sample surface is shown in figure 3.12; this emphasises the high stock removal in the early stages and the effect of changes in the process conditions (table 3.6).

After the first 30 minutes, a strip of shiny crystals was visible at the outer rim of the sample, during experiments 1-7 the strip grew to a width of about 3mm at point 1, 2mm at point 5 and 1mm at points 6 and 10. Using the light microscope the development of a semi-polished region, with time, could be monitored (figure 3.13). The visual form of this region was very interesting and had never been observed in previous diamond polishing studies at Logitech. It appeared as though material had been ploughed off the surface resulting in a smoothed patch. Tracks in the rough surface, where the process was continuing, were also clearly visible. Dektak surface profiling (figure 3.14 A-C, table 3.8) revealed that the

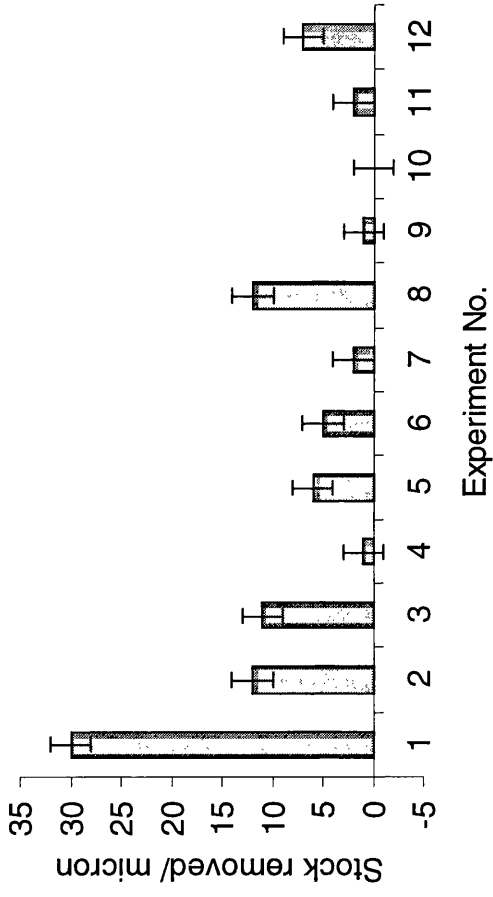


**Figure 3.12** Variation in stock removed at point 1 across sample 11 during experiments 1-12 (tables) 3.6 and 3.7

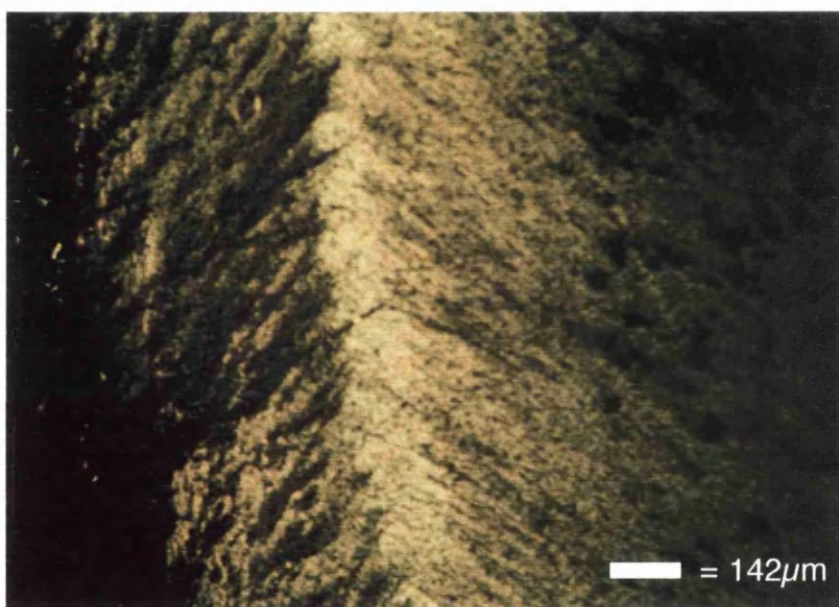
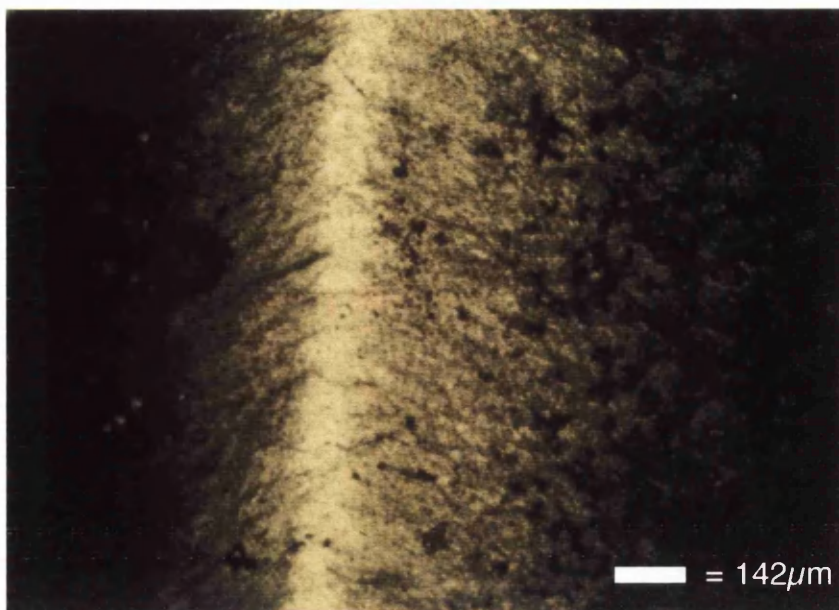


**Figure 3.13** Development of a semi-polished region on the surface of diamond sample 11 after 60, 90 and 120 minutes respectively

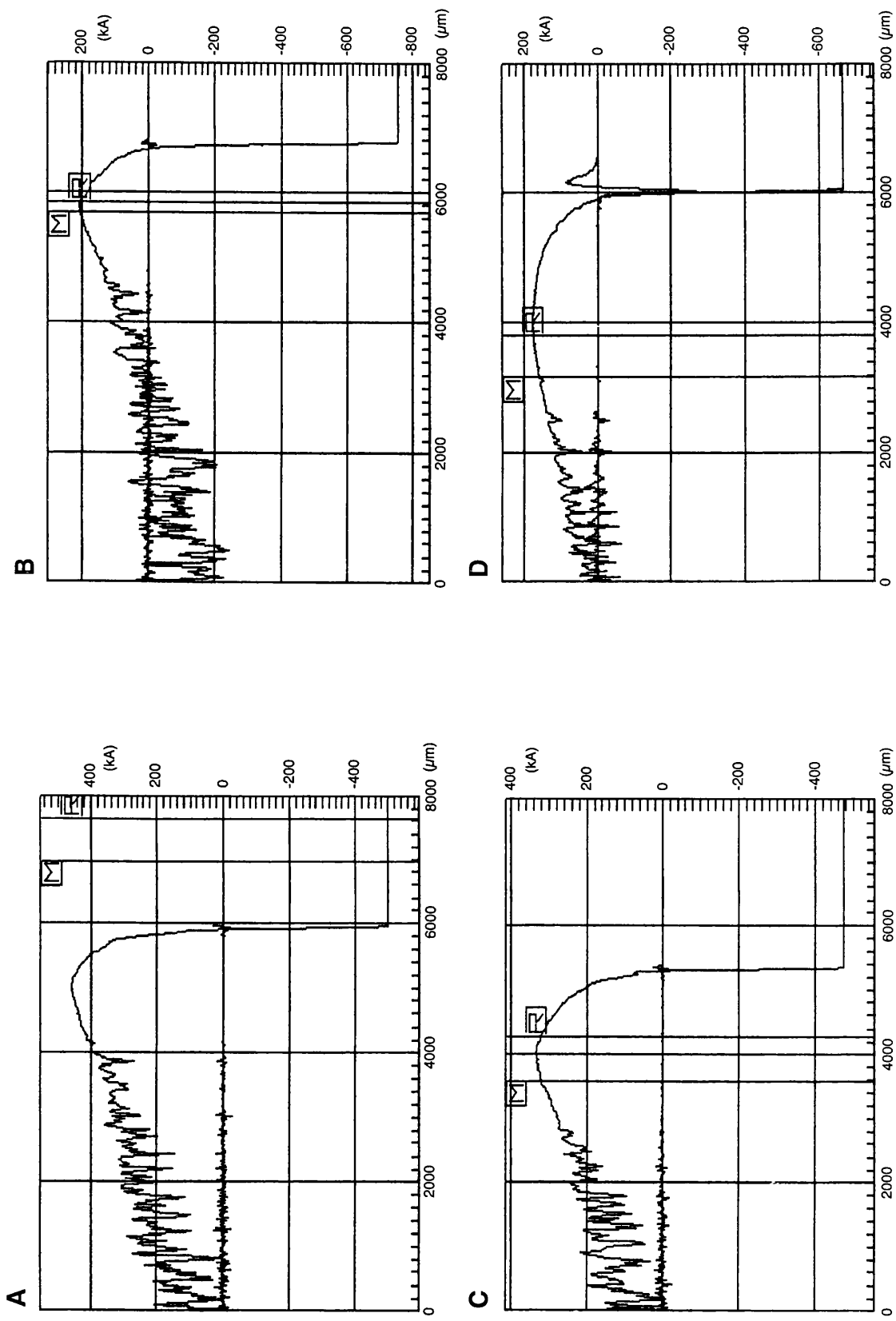


Figure 3.14 Dektak profiles recorded at various stages (Table 3.6) during the polishing of sample 11.

**Table 3.8** Surface roughness measurements obtained at various times during the processing of sample 11 under a range of conditions

Profile	Scan region/ $\mu\text{m}$	Ra/ nm
A, recorded after expt 3	500-1740	$876 \pm 44$
	3021-4021	$340 \pm 17$
	4304-4934	$24 \pm 1$
B, recorded after expt 4	500-1740	$974 \pm 49$
	3021-4021	$530 \pm 26$
	5195-5739	$22 \pm 1$
C, recorded after expt 5	2934-3695	$36 \pm 2$
	3586-4282	$17 \pm 1$
D, recorded after expt 12	3695-4369	$36 \pm 2$
	4434-5086	$33 \pm 2$
	3173-3804	$62 \pm 3$

The error on Ra values measured using the Dektak machine was taken to be  $\pm 5\%$

surface roughness at the semi-polished rim was initially 24 nm improving to 17 nm Ra after experiment 7.

In agreement with the observations made during the processing of sample 10, a green colour formed quickly on the polishing plate and as the experiment progressed this became black; with time the plate took on a glassy appearance. For experiment 12 the polishing rig was reconfigured to promote the removal of this glassy layer, this included the use of a diamond-studded drivering (figure 3.6) and had the effect of cleaning the plate surface, exposing copper. As a result, stock removal, at a reasonable level, was reintroduced (table 3.7, experiment no. 12) across the sample surface. Dektak surface profiling after experiment 12 (figure 3.14D and table 3.8) indicated an increase in the size of the effected area but also a worsening of the surface finish with higher Ra value. It should be noted that material had been removed in the absence of added diamond grit.

These observations were entirely consistent with the suggestion that ploughing of the surface was reoccurring. Ploughing was desirable at this stage in the processing of the sample, since the stock removal rate was much greater than obtained during polishing. Clearly the experimental conditions were approaching an optimum condition for processing diamond film on a copper surface, in the presence of an electrical current and without added diamond as an abrasive.

The total stock removed from, for example, point 1 equates to a rate of 14-20  $\mu\text{m h}^{-1}$ , calculated on the basis of processing time on a copper plate and with an electrical current present. It should be born in mind that traditional lapping processes remove material at a rate of about 5  $\mu\text{m h}^{-1}$ .

At this stage in the project no further time was available for experimental work; it had taken three years but a method for removing material from a diamond film surface at a reasonable rate had been developed. The surface finish, although not of optical quality, was on the nanometre scale and with the correct process conditions could be improved.

However, the process was subject to limitation and complete processing of a 2-inch diameter sample was not achieved. Nevertheless, extensive research had identified the important process parameters, which have been alluded to throughout this chapter. A model for the process is presented in the discussion section of this thesis (section 5.3).

## CHAPTER 4 RESULTS

### Chemical modification of diamond surfaces

#### 4.0 Introduction

This chapter details results obtained from a study of the halogen chemistry possible on polycrystalline diamond surfaces. In chapter 1 the aims of this work were discussed, among these was a desire to develop our understanding of diamond reaction chemistry and correlate this with the success or failure of various polishing regimes.

Diamond powders and films were exposed to a range of halogen (mainly fluorine) containing reagents as outlined in section 2.1.8. The starting point was an FTIR investigation of the volatile products formed in the reaction of diamond powder surfaces, chemically modified in various ways (Table 2.3), with the reagents mentioned previously.

Following this, major focus turned to the diamond surface properties after reaction, concentrating largely on the interaction of hydrogenated powders and films with  $F_2$  or HF. To investigate this, several surface analytical methods were employed with the explicit purpose of elucidating the diamond surface structure, chemical and physical. Extensive use was made of the radiotracer fluorine-18 to probe the behaviour of HF with diamond and the results obtained could be correlated with the surface structure analyses.

## **4.1 FTIR spectroscopic investigation of diamond reaction chemistry**

This part of the work was designed to establish the products of reaction between diamond surfaces and various halogen-containing reagents. Whilst the halogenation of diamond surfaces had been studied previously (chapter 1) there was no analysis of the gaseous phase following reaction. The focal point of work performed previously was to investigate the potential of halocarbons as replacements for methane in the CVD growth process. Analysis was restricted to the diamond surface and the gaseous phase was discarded. In the present study, one of the primary aims was to investigate the polishing properties of chemically modified diamond film. In this respect, it was important to establish the exact nature of the chemical modification. Gas phase analysis was seen to be an important part of this process with FTIR spectroscopy the method used.

### **4.1.1 Reaction of hydrogenated diamond powder and film with Difluorine ( $F_2$ ) and/or Chlorine trifluoride ( $ClF_3$ )**

In order to be useful as a modification process before polishing it was felt that the chemical reaction should induce surface damage. For this reason and the chemically inert behaviour of diamond, aggressive reagents were chosen. The reaction was studied largely with hydrogenated diamond powder since the replacement of hydrogen for fluorine was known to occur easily, even at 263 K. The experimental conditions have been described (chapter 2). Results from the FTIR spectroscopic analysis of the gas phase products are given in table 4.1.

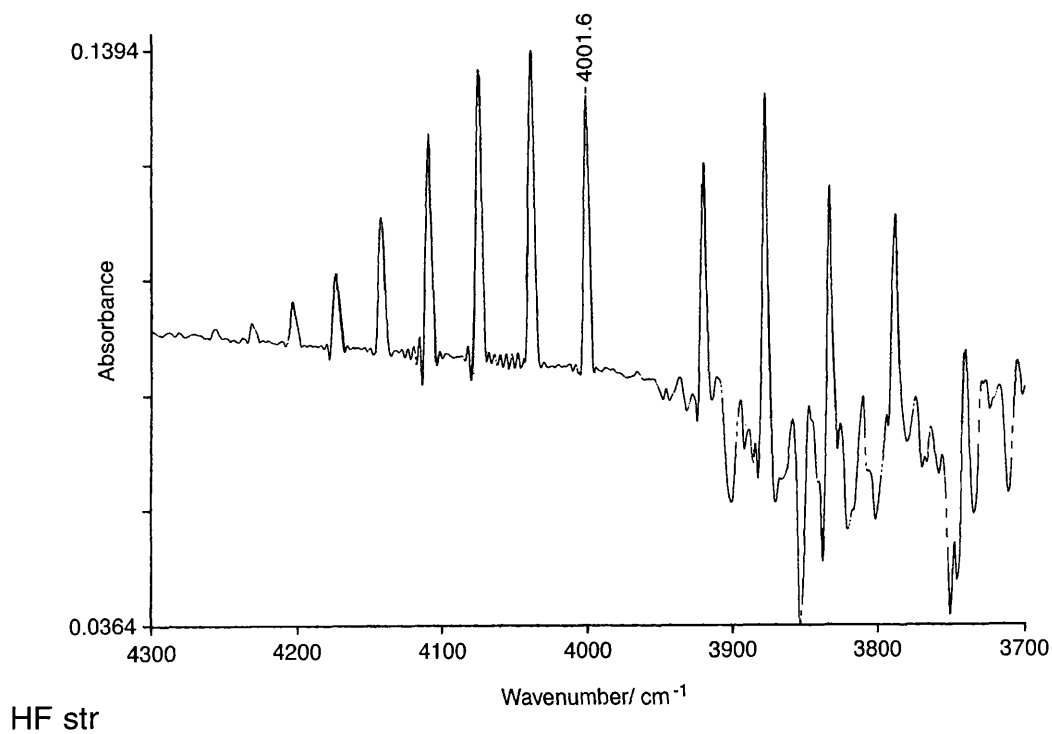
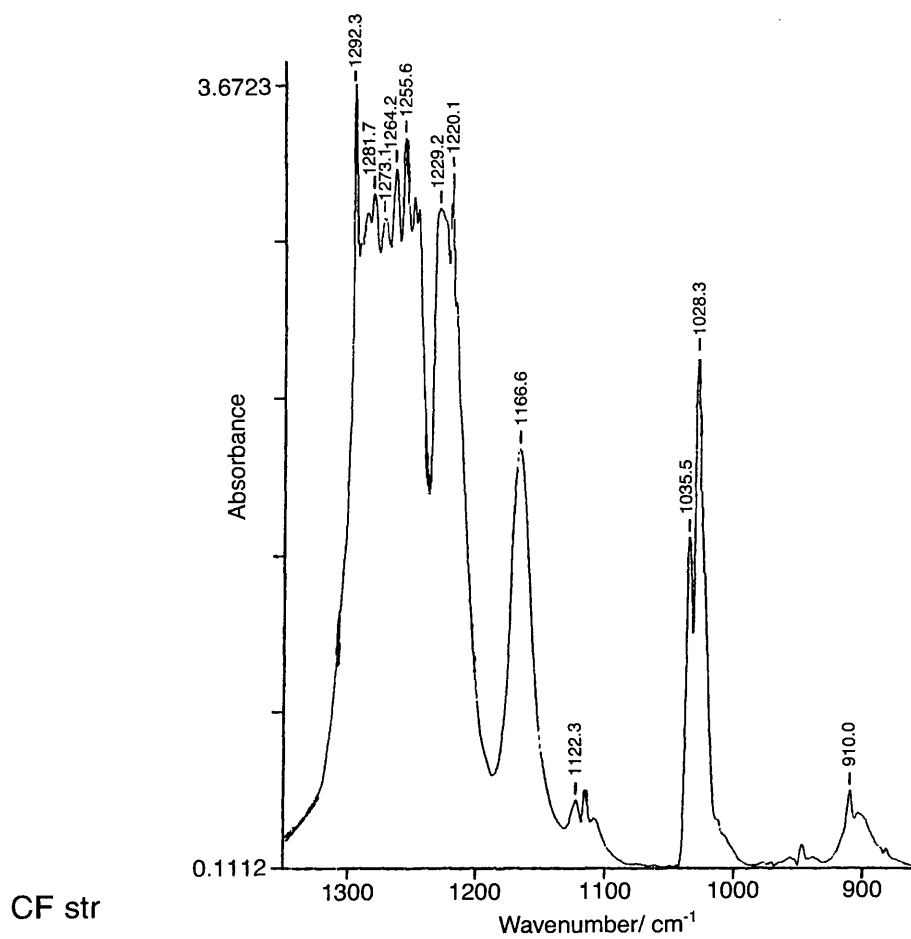
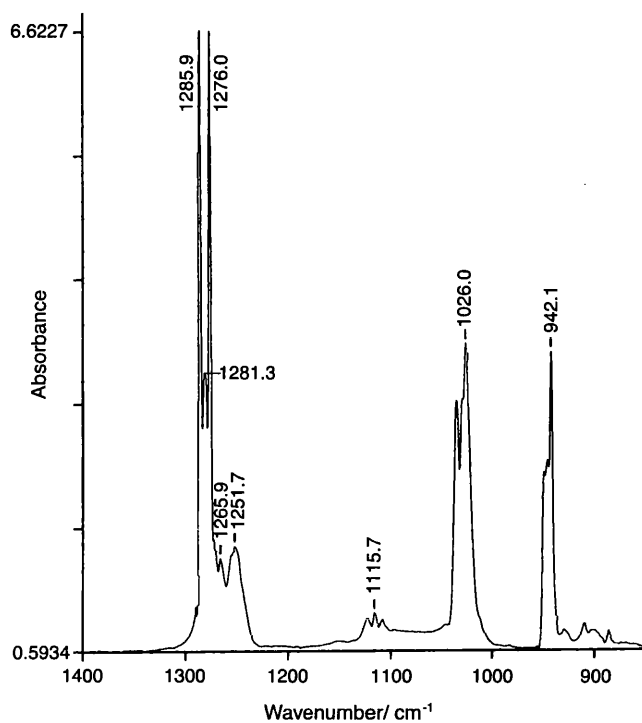
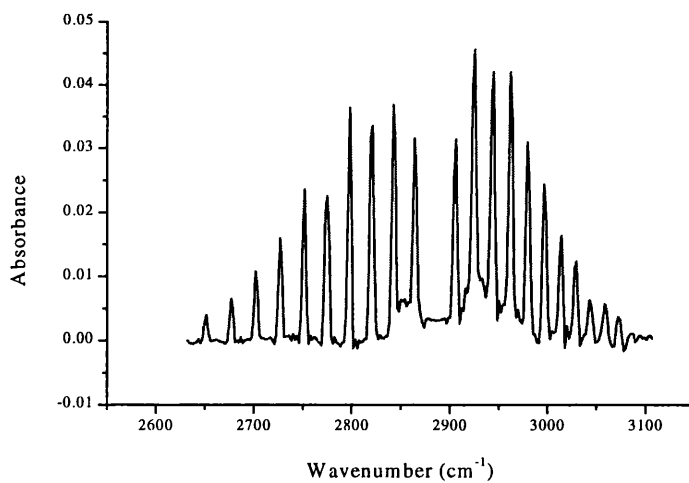


**Figure 4.1** FT-IR analysis of gas phase following reaction of  $\text{F}_2$  with diamond powder at 673 K



CF str



HCl str

**Figure 4.2** FT-IR analysis of gas phase following the reaction of ClF<sub>3</sub> with hydrogenated diamond powder at 673 K (HF also formed)

Table 4.1 FTIR spectroscopic analysis of the gas phase following the reaction of hydrogenated diamond powder and film with F<sub>2</sub> or ClF<sub>3</sub> under a range of conditions

Experimental conditions	Absorption (cm <sup>-1</sup> )	Assignment*
Diamond powder & F <sub>2</sub> at ambient temperature F <sub>2</sub> at 673 K	4000	V <sub>H-F</sub> (HF)
	4000	V <sub>H-F</sub> (HF)
	1295, 1288, 1282, 1276, 1272, 1269, 1264,	V <sub>C-F</sub> (Fluorocarbons)
	1256, 1252, 1247, 1228, 1220, 1166, 1035,	
	1028	V <sub>H-F</sub> (HF)
	Diamond film & F <sub>2</sub> at ambient temperature F <sub>2</sub> at 673 K	4000
4000		V <sub>C-F</sub> (Fluorocarbons)
1372, 1359, 1330, 1313, 1280, 1270, 1258,		V <sub>C-F</sub> (Fluorocarbons)
1248, 1220, 1209, 1153, 1122, 1108, 1034,		
1028, 1006, 901, 735		
ClF <sub>3</sub> at ambient temperature ClF <sub>3</sub> at 673 K	4000	V <sub>H-F</sub> (HF)
	4000	V <sub>H-F</sub> (HF)
	2891	V <sub>H-Cl</sub> (HCl)
	1285, 1281, 1276, 1265, 1251, 1122, 1115,	V <sub>C-F</sub> (Fluorocarbons)
	1035, 1026, 942	

\* Assignments were by comparison with literature spectra for model compounds (125-127)

These are typical results obtained for gas phase aliquots of 5-10 torr. Sample spectra are shown in figures 4.1 and 4.2.

These data suggested that abstraction of hydrogen and carbon atoms from the diamond surface occurred with the latter at 673 K only. These reactions were presumably accompanied by the formation of C-F bonding on the diamond surface. Hydrogen fluoride occurred under all conditions, a diagnostic peak at 4000 cm<sup>-1</sup> exhibiting rotational fine structure was observed. Small quantities of hydrogen chloride were observed following reaction with ClF<sub>3</sub> at 673 K. In the region of the infrared spectrum where C-F bonds absorb light, 800-1300 cm<sup>-1</sup>, an intense and complex feature was observed following reaction with both reagents at 673 K. These bands were thought to be attributable to a mixture of fluorocarbons; however precise assignment was difficult. An indication as to the species present was obtained by cross-referencing the data with literature values for C-F absorption (table 4.2).

**Table 4.2** Literature values (125-127) of the main absorptions for a range of simple fluorocarbons and derivatives

Key: vs: very strong, s: strong, m: medium and w: weak

Compound	Absorption (cm <sup>-1</sup> )
CF <sub>4</sub>	1283 (vs)
C <sub>2</sub> F <sub>6</sub>	1250 (vs) 1116 (s) 713 (w)
C <sub>3</sub> F <sub>8</sub>	1316 (m) 1262 (vs) 1209 (m) 1155 (s) 1117 (w) 1034 (s) 948 (m) 928 (w)
C <sub>4</sub> F <sub>10</sub>	1330 (w) 1290 (vs) 1260 (vs) 1220 (vs) 1160 (m) 1110 (m) 940 (m) 910 (m)
C <sub>5</sub> F <sub>12</sub>	1330 (w) 1260 (vs) 1220 (s) 1150 (m) 1130 (w) 1025 (s) 925 (w) 730 (s)
C <sub>2</sub> F <sub>4</sub>	1350 (w) 1261 (vs) 920 (m)
CHF <sub>3</sub>	3010 (w) 1350 (w) 1230 (w) 1220 (m) 1150 (s)
CF <sub>3</sub> Cl	1215 (vs) 1107 (s) 783 (w)
CF <sub>2</sub> ClCFClCF <sub>3</sub>	1278 (vs) 1237(s) 1131 (m) 1042 (s) 967 (m) 907 (w) 726 (m)

The values in bold type are those peaks, which were present in the literature spectra for a range of fluorocarbons and spectra recorded following reaction between diamond powder or film and  $F_2$  or  $ClF_3$  at 673 K. Clearly there was a range of potential products. The greatest agreement was observed with the first six compounds quoted with, in general, only the weak bands absent in the experimental spectra. Formation of C1-C5 fluorocarbons was evident. Hydrofluorocarbons were less evident due to an absence of C-H stretching but  $CHF_3$  could not be ruled out completely and chlorofluorocarbons may be present following reaction with  $ClF_3$ .

Other methods of analysis, such as GCMS or  $^{19}F$  NMR, were considered to elucidate further the identity of the products. However, for practical reasons these analyses were not performed; in addition it was considered that precise assignment of the reaction products was not of primary importance in this work.

Instead, further fluorine treatment of the etched powder surface was performed to determine if more carbon, in whatever form, could be removed or etched from the surface. FTIR analysis following reaction at 673 K with  $F_2$  or  $ClF_3$  revealed a massive reduction in C-F activity. Table 4.3 compares the intensity of selected absorptions in the C-F region after the first, second and a final third exposure to the fluorinating agent.

**Table 4.3** Infrared band intensities following successive exposure of hydrogenated diamond powder to F<sub>2</sub> or ClF<sub>3</sub>

Reagent	Absorption (cm <sup>-1</sup> )	Intensity (absorbance units)		
		1 <sup>ST</sup>	2 <sup>ND</sup>	3 <sup>RD</sup>
F <sub>2</sub>	1282	3.11	0.18	0
	1260	3.28	0.12	0
	1229	3.22	0.07	0
	1162	2.01	0.21	0
	1029	2.29	0.2	0
ClF <sub>3</sub>	942	3.49	0.26	0
	1035	3.02	0.11	0
	1276	6.62	0	0
	1281	3.31	0.74	0
	1285	6.63	0	0

The conditions used for sampling gas phase aliquots were kept as close to identical as practicable to ensure validity. The pressure of gas sampled was kept constant (10 Torr) and the same infrared cell was used for every measurement.

This table illustrates that upon exhaustive fluorination C-F containing products are not formed. A sharp decrease in C-F activity was observed following a

second exposure to the fluorinating agent and after a third exposure this had decreased to zero. A change in the behaviour of the diamond surface was apparent and removal of carbon was no longer occurring. The inert behaviour of the fluorinated diamond surface was comparable to that known for polytetrafluoroethylene where a sheath of fluorine atoms prevents further fluorination of the carbon backbone (127).

#### 4.1.2 Surface area analysis of diamond powder

The surface areas of a number of diamond powder samples were determined using the methods outlined in chapter 2 (2.1.11). The results obtained are reported in table 4.4.

**Table 4.4** Surface area analysis of various diamond powders

Sample	BET area ( $\text{m}^2\text{g}^{-1}$ )	BJH area ( $\text{m}^2\text{g}^{-1}$ )	A ( $\text{cm}^3\text{g}^{-1}$ )	B (nm)
Hydrogenated	12.9990	6.3995	0.0249	15.6171
Fluorinated	10.2126	12.8185	0.0646	20.1780
Oxygenated	14.3190	-	-	-

A: BJH desorption cumulative volume of pores between 1.7 and 300 nm in diameter

B: BJH desorption average pore diameter

The surface areas determined by the BET method, defined in section 2.1.11, varied across the sample range but the differences were not considered significant. Interestingly, BJH analysis suggested porosity. Inspection of pore volume distribution plots for these samples revealed a broad range of pores with small volume (figure 4.3). When compared with a highly porous material such as a zeolite, these pore volumes were an order of magnitude smaller. In addition a narrow range of pore sizes are observed for truly porous materials. Therefore, it was more likely that BJH analysis was indicating an irregular surface and not a porous material. Surface defects, grain boundaries or pitting are possible irregularities and, particularly in the case of the fluorinated diamond sample are, not insignificant. The cumulative surface area of pores for this sample was greater than the surface area measured using the BET method. In addition, there was an obvious distinction between the hydrogenated and fluorinated samples in terms of pore sizes with the cumulative volume of the latter three times larger than the former. The fluorination of this sample was performed at 673 K and increased surface irregularity may be a consequence of the etching reaction, which was evidenced in the FTIR study.

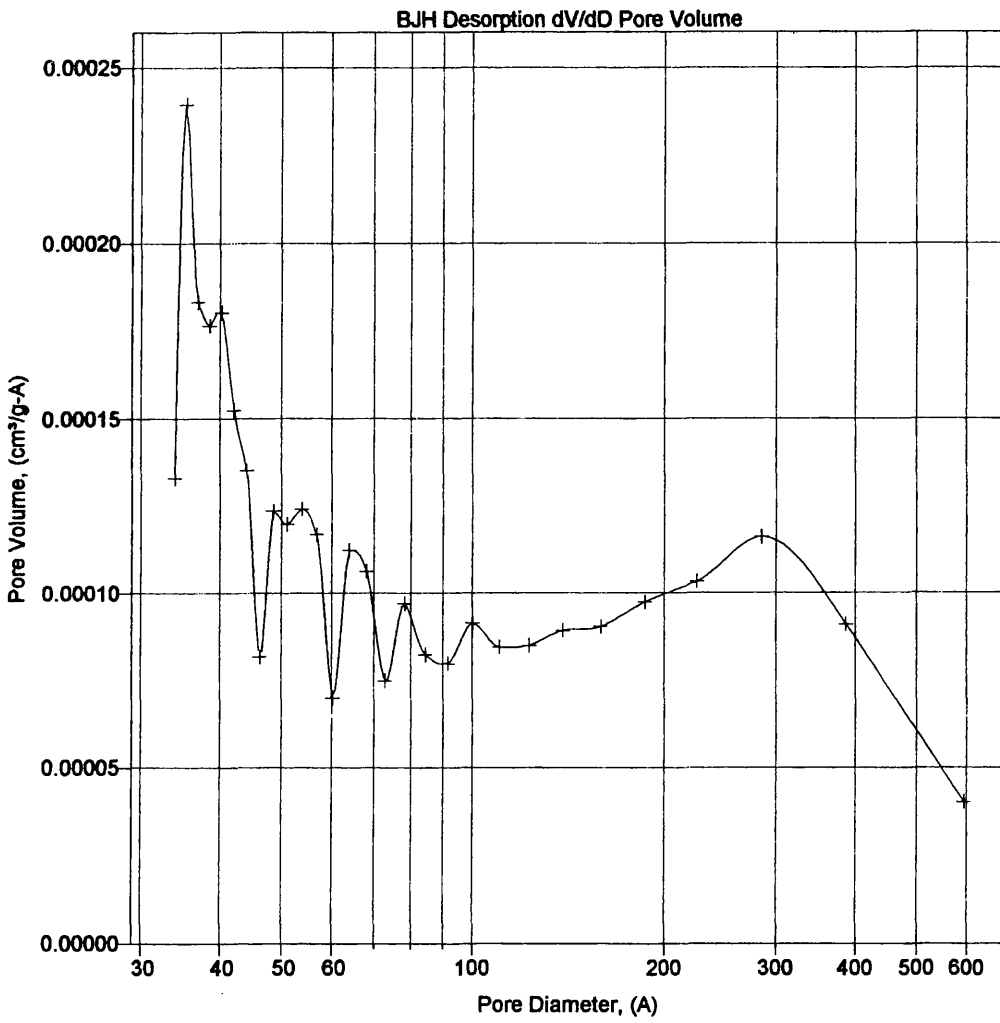


**Figure 4.3** Pore volume analysis of diamond powder

## 4.2 Diamond surface structure analysis following fluorination

### 4.2.1 Diffuse Reflectance Infrared Fourier Transform Spectroscopy, DRIFTS

The availability of this method for use in the present study was limited, for this reason analyses were performed on a restricted number of samples. The aim was to characterise the diamond surface after chemical treatment and confirm that the desired result had occurred. Spectra were recorded from powder samples (1 $\mu$ m) which had received hydrogenation, oxygenation and fluorination (F<sub>2</sub>) treatments with the expected result being surface termination in hydrogen, oxygen and fluorine respectively.

The data obtained are given in tables 4.5-4.7 and sample spectra are shown in figures 4.4-4.6.

**Table 4.5** DRIFTS analysis of hydrogenated diamond powder

$\nu_{\max}$ (cm <sup>-1</sup> )	Assignment
2937	$\nu_1(\text{CH asym str}) \text{CH}_2$
2860	$\nu_2(\text{CH sym str}) \text{CH}_3$
2837	$\nu_3(\text{CH sym str}) \text{CH}_2$

These band positions are in good agreement with literature (78-80) values for methylene (CH<sub>2</sub>) and methyl (CH<sub>3</sub>) surface groups; methine (CH) is believed to occur below a treatment temperature of 923 K but is not observed here. However, the presence of CH groupings cannot be ruled out since it is possible that the band at 2860 cm<sup>-1</sup>, attributed to the CH<sub>3</sub> symmetric stretching vibration, was masking the presence of the CH stretching vibration which would occur at 2780 cm<sup>-1</sup> (80). This was reasonable given that the treatment temperature in the present study was 1173 K and a significant concentration of CH<sub>3</sub> groupings are likely.

**Table 4.6** DRIFTS analysis of oxygenated diamond powder

$\nu_{\max}$ (cm <sup>-1</sup> )	Assignment
3453	$\nu(\text{OH str}) \text{H}_2\text{O}$
1774	$\nu(\text{C=O str}) \text{ROOCO, RCOR, RCOOH, RCOO}$
1645	$\nu(\text{OH bend}) \text{H}_2\text{O}$
1457	-
1128	$\nu(\text{C-O str}) \text{ROR}$

These results are again consistent with literature reports on the oxidation of hydrogenated diamond surfaces. The absence of CH stretching modes confirms the replacement of hydrogen with oxygen. In their paper (81) Ando *et al.* observed the survival of surface hydrogen up to an oxidation temperature of 673 K after which only oxygenated species were observed. In the present study the

oxidation temperature was 673 K and a similar result was obtained. Surface carbonyl groups result with a range of species possible as indicated above, a C-O moiety was also observed which is consistent with a cyclic ether grouping. The presence of hydroxyl stretching and bending modes can be explained as either the formation of surface OH groups or the adsorption of water molecules from the atmosphere. Both of these explanations are reasonable and it is likely that a combination of effects was occurring.

**Table 4.7** DRIFTS analysis of fluorinated diamond powder

$\nu_{\max}$ (cm <sup>-1</sup> )	Assignment
1358	$\nu_1(\text{CF})$ CF <sub>2</sub> and CF <sub>3</sub>
1260	$\nu_2(\text{CF})$ CF
1090	$\nu_3(\text{CF})$ CF

These data were acquired from a sample, which had received a hydrogenation treatment followed by fluorination using F<sub>2</sub> at 673 K. A spectrum was also acquired following room temperature fluorination, but this was less well defined exhibiting broad bands in the CF region. In both cases it is clear that a replacement of hydrogen for fluorine was occurring and, not surprisingly, the fluorination process was more extensive at higher temperature. It is also worth noting that, unlike the oxygenated surface, there was no evidence for adsorption of water confirming the expected hydrophobicity of the fluorine-terminated surface. Due to restrictions on the use of the DRIFTS method in this work, the

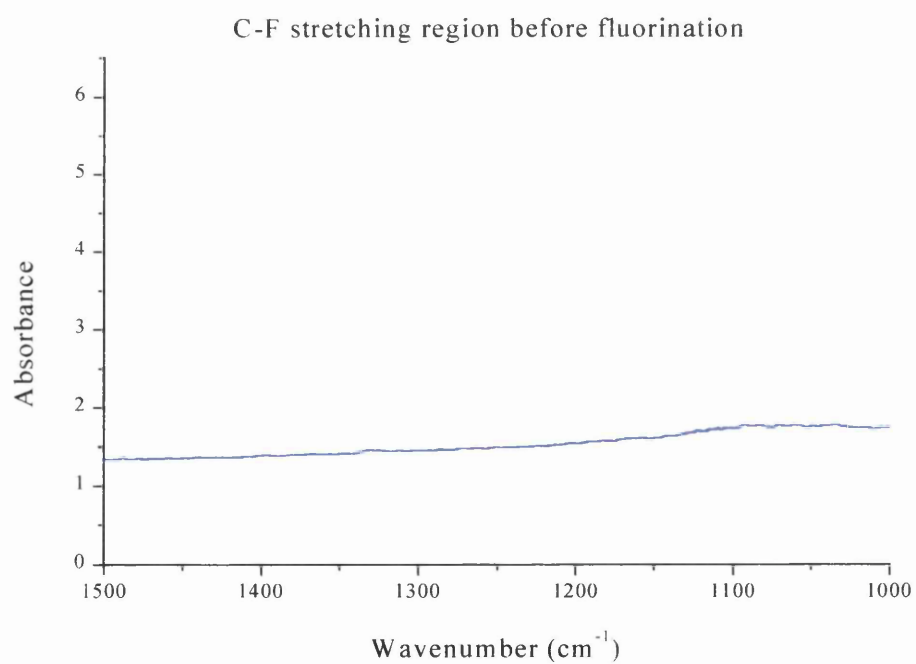
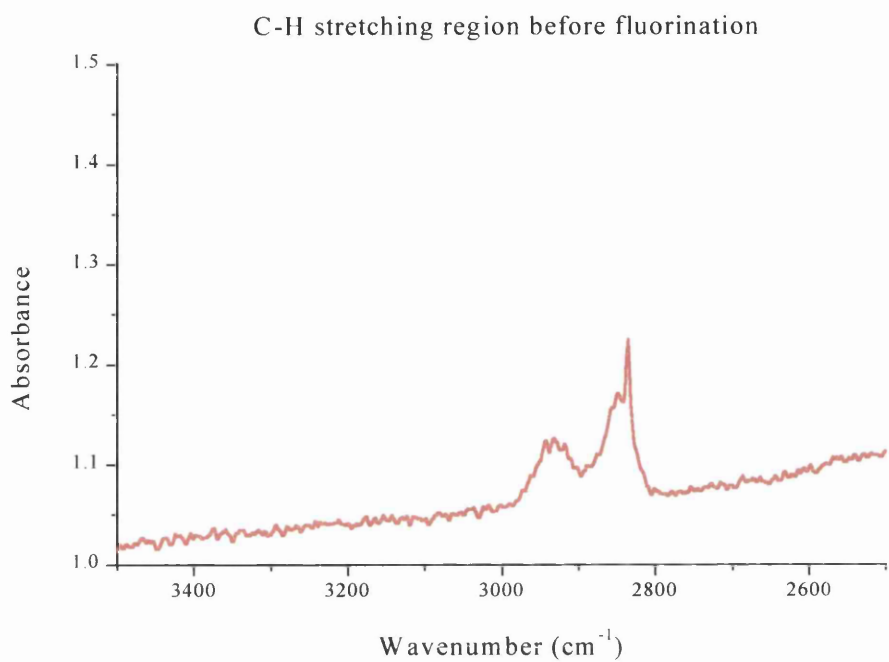


**Figure 4.4** DRIFT spectrum, in the C-H and C-F stretching regions, of a hydrogenated diamond powder surface prior to exposure to  $\text{F}_2$

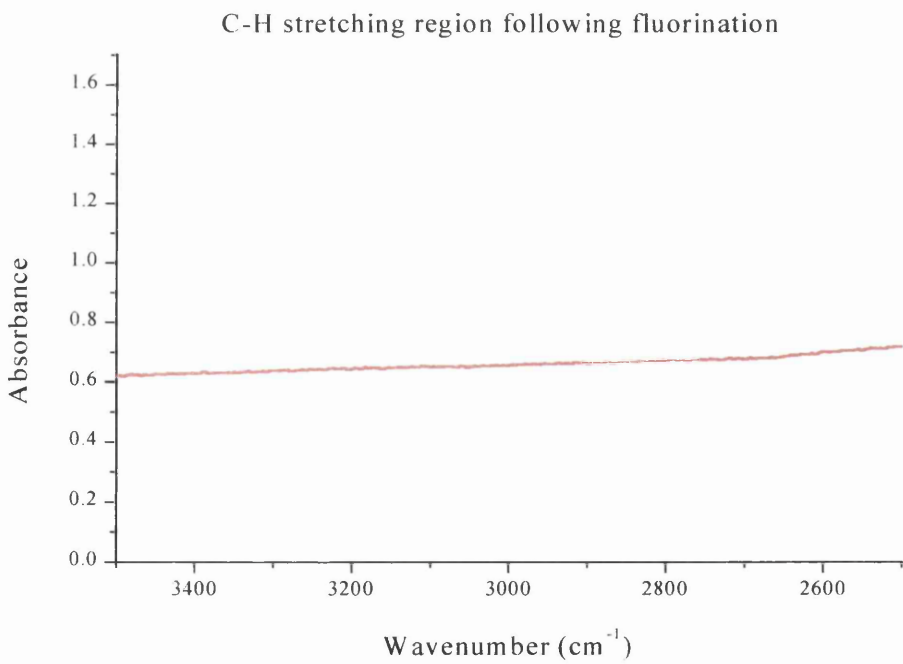
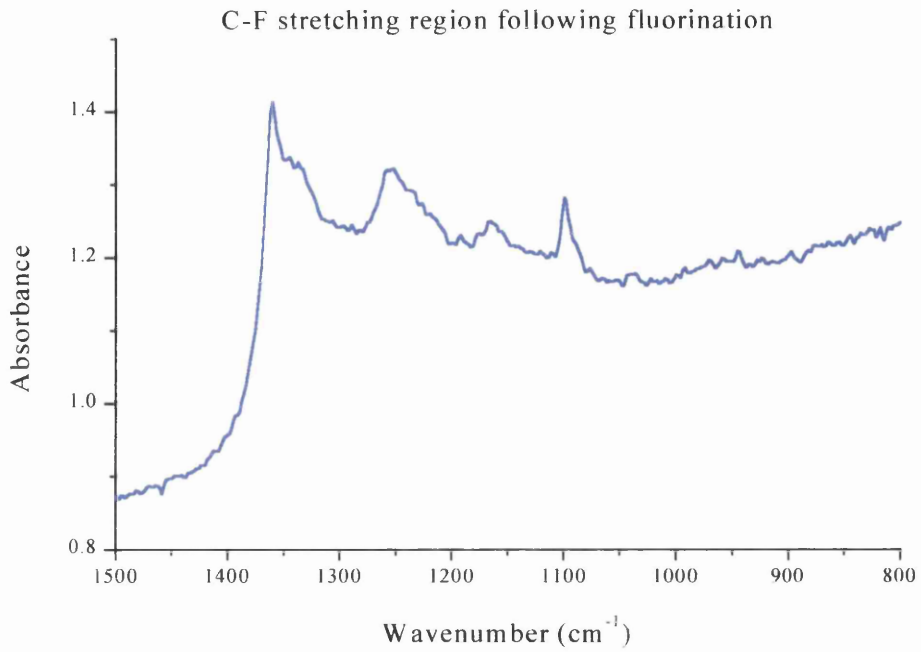


**Figure 4.5** DRIFT spectrum, in the C-F and C-H stretching regions, of a hydrogenated diamond powder surface after exposure to  $\text{F}_2$  at 673 K

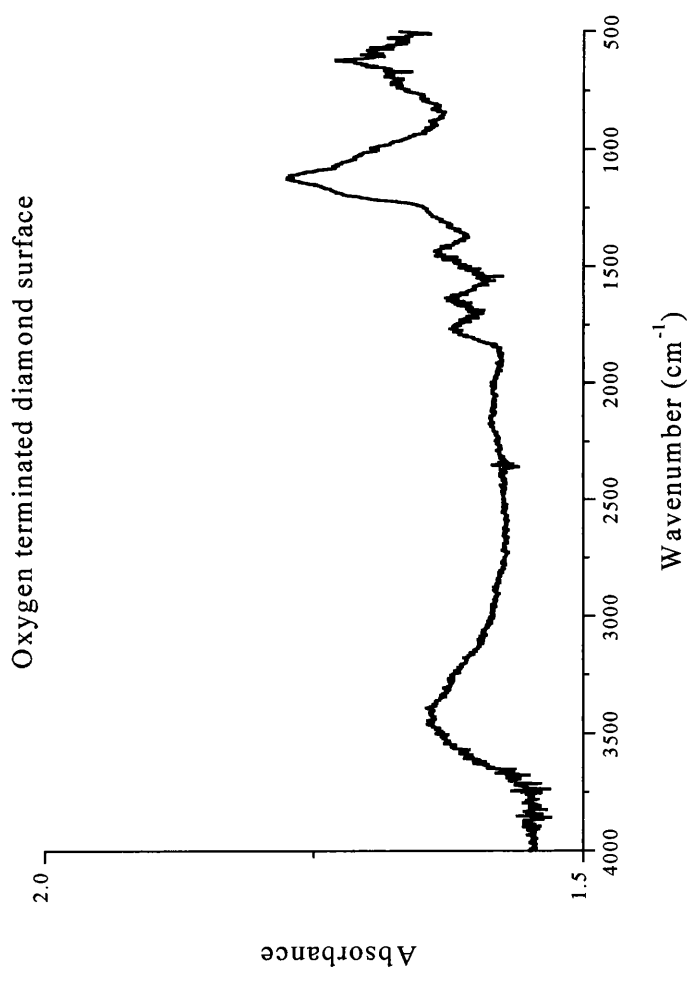


**Figure 4.6** DRIFTS analysis of diamond powder surface following oxygenation treatment

fluorination of oxygenated diamond was not studied, however other workers (90, 91) have shown that fluorination was more difficult with oxygen surviving on the surface below 773 K.

As a result of the DRIFTS study a high level of confidence in the experimental methods employed for the hydrogenation, oxygenation and fluorination of diamond surfaces was justified. In addition, the surface groups present following treatment could be reasonably well characterised and this information used to explain observations in later work.

#### **4.2.2 Scanning Electron Microscopy, SEM**

The FTIR analysis of the reaction between a hydrogenated diamond surface and  $F_2$  or  $ClF_3$  at 673 K suggested that, in the early stages of reaction, etching of carbon to produce fluorocarbons was an important feature. To investigate this further, the surface morphology of polycrystalline diamond film and powder samples, before and after treatment with  $F_2$ , was studied using SEM.

Figures 4.7-4.9 show SEM images acquired at various magnifications from three diamond film samples which had received hydrogenation,  $F_2$  at room temperature and  $F_2$  at 673 K treatments respectively. Figure 4.10 shows SEM images of a diamond powder sample before and after reaction with  $F_2$  at 673 K.

All samples were prepared from the same parent sample, film or batch of powder, to ensure that any significant change in surface morphology, as result of reaction would be easily detectable.

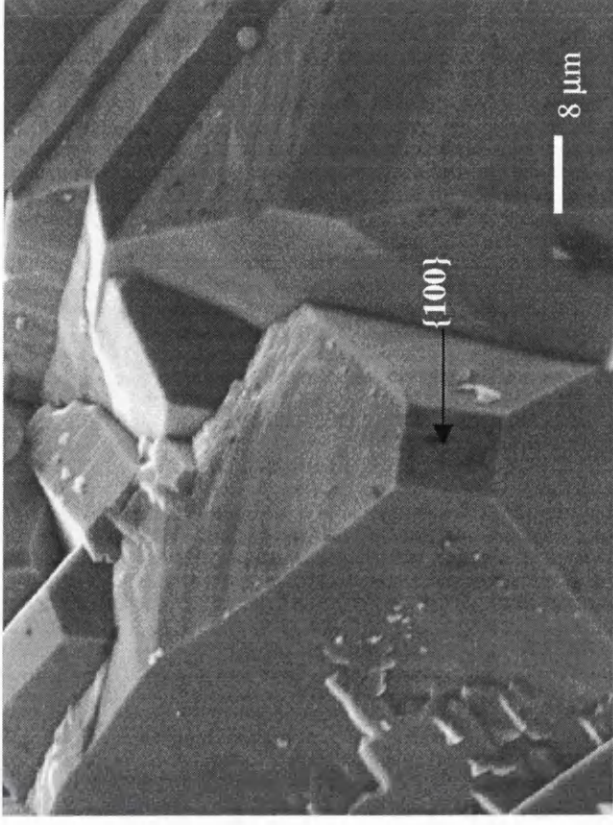
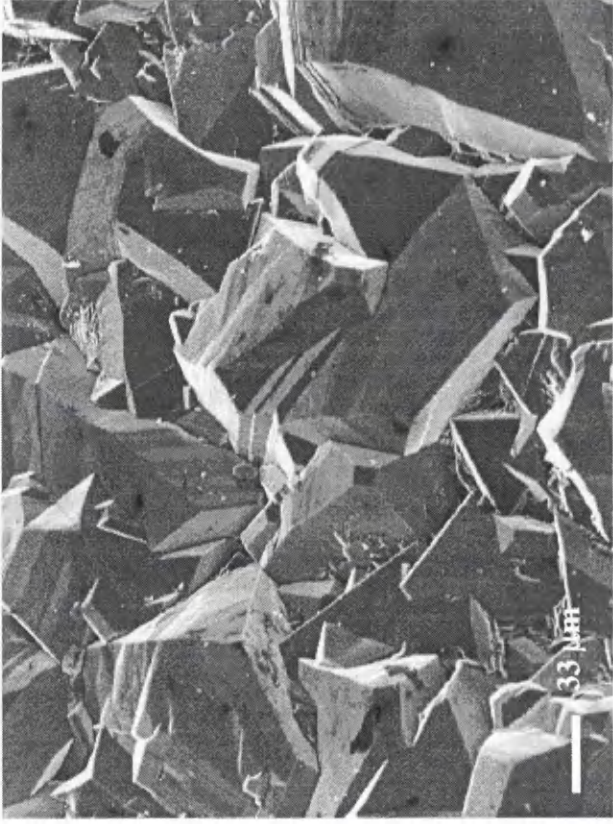


**Figure 4.7** Surface morphology of diamond film following hydrogenation and an example of a {100} type crystal plane

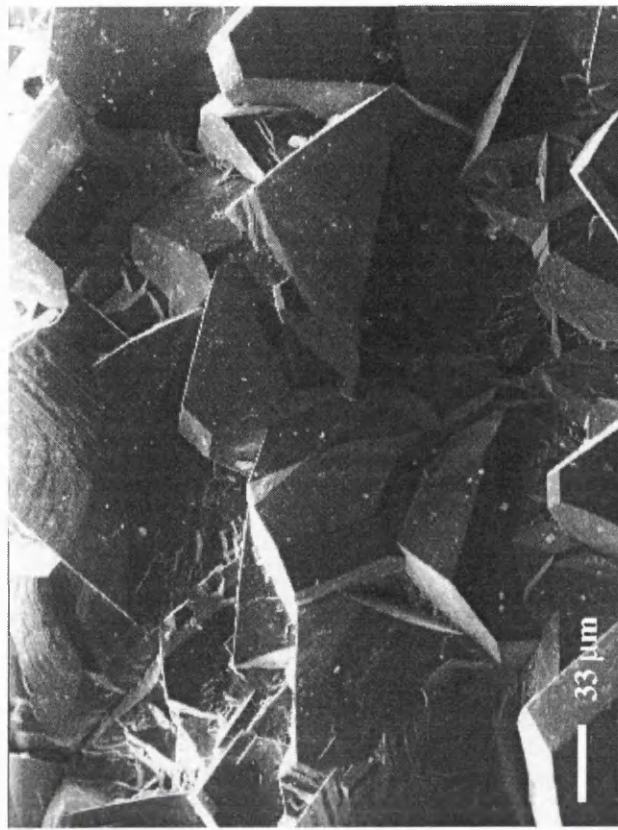
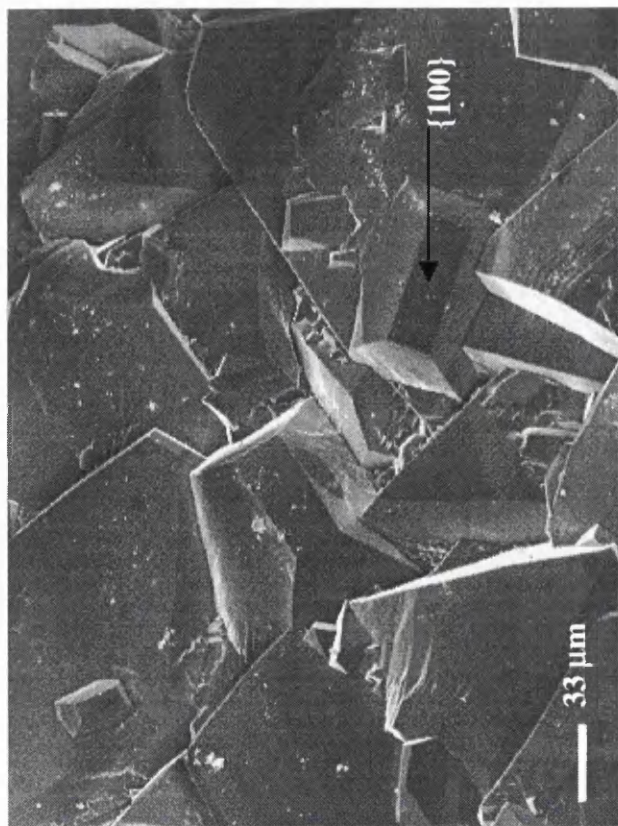


**Figure 4.8** Diamond film surface morphology following treatment with F<sub>2</sub> at ambient temperature (left) and 673 K (right)

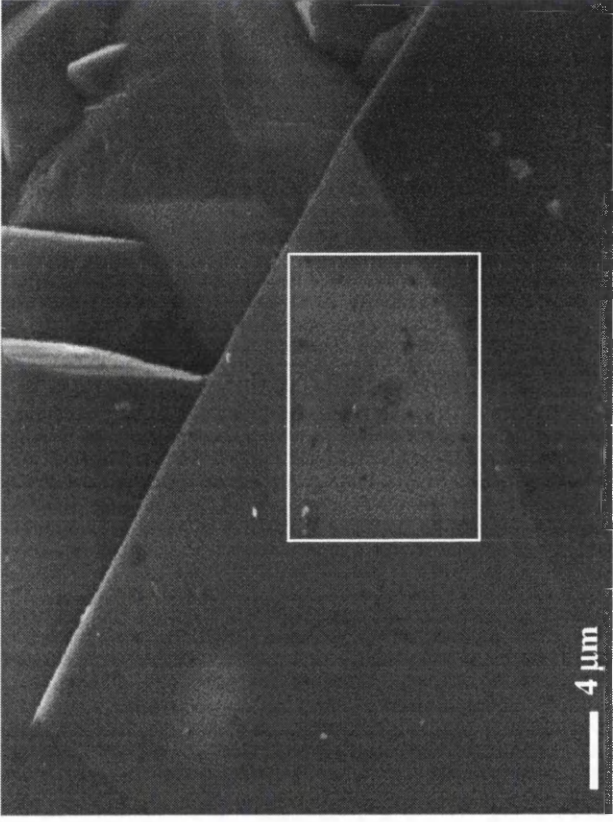


**Figure 4.9** Apparent removal of a surface layer in the electron beam

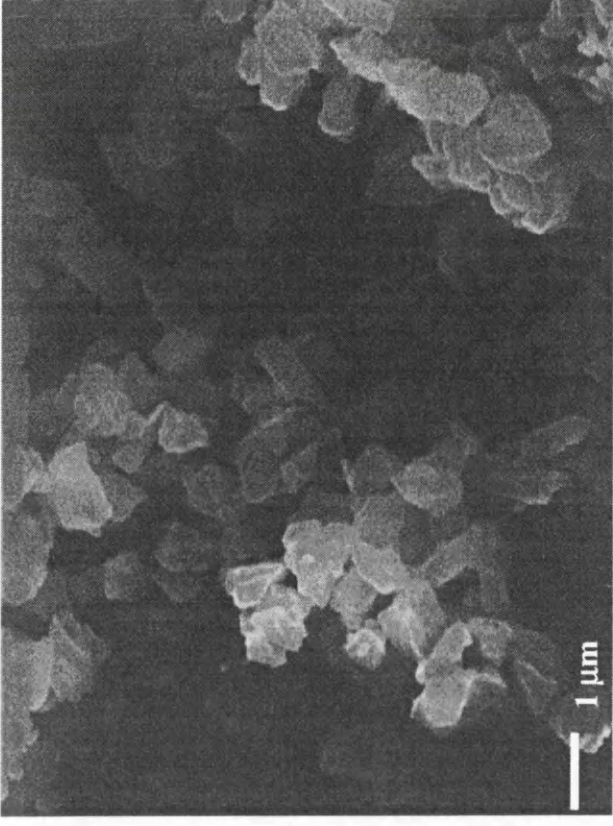
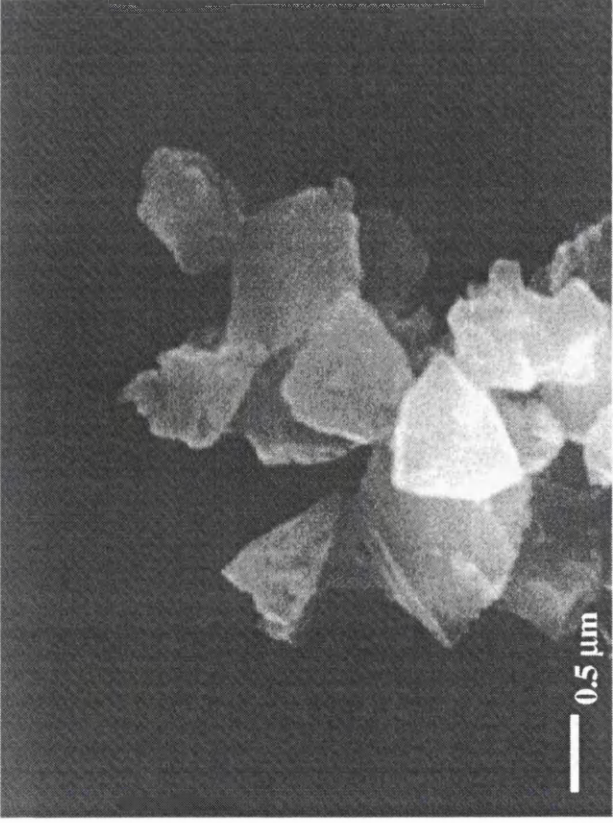


**Figure 4.10** Morphology of diamond powder (1 μm) particles before and after difluorine treatment at 673 K

The images shown in figure 4.7 illustrate clearly the polycrystalline nature of the diamond film sample; crystallites are orientated in various directions, which is a result of random nucleation in the CVD growth process (chapter 1).

It can also be seen that the surface could be described as a combination of {100}, {110} and {111} type crystal planes. A {100} type plane is highlighted. This was important for comparison, since much of the literature studies involving diamond surface chemistry has been performed on distinct crystal planes.

Following difluorine treatment at ambient temperature or 673 K the SEM images obtained (figure 4.8) illustrate that the gross surface morphology of the film surface has been preserved. The crystallites were still faceted, with well defined crystal planes evident.

Despite the fact that the FTIR study showed the production of fluorocarbon products following reaction at this temperature, there was no evidence of pitting or rounding of peaks which would be expected if the reaction was extensive. In contrast, the reaction of polycrystalline diamond film with molecular oxygen at 723 K results in a severely pitted surface with the formation of CO and CO<sub>2</sub> (85).

The gross morphology of the diamond surface following fluorine treatment was apparently unchanged, but there was some evidence that the chemical nature of

the surface was different. Unlike the other materials, the surface appeared to be susceptible to electron beam damage (Fig 4.9).

The square area indicated on the image occurred following focussing of the microscope and shows the apparent removal of a surface layer. The identity of this surface layer could not be determined here, however fluorination to produce CF species is known to occur on powder surfaces and evidence for this has been obtained here using DRIFTS (4.2.1). It was therefore likely that the electron beam was causing the removal of fluorine atoms and or fluorocarbon species from the fluorine-terminated film surface.

The examination of diamond powder samples before and after treatment with difluorine has also been performed (figure 4.10). These images provided useful information with regard to the morphology of powder particles. Inspection of the images revealed the presence of particles that are non-spherical and show evidence of facets. However, the particles are not perfectly faceted and there is some evidence of irregular surfaces. Following difluorine treatment at ambient and elevated temperatures, there was still evidence for faceted particles. In agreement with studies performed on diamond film surfaces, the pictures before and after reaction with  $F_2$  were similar, suggesting the absence of a massive etching reaction. In figure 4.11 possible sites from which etching may occur are shown.

SEM proved a useful way of investigating the surface morphology of diamond, polycrystalline films and powders. The qualitative information obtained could

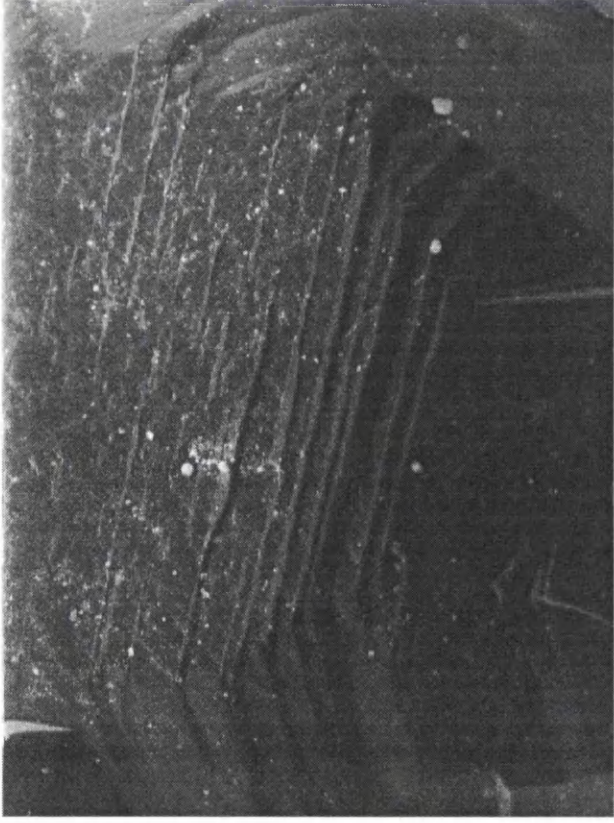


**Figure 4.11** Step-like structure and grain boundaries on the surface of polycrystalline diamond film

be used to model the interactions of diamond surfaces and fluorinating reagents. The results have also provided some physical evidence for the formation of a surface resistant to massive etching in the reaction between difluorine and diamond.

However, it was important in this work to obtain a profile of the extent of reaction between the diamond surface and difluorine on the atomic scale. This could be done using x-ray photoelectron spectroscopy (XPS).

The debris observed on the fluorinated film surfaces (figure 4.8) was determined using energy-dispersive x-ray (EDX) analysis to be  $\text{NiF}_2$  contamination, the main cause of which was the Ni sample boat. Using a Teflon sample boat and also by coating the inner surface of the reactor using a Teflon spray eliminated this problem. Whilst the contamination was on a microscopic scale this measure was considered worthwhile since sample preparation for XPS analysis was intended.

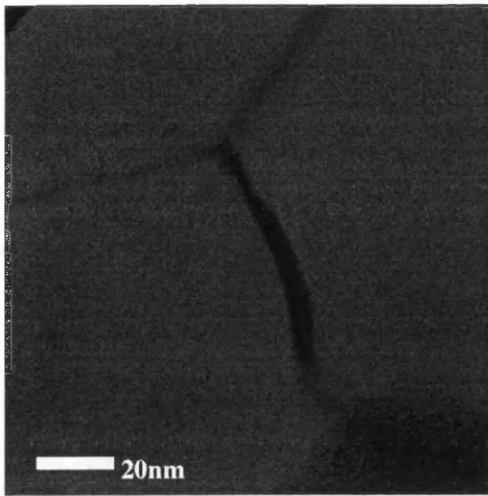
### 4.2.3 Energy Filtered Transmission Electron Microscopy, EFTEM

This technique allows bonding level maps of bulk materials to be produced and the information obtained is very useful for monitoring any changes in bonding as a result of chemical reaction. In this study, changes in carbon hybridisation, due to fluorination was the feature of interest. Figure 4.12 shows the  $sp^2$  and  $sp^3$  maps obtained for as grown and fluorine ( $ClF_3$ ) treated diamond film samples respectively. The theory behind the use of this technique and its practical application in this work has been discussed in section 2.1.11.

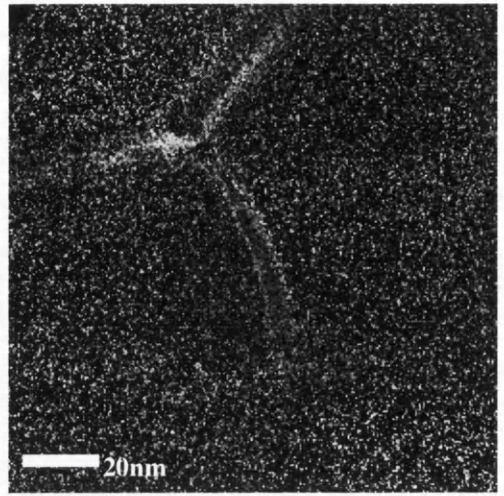
Examination of the micrographs obtained for the untreated sample revealed the presence of  $sp^2$  hybridised carbon at the grain boundary. This is observed as a region of bright contrast on the  $sp^2$  map and a region of dark contrast on the  $sp^3$  map. The EELS spectrum in the boundary region showed a peak representing the  $\sigma \rightarrow \pi^*$  transition in addition to the  $\sigma \rightarrow \sigma^*$  transition. In the bulk region of the grain only  $sp^3$  bonding is present and the EELS spectrum showed only the  $\sigma \rightarrow \sigma^*$  transition.

Given the results obtained on the as-grown sample it was reasonable to predict a high degree of  $sp^2$  hybridised carbon at grain edges such as the one examined on the fluorine treated sample. Inspection of the micrographs obtained from the fluorine treated sample revealed that there was no evidence for  $sp^2$  carbon at the grain edge, instead of a bright contrast, noise was observed.

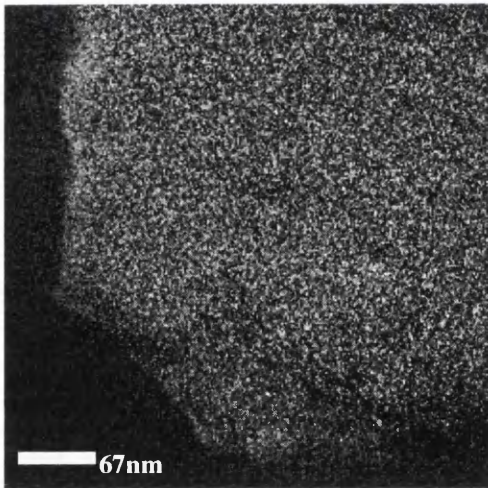
The absence of  $sp^2$  carbon on the fluorine treated sample can be explained as a result of reaction with  $ClF_3$  to produce carbon-fluorine bonding. It was also



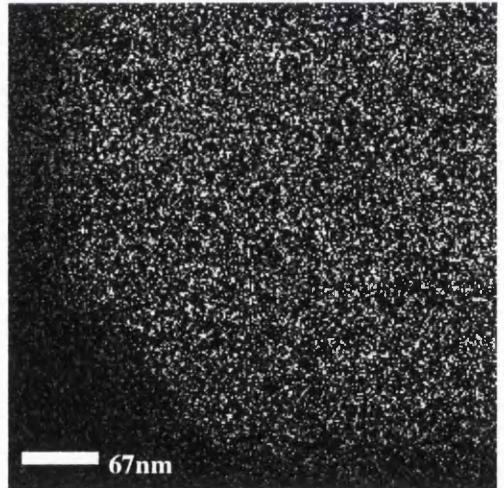
sp<sup>3</sup> map



sp<sup>2</sup> map



sp<sup>3</sup> map



sp<sup>2</sup> map

**Figure 4.12** EFTEM analysis of diamond film, as-made (top) and fluorinated (bottom) samples

clear that graphitisation was not a feature of the fluorination reaction and the surface was most likely terminated with atoms of fluorine.

The EFTEM study provided new information on the nature of fluorination reactions between diamond surfaces and highly aggressive reagents like  $F_2$  and  $ClF_3$ . The involvement of  $sp^2$  hybridised carbon, present at defects or cracks cannot be ignored. Hydrogenation would be expected to remove most, if not all, graphitic carbon. However, if the hydrogenation was incomplete or graphite formation occurred after hydrogenation as a result of the clipping of dangling bonds for example, then the fluorination of  $sp^2$  hybridised carbon becomes important. Such  $sp^2$  hybridised carbon is likely to react preferentially to  $sp^3$  hybridised carbon in the early stages of reaction. This means that grain boundaries or edges will be the high-energy sites where initial reaction is favoured. An etching reaction to produce fluorocarbons is possible and, if unlimited, a large pit would be formed. The SEM study showed that pitting did not occur on a gross scale, supporting the FTIR evidence for a self-limiting reaction. However, EFTEM showed that surface defects such as cracks can occur and pore volume analysis of fluorinated diamond powders indicated an irregular surface. Whilst the etching reaction was not apparent on a gross scale, as already highlighted, it was important to establish the chemistry on the nanometre scale.

#### **4.2.4 X-ray Photoelectron Spectroscopy, XPS**

The use of this method for the analysis of fluorinated carbon materials is commonplace with many literature examples (86, 87, 105-109). As a result, an

extensive source of reference data was available for comparison with the experimental data obtained in this work. Some of the more important reference data is given in table 4.8.

**Table 4.8** C(1s) binding energy shifts for a range of fluorinated carbons (105-109)

Carbon material (normalised C(1s) binding energy eV)	Binding energy shift (+eV)	Assignment
Fluoropolymers (285)	Primary effects	
	3.0	CF
	6.1	CF <sub>2</sub>
	7.7	CF <sub>3</sub>
	Secondary or β-effects (additive)	
	0.6	R <sub>3</sub> C-CF or CF <sub>x</sub> -CF
1.4	FC-R <sub>2</sub> C-CF or R <sub>3</sub> C-CF <sub>2</sub> or CF-CF <sub>x</sub> -CF or F <sub>x</sub> C-CF <sub>2</sub>	
Graphite fluorides (284.4)	6.1	CF [(CF) <sub>n</sub> ]
	5.8	CF [(C <sub>2</sub> F) <sub>n</sub> ]
	7.8	CF <sub>2</sub> [(CF) <sub>n</sub> ]
	8.1	CF <sub>2</sub> [(C <sub>2</sub> F) <sub>n</sub> ]
	9.8	CF <sub>3</sub> [(CF) <sub>n</sub> , (C <sub>2</sub> F) <sub>n</sub> ]
Carbon black (284.4)	3.8	CF
	5.8	CF <sub>2</sub>
	7.9	CF <sub>3</sub>
Pitch carbon (284.4)	5.8	CF
	7.8	CF <sub>2</sub>
	9.8	CF <sub>3</sub>
Carbon fibre (284.6)	3.0-4.6	CF
	4.3-7.3	CF <sub>2</sub>
	7.1-11.7	CF <sub>3</sub>

As can be seen from the data presented in table 4.8, fluorination of carbon results in shifting of the C(1s) binding energy to higher values. This is because the electronegative fluorine atom removes electron density from the carbon atom,

which causes the effective charge per electron ( $Z_{\text{eff}}$ ) in the C(1s) shell to be increased. As a result, the 1s core electrons of the carbon atom are held more tightly to the nucleus and more energy is required for their ejection. The size of the binding energy shift depends principally on the number of fluorine atoms bound to the carbon atom. The degree of fluorination is often a result of the conditions employed, as in the case of carbon fibre where higher C(1s) binding energies were observed when more vigorous conditions were employed. It is also clear that the surrounding environment of the carbon atom in question is important, secondary effects can further shift the binding energy. This feature must be considered whenever an extensive reaction is expected.

The F(1s) binding energy also increases with increased fluorination, but the effect is much less marked compared with C(1s). As more fluorine atoms are added to the carbon atom, the electron density of the carbon must be shared, this results in a reduction of electron density about the fluorine atoms of a CF<sub>2</sub> compared with the fluorine atom of a CF group, and an increase in the binding energy of the F(1s) core electron. In practice, differentiating among CF, CF<sub>2</sub> and CF<sub>3</sub> groups using F(1s) data is difficult, therefore assignments are usually made on the basis of the C(1s) data. The F(1s) binding energy is still useful since it provides some information as to the type of bonding present, a value of around 684 eV occurs for ionic species (e.g LiF) whilst a higher value of 689 eV suggests covalent bonding (e.g CF graphite fluoride). Table 4.8 has been used in conjunction with the experimental data obtained in this work, providing a good indication as to the identity of the diamond surface species resulting from the fluorination reaction.

Previous XPS studies involving diamond have investigated the chemisorption of hydrogen, oxygen and halogen atoms on well defined single crystal surfaces (section 1.5). Fluorine chemisorption (86, 87) was characterised by the appearance of a shoulder on the high energy side of the bulk carbon peak in the C(1s) spectrum. This feature, occurring at 286.8 eV (Binding energy shift: +1.8 eV), has been attributed to a carbon-monofluoride (CF) species which forms an adlayer with a coverage of about three-quarters of a monolayer. There was no evidence for more highly fluorinated species like CF<sub>2</sub> or CF<sub>3</sub> and, when compared with the data presented in table 4.8, a binding energy shift of 1.8 eV is smaller than expected for the formation of a covalent C-F bond. This was rationalised as being a consequence of the less than monolayer coverage, presumably due to the absence of a significant secondary effect (87).

In this work, the fluorination of polycrystalline diamond film was investigated under the conditions outlined in section 2.1.11, the raw C(1s) and F(1s) data obtained are presented in figures 4.13-4.16. Inspection of these raw spectra revealed that the C(1s) binding energy envelopes were composed of subpeaks, the primary indication of this was a non-gaussian peak shape. Fitting of the C(1s) and F(1s) data, using a peak fitting module available with Origin data analysis and technical graphics packages (Microcal<sup>TM</sup> Software, Inc.), has been performed and the results are presented alongside the raw binding energies ( $E_B$ ) in table 4.9. The fitting procedure employed was as outlined in section 2.1.11. The quality of the fit was determined by inspecting the residual spectrum, which

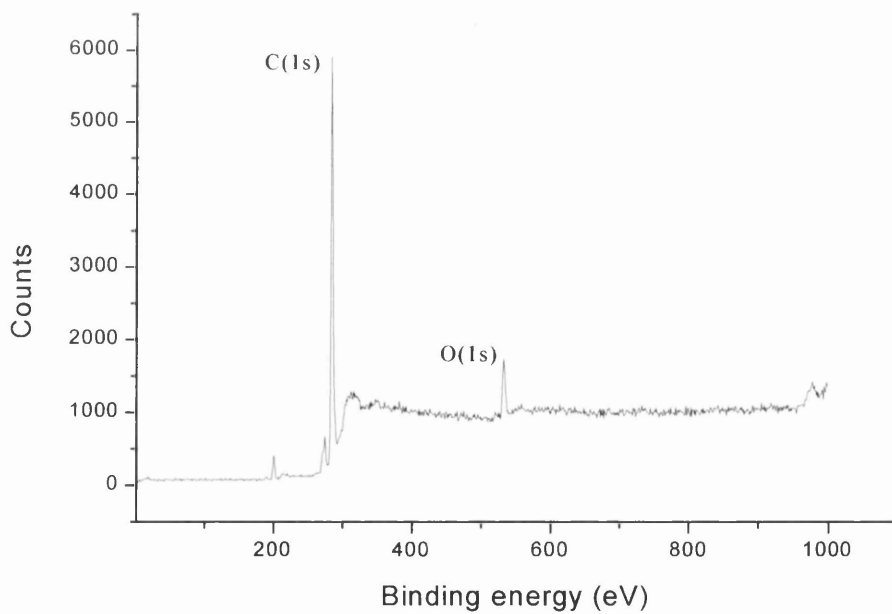
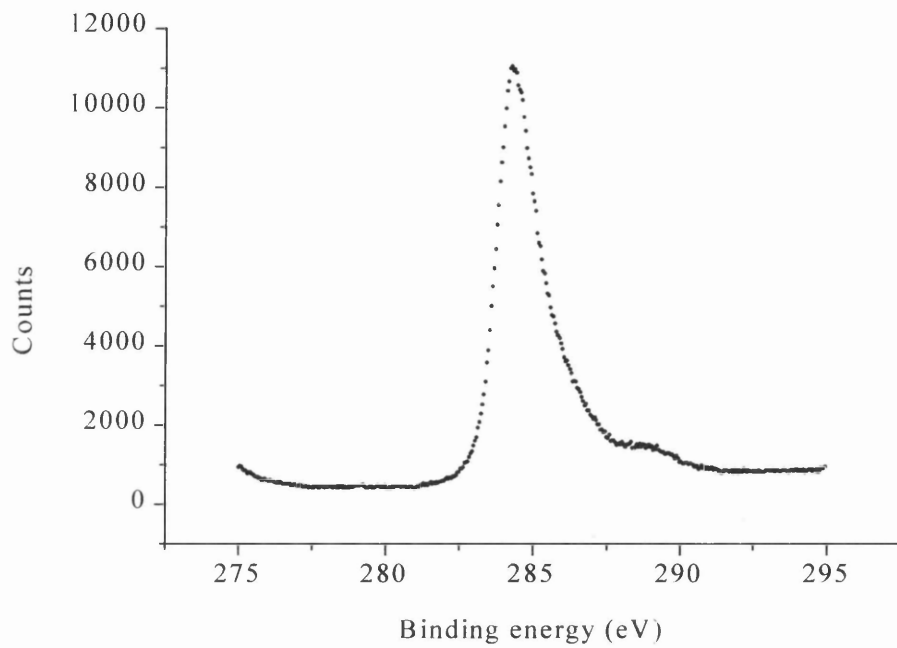


**Figure 4.13** C(1s) binding energy envelope and long range XPS spectrum obtained from analysis of hydrogenated diamond film

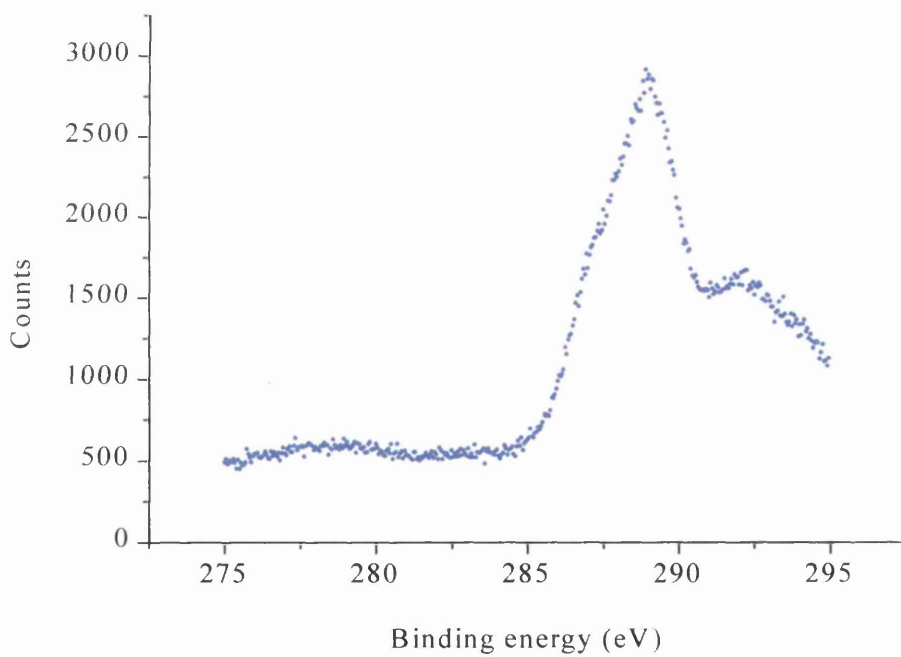
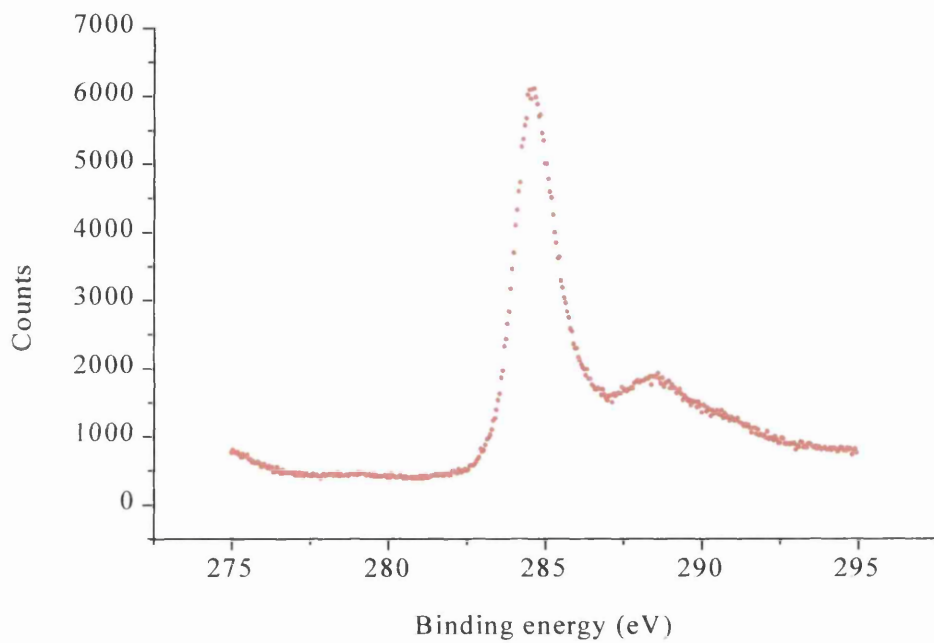


**Figure 4.14** C(1s) binding energy envelopes for diamond film following exposure to F<sub>2</sub> at ambient temperature (red line) and 523 K (blue line)

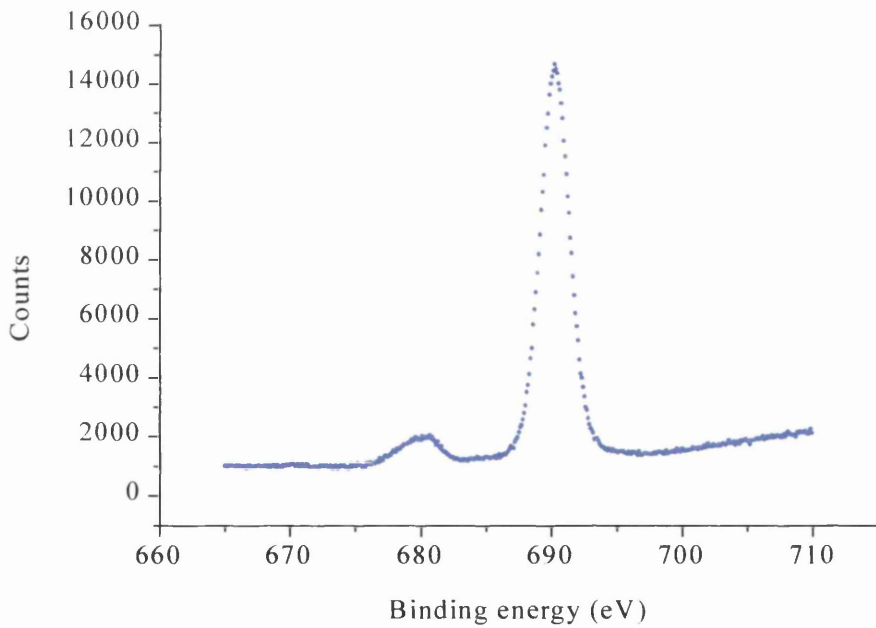
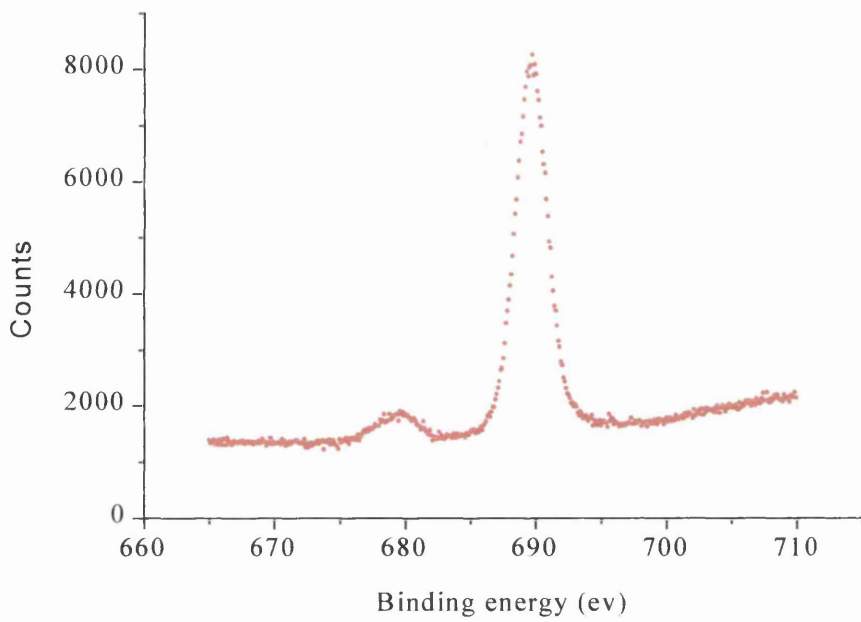


**Figure 4.15** F(1s) binding energy envelopes for diamond film following exposure to  $F_2$  at ambient temperature (red line) and 523 K (blue line)

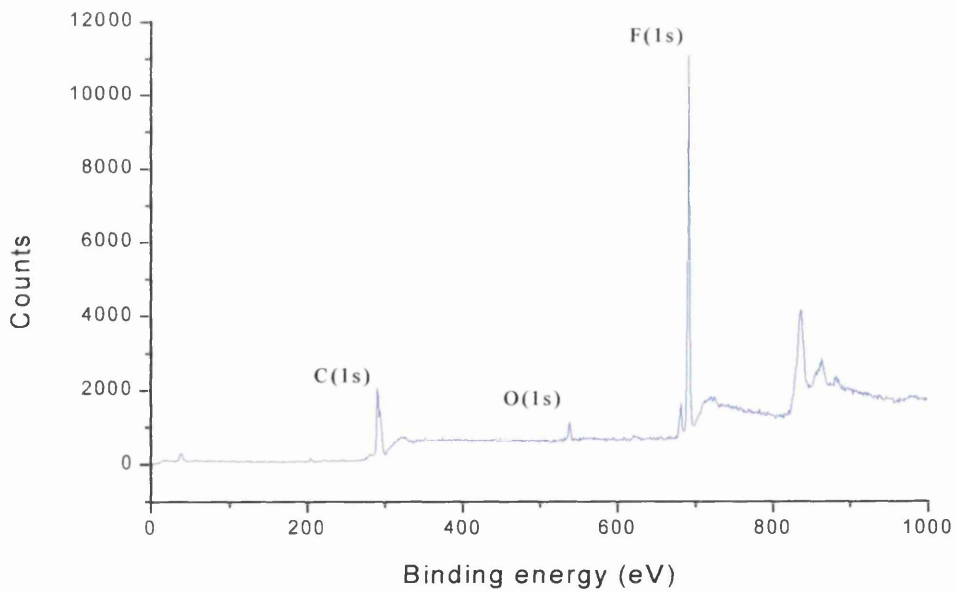
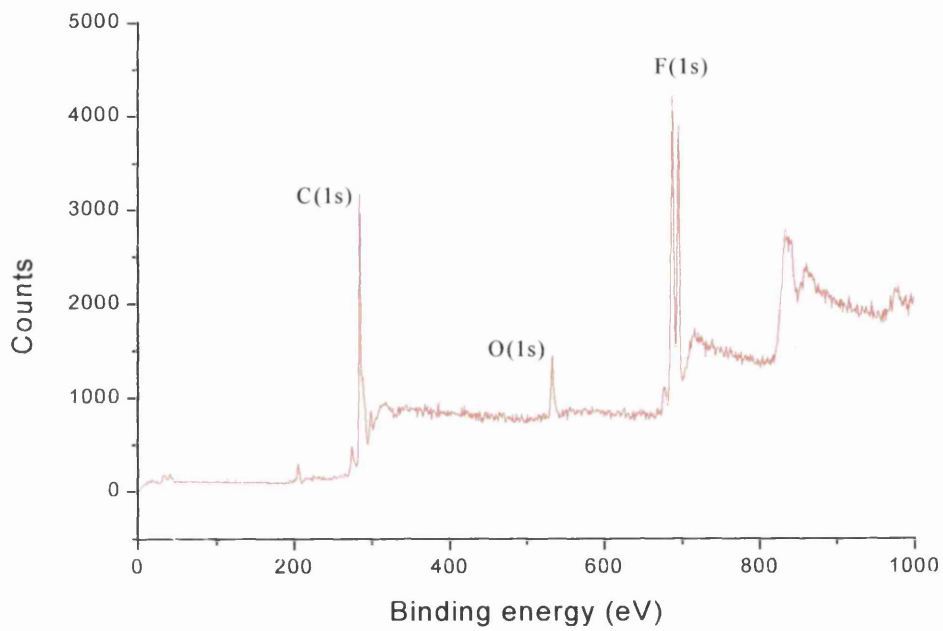


**Figure 4.16** Long range XPS analysis of diamond film following exposure to F<sub>2</sub> at ambient temperature (red line) and 523 K (blue line)

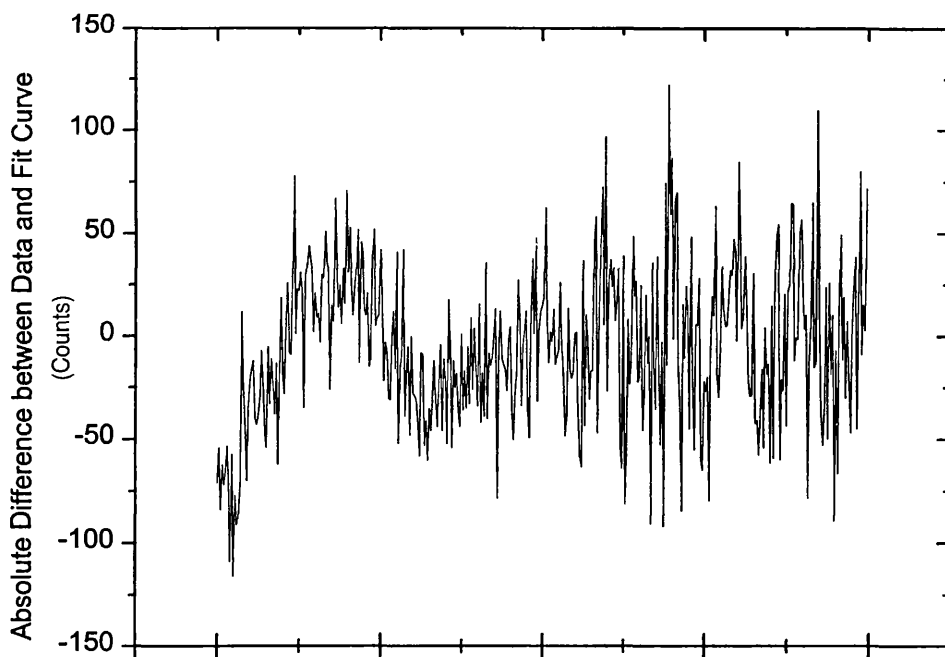
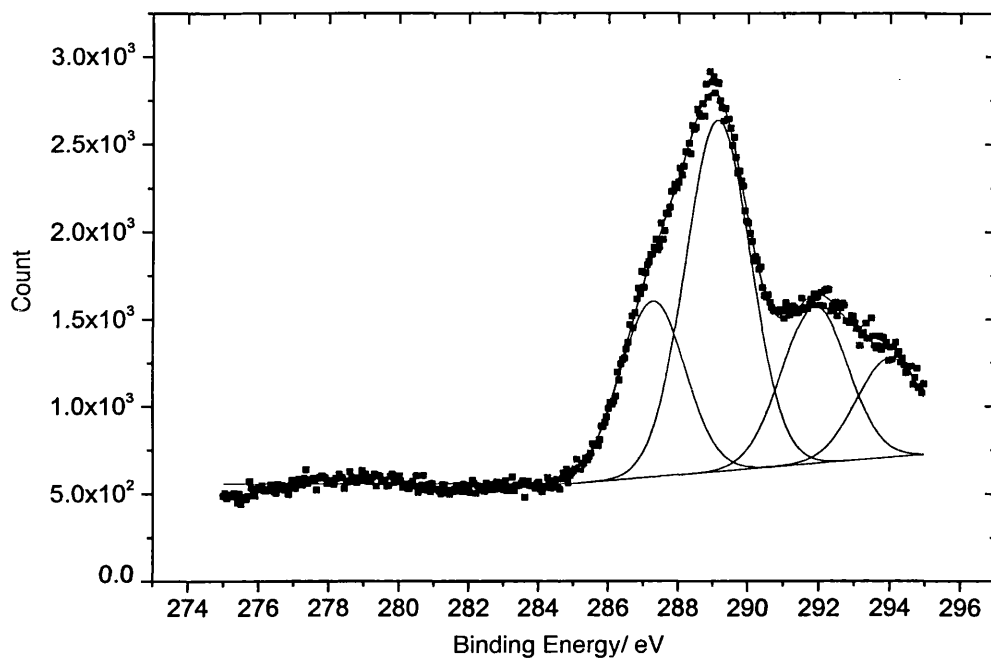


**Figure 4.17** XPS fit data for C(1s) peak of diamond sample fluorinated at 523 K

represents the difference between the experimental and fitted data. An example of a fitted spectrum and its residual is given in figures 4.17.

**Table 4.9** C(1s) and F(1s) binding energy data for fluorinated diamond film

Sample	C(1s) E <sub>B</sub> (eV)		F(1s) E <sub>B</sub> (eV)
	Raw	Fitted	
Reference (Hydrogenated)	284.3	284.3	-
	288.3	285.1	
		286.5	
		288.3	
Fluorinated RT	284.7	284.4	689.7
	288.6	285.1	
		286.4	
		288.4	
Fluorinated 523 K	288.9	287.2	690.2
	292.2	289.1	
		291.8	
		294.0	

There were a number of important observations to be made following examination of this data. In agreement with previous studies, fluorine treatment resulted in the formation of peaks in the C(1s) binding energy envelope which

were shifted to higher binding energy. Fluorine was present on the surface as evidenced by the strong peaks in the F(1s) region. The main component of the C(1s) binding energy envelope (centred on approx. 284.4 eV) for the reference and room temperature, F<sub>2</sub> treated, samples could not be fitted to a single Gaussian function. A good fit could only be obtained by the addition of a second gaussian function at 285.1 eV. This would appear to suggest that 2 forms of carbon are present at the surface region of the sample; however great care must be taken in this analysis since the C(1s) binding energy is known to be difficult to measure accurately (69) and depends among other things upon the method used to calibrate the spectrometer. In this regard, the method used in the present study, involving calibration on the photoelectron lines of the gold coat, is thought to be the most reliable method in the XPS analysis of insulating materials.

Laser raman spectra (R2000 spectrometer, Perkin Elmer, Institute of Inorganic Chemistry, LMU, Munich, Germany) of hydrogenated and fluorinated diamond film and powder samples were characterised by the appearance of a sharp peak at 1332 cm<sup>-1</sup> only, with no evidence for non-diamond carbon forms such as graphite in the 1500-1600 cm<sup>-1</sup> region of the spectra. This observation is entirely consistent with DRIFTS evidence obtained (section 4.2.1) for termination of the diamond surface with hydrogen or fluorine.

Remarkably, following reaction at 523 K, there was no evidence for non-shifted or bulk carbon in the C (1s) XPS spectrum (figure 4.14) i.e. there was no peak at 284 eV. The C(1s) binding energy shifts, from the main component (284.4 eV)

of the C(1s) binding energy envelope, and assignments are given in table 4.10 which is followed by some explanation regarding the assignments made.

**Table 4.10** C(1s) binding energy shifts ( $\Delta E_B$ ) and assignments for a range of diamond film samples

Sample	$\Delta E_B$ (+eV)	Assignment	F/C ratio
Reference	2.2	COH or COC	
	4.0	CO	
Fluorinated RT	2.1	CF and COH or COC	$0.31 \pm 0.006$
	4.1	CO and CF	
	6.3	CF <sub>2</sub>	
Fluorinated 523 K	2.9	CF	$1.13 \pm 0.02$
	4.6	CO and CF	
	7.4	CF <sub>2</sub>	
	9.5	CF <sub>3</sub>	

These data represent shifts from the bulk carbon peak, which was centred on 284.3 eV and can be explained as follows. For the reference sample, the weak shoulder on the high energy side of the main component could be fitted to two peaks at 286.5 eV and 288.3 eV. These were attributed to oxygenated species as shown. It was standard practice, when performing XPS analysis, to record a long-range (0-1000 eV) spectrum to examine the gross features, the long-range spectra obtained for the three diamond samples are shown figures 4.13 and 4.16.

The presence of oxygen was confirmed in the long-range spectrum with a weak peak occurring at 533 eV. Assignments were made in accordance with literature (69) values for CO bonding. Following fluorination at room temperature, a similar situation was observed and the high-energy shifted shoulder fitted to three subpeaks at 286.4, 288.4 and 290.6 eV, which were assigned as shown. As before, the long-range spectrum revealed the presence of surface oxygen at the slightly shifted value of 534 eV and a new peak at 689.7 eV, which was due to covalently bound fluorine atoms. Interestingly, this peak appeared to be split into two separate components, however the F(1s) binding energy envelope (figure 4.15) for both F<sub>2</sub> treated samples could be fitted to a single gaussian function.

The occurrence of oxygen made precise assignment of the C(1s) subpeaks difficult, since CO and CF groups occur at a similar binding energy. However, there was no doubt that a large amount of fluorine was present and given the small intensity of the O (1s) peak in the long range spectrum, it was reasonable to predict that the contribution, from CO species, to the peaks at 286.4 and 288.4 eV was small.

The C(1s) binding energy envelope following fluorination at 523 K was greatly altered when compared with the reference and room temperature fluorine treated samples. Interestingly, there was no peak at 284.4 eV, which represents C-H or C-C groups present at the diamond surface and bulk regions. This strongly suggests the occurrence of a reaction, which proceeds beyond the first layer of carbon atoms on the diamond surface, involving fluorination of bulk material. The parent peak could be well fitted to four sub-peaks, which were

assigned as shown. The assignments for the CF, CF<sub>2</sub> and CF<sub>3</sub> groupings were in good agreement with the reference data (table 4.8) and indicative of a highly fluorinated material exhibiting secondary effects. Secondary effects are those caused by the presence of other CF groupings in the local environment. Once more the long-range spectrum revealed the presence of oxygen at the shifted value of 538 eV; it was also notable that the intensity of the oxygen peak was further reduced when compared with the room temperature fluorine treated sample. A very strong fluorine peak was observed at 690.2 eV confirming the presence of surface fluorine. Secondary effects were the likely cause of shifting of the oxygen binding energy, whilst replacement of oxygen for fluorine at 523 K would account for the reduction in signal intensity and the absence of COC groupings which are less stable to F<sub>2</sub> than C=O groups.

The F/C ratios for both F<sub>2</sub> treated samples are also shown in table 4.10; these were calculated using equation 2.13. These numbers represent the ratio of fluorine to carbon in the region of the sample from which photoemission can be detected. In the case of the room temperature, F<sub>2</sub> treated sample; an F/C value of 0.31 indicates the presence of fluorinated and non-fluorinated carbon. In contrast, an F/C value of 1.13 for the sample treated with F<sub>2</sub> at 523 K suggests that, on average every carbon is bonded to 1.13 fluorine atoms. In reality, this is not possible and the value of 1.13 is indicative of the presence of CF<sub>2</sub> and/or CF<sub>3</sub> groups, in addition to CF, which is in good agreement with the fit data for the sample.

It is generally accepted that the XPS sampling depth varies from a minimum given by the inelastic mean free path of the photoelectron,  $\lambda$ , to a maximum of three times the inelastic mean free path of the photoelectron,  $3\lambda$  (69, 110). The actual value is dependent upon factors such as the position of the detector relative to the sample. The upper limit represents the depth into the sampling for which 95% of the total photoemission is detected.

In this work,  $\lambda$  could be estimated using equation 2.12, taking the monolayer thickness as an average of the interplanar distances for the {100}, {110} and {111} crystal planes of diamond, 2.715 angstroms. The result is a value of approximately 7 angstroms for  $\lambda$  and therefore a range on the XPS sampling depth of 7 to 21 angstroms. Clearly, calculations of  $\lambda$  will be most accurate for photoemission from a monocrystalline surface where the monolayer thickness is known. In this work, the material is a polycrystalline diamond film, it was therefore necessary to use an average value for the monolayer thickness to account for the range crystal surfaces which are present. The {100}, {110} and {111} planes were chosen since, the SEM analysis performed in this work (section 4.2.2) and other studies in diamond film surface morphology (section 1.2) have suggested that the {100}, {110} and {111} types are dominant on the polycrystalline material.

It should be stressed that the range of sampling depths quoted above will be subject to some error as a result of the method used to evaluate  $\lambda$  and is only a first approximation which can be used in the analysis of the XPS results obtained. In this regard, the depth into the diamond sample where fluorine

occurs following reaction at 523 K can be considered to be at least 7 to 21 angstroms. This is indicative of a fluorination reaction, which proceeds to the subsurface region of the diamond sample, resulting in the fluorination of 2.5-7.7 layers (evaluated using an average monolayer thickness of 2.715 angstroms). The implications of this result are considered further in the next chapter of this thesis.

Whilst the results presented in sections 4.2.1-4.2.4 enable the nature of the diamond surface after reaction with  $F_2$  and related reagents to be described in some detail, FTIR, microscopy and XPS do not yield any direct information concerning the subsequent chemical behaviour of a fluorinated diamond surface. By making analogies with the known properties of perfluorocarbon polymers (105) and highly fluorinated carbon compounds such as graphite fluorides (108), it could be argued that these surfaces will be highly hydrophobic and, therefore, not interact to any great extent with polar molecules. It can also be reasonably assumed that surface C-F bonds in  $CF$ ,  $CF_2$  and  $CF_3$  groups will be kinetically inert with respect to substitution. Radiotracer experiments using  $H^{18}F$  were performed in order to provide direct evidence for these postulations and to compare the behaviour of diamond surfaces terminated with  $-H$ ,  $-O$  or  $-F$  towards the highly polar molecule  $H-F$ . This part of the work has also enabled the behaviour of  $HF$  as a fluorinating agent towards diamond to be assessed.

#### 4.2.5 The reaction of various diamond powders with anhydrous fluorine – 18 radiolabelled hydrogen fluoride vapour, H<sup>18</sup>F, under a range of conditions

##### 4.2.5.1 Handling of fluorine-18 raw counting data

There were four factors to be considered here:

- (i) Decay correction
- (ii) Counting error
- (iii) H<sup>18</sup>F specific activity
- (iv) Weight of diamond sample

The aim of this section is to illustrate the conversion of raw counting data into fluorine uptake, measured in mmol g<sup>-1</sup>.

As a consequence of the relatively short fluorine-18 half-life, experimental counting data must be corrected for decay. The radioactive decay law, equation 2.17, was used to do this. The corrected count was then converted into a count rate, dividing by the counting time in seconds. This yields a quantity with units, count sec<sup>-1</sup>.

In this work, the counting error is given as  $\sqrt{n}$  where  $n$  is the experimental count, in practice  $n$  was large due to high fluorine-18 activities. In all cases, greater than 10,000 counts were achieved in less than 600 seconds (10 minutes) with the large majority in the 60-150 second range. Only those samples exhibiting small fluorine uptake required longer counting times. As a result, the relative error on the experimental count ( $\sqrt{n}/n \times 100\%$ ) was small (0.75-1.5%).

The specific count rate is the activity of a known amount of radiolabelled material and is expressed in count sec<sup>-1</sup> mmol<sup>-1</sup>. This quantity was used to convert the activity measured on a diamond sample from a corrected count rate (count sec<sup>-1</sup>) into a fluorine uptake value expressed in millimoles (mmol). Finally, since the diamond sample weight (g) was known, fluorine uptake values could be expressed in millimoles per gram (mmol g<sup>-1</sup>). In this work all counts were obtained for solids which maximises the efficiency of the counter and hence the accuracy of the results, this is why H<sup>18</sup>F vapour was counted as its solid CsF adduct, CsF:H<sup>18</sup>F. An example of these data handling steps is given in table 4.11, illustrating clearly the method employed. Unless otherwise stated this method was used exclusively.

**Table 4.11** Fluorine-18 data handling example

Experimental count	10240 ± 101
Decay time from experimental t <sub>0</sub> (min)	247
Decay corrected count	= 10240/ e <sup>-(0.0063x247)</sup> = 10240/0.21 = 48761 ± 481
Counting time (sec)	130
Count rate (count sec <sup>-1</sup> )	= 48761/130 = 375 ± 3.7
Sample mass (g)	0.62
Count rate per gram of sample	= 1/0.62 x 375 = 604.8 ± 5.97
Specific Activity of H <sup>18</sup> F determined independently (count sec <sup>-1</sup> mmol <sup>-1</sup> )	723 ± 3.47
Fluorine uptake (mmol g <sup>-1</sup> )	= 604.8/723 = 0.836 ± 0.0047

The results quoted above were measured for an oxygenated diamond powder sample following reaction with H<sup>18</sup>F at room temperature. As shown, an experimental count of greater than 10000 was achieved in just over 2 minutes

even after 4 hours into the experiment. This example represents data obtained towards the end of the experimental day and was chosen to illustrate the reliability of the technique.

The relative error, best calculated for the experimental count to avoid artificial minimisation of the error, is  $\pm 0.99\%$ . This value has been used to calculate the error on all values shown above except the fluorine uptake value where a combination of the error on the sample activity and that on the specific activity was calculated.

Fluorine uptake studies were performed for a range of diamond powder (1 $\mu$ m particle size) surfaces, which had been defined chemically using the methods outlined earlier in this chapter. Specifically, the surfaces studied were hydrogen, oxygen and fluorine terminated. The conditions employed for hydrogenation and oxygenation treatments of diamond samples were constant (section 2.1.2); however the conditions for fluorine treatment of the diamond sample could be varied in a number of ways (Table 2.3):

1. Before all fluorine treatments the diamond sample was first given a hydrogen or oxygen treatment.
2. Reaction temperature: the fluorine treatment was performed at ambient temperature and at 573 K
3. The reagent used for fluorine treatment could be varied; in this work  $F_2$ ,  $ClF_3$  and HF were the reagents employed.

Each reaction was repeated at least once to establish reproducibility, in a few cases further repeat reactions were possible, providing a larger dataset. Unfortunately, due to time constraints and the large number of reactions for study, this was not always possible. However, similarities in the trends observed for each surface type made it possible to make conclusions with some confidence.

The data obtained and the themes that emerged are presented now, with each surface type handled in turn.

#### 4.2.5.2 Hydrogen-terminated diamond powder surfaces

**Table 4.12** Fluorine uptake data measured on hydrogen-terminated diamond surfaces following reaction with anhydrous H<sup>18</sup>F vapour

Sample	Reaction temperature	Fluorine uptake (mmol g <sup>-1</sup> )
1	Ambient	0.578 ± 0.008
2		0.821 ± 0.004
3		0.600 ± 0.003
4		0.739 ± 0.003
5		0.909 ± 0.008
6	573 K	0.577 ± 0.003
7		0.518 ± 0.002
8		0.458 ± 0.002
9		0.359 ± 0.003
10		0.489 ± 0.001

As shown in this table, there was a significant reaction between hydrogen-terminated diamond surfaces and anhydrous H<sup>18</sup>F vapour under the conditions described. This was unexpected; therefore the reaction was studied extensively to ensure the results were real and to establish reproducibility. Consequently, it can be seen that fluorine uptake ranges from 0.57-0.89 and 0.36-0.58 mmol g<sup>-1</sup> following reaction at room temperature and 573 K respectively. There was some data scatter, which is common in this type of study and most likely due to

variations in the behaviour of the HF vapour on a given working day. Taking account of data scatter it can be seen that fluorine uptake was greatest following reaction at room temperature. This is highlighted in figure 4.18, which also illustrates the variation in uptake observed on different working days.

#### 4.2.5.3 Oxygen-terminated diamond surfaces

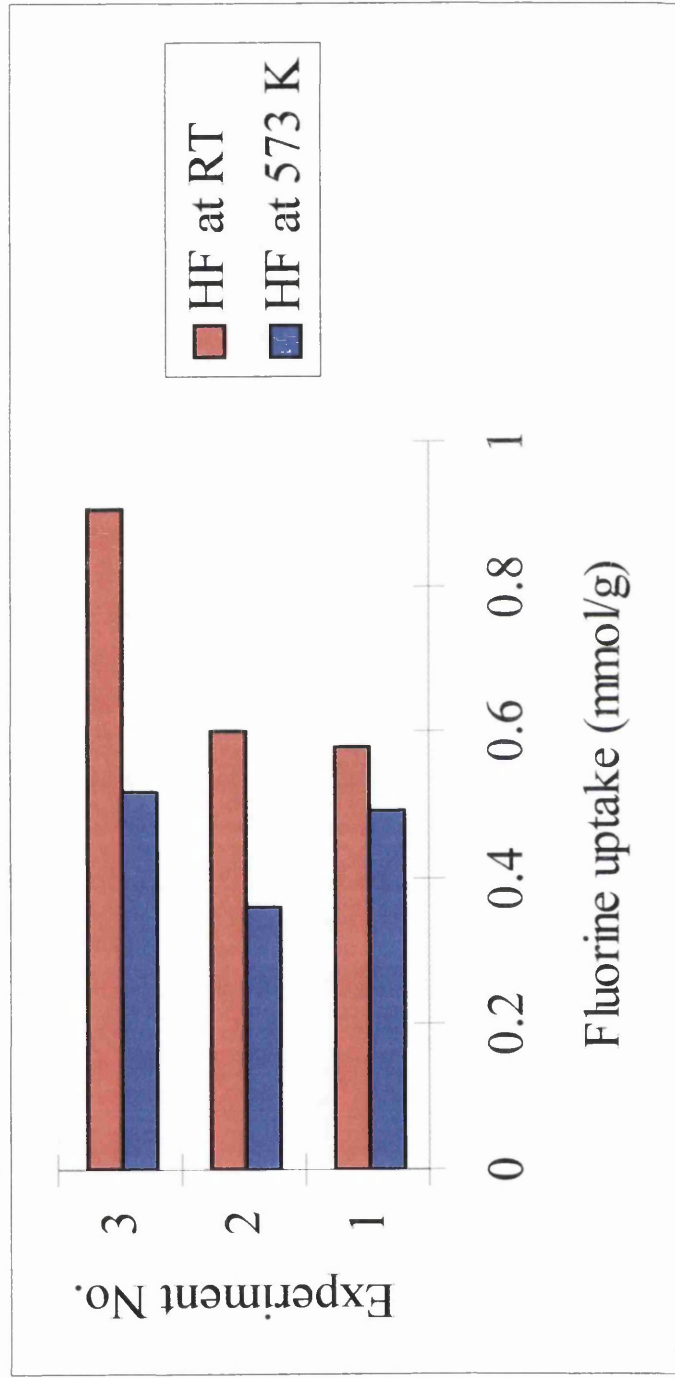
These results (table 4.13) were similar to those obtained for hydrogen-terminated surfaces, with comparable fluorine uptake values. This indicated that a significant reaction had occurred on the oxygen-terminated surface also. The fluorine uptake was consistently greater following reaction at room temperature agreeing with the general pattern observed previously for hydrogen-terminated surfaces.

**Table 4.13** Fluorine uptake data measured on oxygen-terminated diamond surfaces following reaction with  $\text{H}^{18}\text{F}$  vapour under various conditions

Sample	Reaction temperature	Fluorine uptake ( $\text{mmol g}^{-1}$ )
11	Ambient	$0.836 \pm 0.004$
12		$1.116 \pm 0.003$
13		$0.939 \pm 0.002$
14	573 K	$0.435 \pm 0.002$
15		$0.649 \pm 0.003$
16		$0.510 \pm 0.002$

**Figure 4.18**

Variations in fluorine uptake on hydrogen-terminated diamond powder following exposure to anhydrous  $\text{H}^{18}\text{F}$  vapour



This was an unusual feature and not predicted in the light of work presented earlier in this chapter. In the reaction of powder or film surfaces with F<sub>2</sub> there was clear evidence, using DRIFTS and ESCA analysis, for greater fluorination at higher reaction temperatures.

#### 4.2.5.4 Fluorine-terminated diamond surfaces

An obvious distinction in the behaviour of HF and F<sub>2</sub> towards diamond was apparent and several methods, including exchange studies, were employed in an attempt to elucidate the nature of the HF reaction. Before discussing the outcome of those studies results obtained following exposure of pre-fluorinated samples to anhydrous H<sup>18</sup>F are presented.

**Table 4.14** Fluorine uptake data measured on F-terminated diamond powder surfaces, prepared from H-terminated powder surfaces and following reaction with anhydrous H<sup>18</sup>F under various conditions

Sample and fluorination conditions	Reaction temperature	Fluorine uptake (mmol g <sup>-1</sup> )
17 (H <sub>2</sub> + F <sub>2</sub> at RT)	Ambient	0.118 ± 0.0006
18 (H <sub>2</sub> + F <sub>2</sub> at 400 °C)		0.090 ± 0.0007
19 (H <sub>2</sub> + ClF <sub>3</sub> at RT)		0.068 ± 0.0003
20 (H <sub>2</sub> + ClF <sub>3</sub> at 400 °C)		0.038 ± 0.0002
21 (H <sub>2</sub> + F <sub>2</sub> at RT)	523 K	0.091 ± 0.0004
22 (H <sub>2</sub> + F <sub>2</sub> at 400 °C)		0.082 ± 0.0003
23 (H <sub>2</sub> + ClF <sub>3</sub> at RT)		0.052 ± 0.0002
24 (H <sub>2</sub> + ClF <sub>3</sub> at 400 °C)		0.021 ± 0.0002

The most obvious feature of these results, when compared with those obtained previously for hydrogen-terminated surfaces, was the marked reduction in fluorine uptake. Approximately a ten-fold decrease had occurred as a consequence of surface fluorination (tables 4.12 & 4.14). Since the fluorination of hydrogenated diamond using  $F_2$  was now well characterised; the reaction of such fluorinated surfaces with HF could be used as a model system for comparison with other systems. The usefulness of this model was highlighted upon consideration of the fluorine uptakes observed on surfaces pre-treated with  $ClF_3$ . Chlorine trifluoride is known to be a vigorous fluorinating agent, fluorine uptake values as low as  $0.021 \text{ mmol g}^{-1}$  confirm that a high degree of fluorination has occurred. This model assumes that no exchange occurs between surface C-F and  $H^{18}F$ , which will be discussed further later. Whilst this result was not surprising it was important since it supported earlier FTIR and EFTEM evidence for diamond surface fluorination using this reagent.

A large reduction in the extent of reaction between anhydrous  $H^{18}F$  and fluorine treated diamond surfaces had occurred but there was still a measurable uptake of the radiolabel which could not be ignored. If it is assumed that uptake of the radiolabel involved some kind of interaction with surface atoms, two explanations for reduced uptake were possible. Firstly, incomplete fluorination with the survival of surface hydrogen or secondly, reduced interaction of C-F with HF compared with C-H groupings. In order to shed light on this problem it was necessary to study a system where incomplete fluorination was known to

occur. Conveniently, this was the case for oxygen-terminated diamond surfaces where CO groupings are much more resistant to fluorination. (Table 4.15)

**Table 4.15** Fluorine uptake data measured on F-terminated diamond powder surfaces, prepared from O-terminated powder surfaces and following reaction with anhydrous  $\text{H}^{18}\text{F}$  under various conditions

Sample and fluorination conditions	Reaction temperature	Fluorine uptake ( $\text{mmol g}^{-1}$ )
25 ( $\text{H}_2 + \text{O}_2 + \text{F}_2$ at RT)	Ambient	$0.361 \pm 0.001$
26 as 25		$0.531 \pm 0.001$
27 ( $\text{H}_2 + \text{O}_2 + \text{F}_2$ at 623 K)		$0.139 \pm 0.0007$
28 as 27		$0.183 \pm 0.0007$
29 ( $\text{H}_2 + \text{O}_2 + \text{F}_2$ at RT)	523 K	$0.259 \pm 0.001$
30 as 29		$0.408 \pm 0.002$
31 ( $\text{H}_2 + \text{O}_2 + \text{F}_2$ at 623 K)		$0.107 \pm 0.0005$
32 as 31		$0.086 \pm 0.0004$

These results are very important since they highlight a key factor in the control of fluorine uptake levels. The fluorine uptake values observed on samples (25,26,29 and 30), which were pre-treated with  $\text{F}_2$  at room temperature are most useful. Under these conditions survival of surface oxygen was known to occur (81), the fluorine uptakes are significantly higher when compared to those

observed on a surface known to be highly fluorinated (Table 4.15). However, when the reaction with  $F_2$  was performed at 623 K (samples 27,28,31 and 32) the fluorine uptake values following reaction with  $H^{18}F$  were reduced. Under these conditions CO groups were much less resistant to fluorination and the uptake values agreed with the profile of a highly fluorinated surface. The fluorine uptake on highly fluorinated surfaces was still significant and confidently assigned to reaction with surviving oxygen atoms, which cannot be completely removed by  $F_2$  below 723 K. Fluorine uptakes on hydrogen, oxygen and fluorine terminated diamond surfaces, derived from hydrogen or oxygen terminated surfaces, are compared in figures 4.19 and 4.20. These bar charts show how the interaction with HF varied as a result of pre-treatment with  $F_2$  or  $ClF_3$  compared against an average of the highest and lowest uptake without fluorination.

#### **4.2.5.5 Room temperature fluorine exchange reactions between $^{18}F$ -radiolabelled diamond powder surfaces and non-labelled anhydrous HF vapour**

As noted earlier, the behaviour of anhydrous HF vapour towards diamond was not typical of a fluorination reaction. The main evidence for this was a general feature involving decreased uptake of the radiolabel,  $^{18}F$ , at 573 K compared with ambient temperatures. In an attempt to explain this feature and to elucidate the nature of the HF reaction on the various surfaces, a number of exchange experiments were designed. The techniques used and the results obtained are presented below.

**Figure 4.19** Comparison of fluorine uptake values on hydrogenated diamond powder surfaces following exposure to anhydrous  $H^{18}F$  vapour

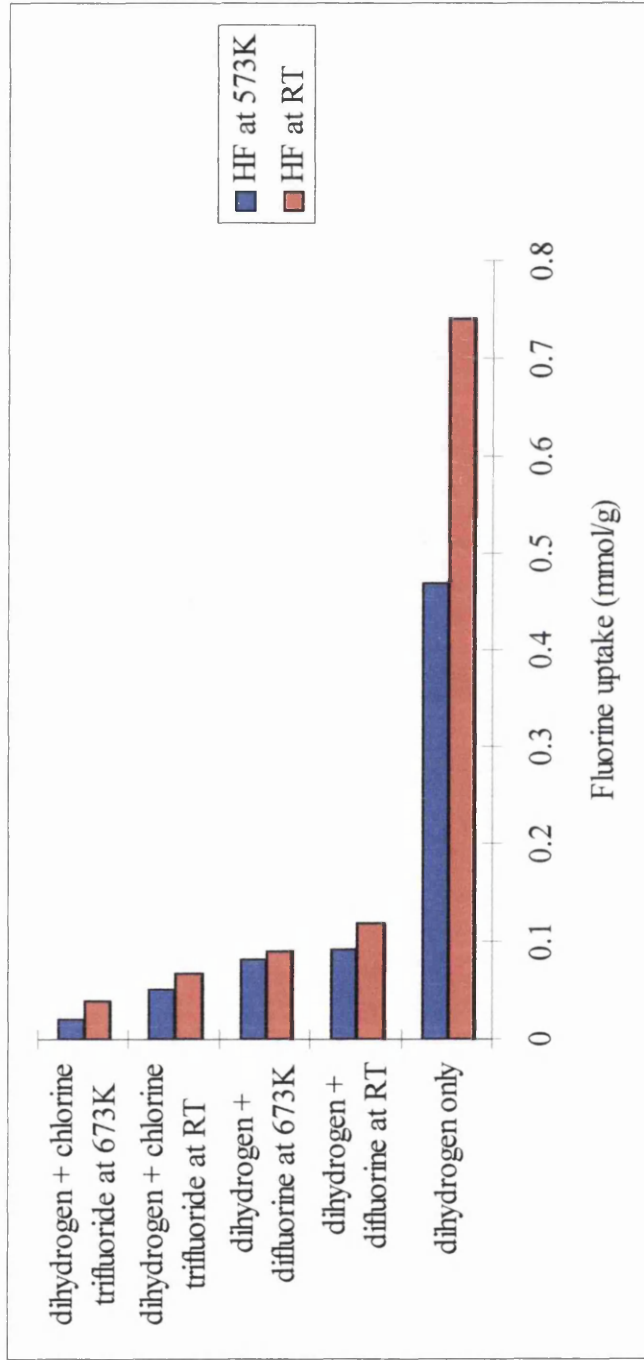
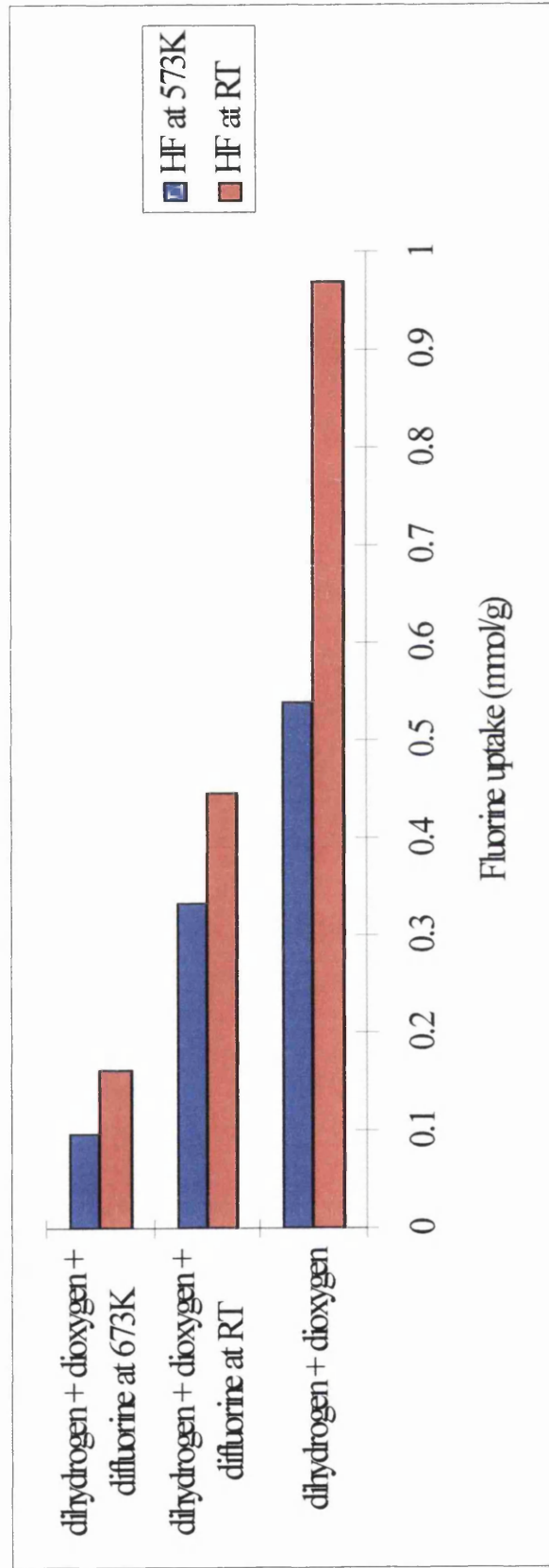
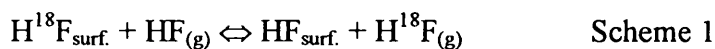


**Figure 4.20** Comparison of fluorine uptake values on oxygenated diamond powder surfaces following exposure to anhydrous H<sup>18</sup>F vapour



These experiments were designed to assess the extent to which the reaction, left to right, given in scheme 1 occurred. The labelled diamond sample contained in the FEP/PTFE tube vessel was degassed at 77 K under static vacuum before anhydrous HF (142torr, 1mmol) was condensed into the vessel. Following warming to room temperature and allowing to stand for 30 minutes, the volatiles were removed under static vacuum to the waste trap. All of these procedures were performed using the Monel vacuum system for handling anhydrous HF vapour, which was described in chapter 2. The diamond sample was then removed from the vacuum system and the activity measured using a well counter. The procedure was repeated at least twice for each sample to obtain an exchange profile with 4 data points. A total of 4 samples was studied, two hydrogenated (3 and 4 Table 4.12) and two oxygenated (12 and 13 Table 4.13). Protocols for handling raw counting data were as described earlier. After each experiment the FEP tube containing the sample was weighed on a balance housed behind some lead bricks. This was to ensure that the sample mass was remaining constant.



The results that were obtained are shown in table 4.16 and represented graphically in figure 4.21.

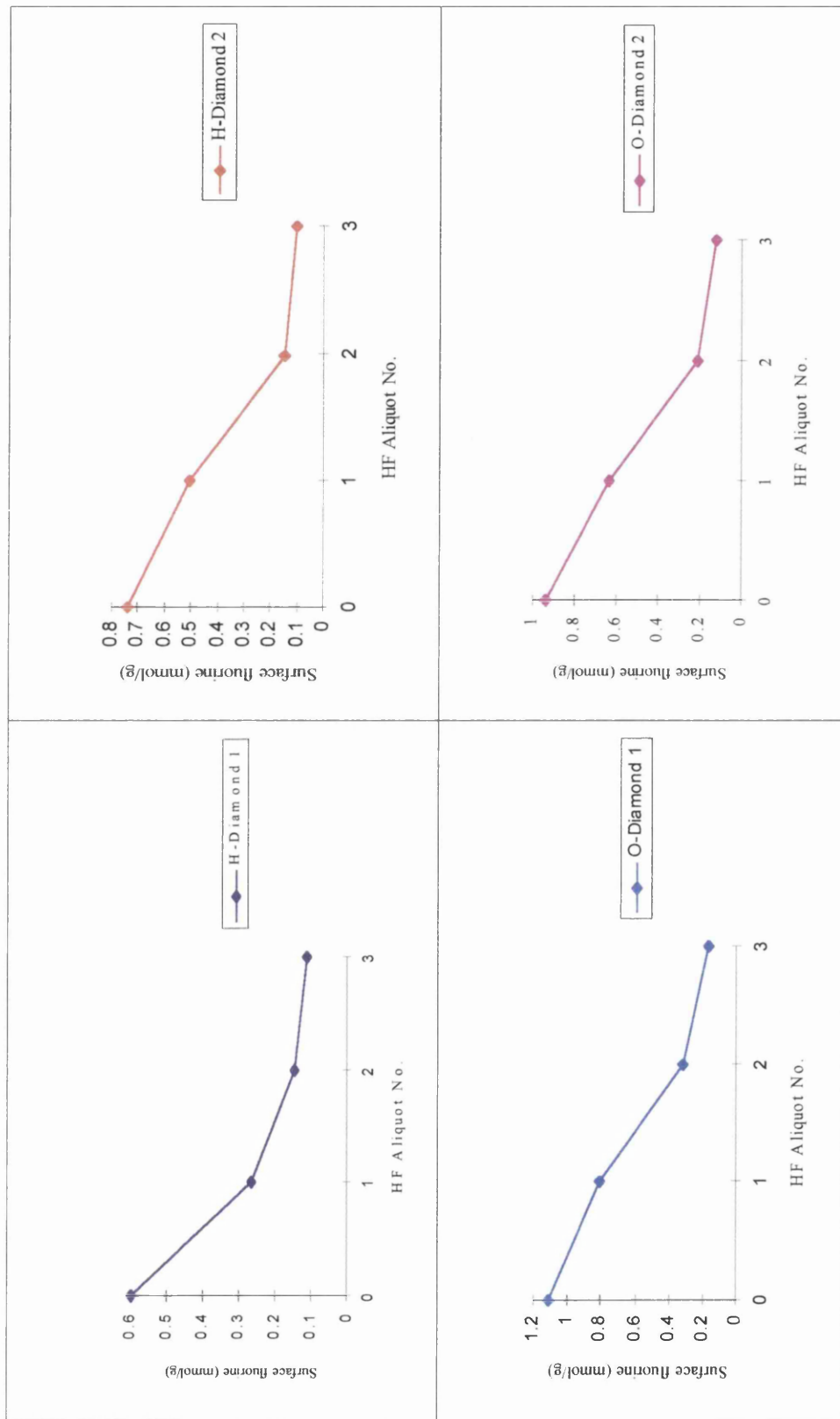
**Table 4.16** Room temperature fluorine exchange reaction between  $^{18}\text{F}$ -radiolabelled diamond powder and anhydrous HF vapour

Diamond sample	HF aliquot No.	$^{18}\text{F}$ (mmol g <sup>-1</sup> )	% $^{18}\text{F}$ age original remaining	Relative F-exchange
3	0	$0.60 \pm 0.003$	100	0
	1	$0.265 \pm 0.001$	44.1	55.9%
	2	$0.147 \pm 0.0006$	24.6	45.6%
	3	$0.115 \pm 0.0005$	19.2	21.7%
4	0	$0.739 \pm 0.003$	100	0
	1	$0.505 \pm 0.002$	68.3	31.6%
	2	$0.152 \pm 0.0006$	20.7	69.9%
	3	$0.104 \pm 0.0004$	14.1	31.5%
12	0	$1.116 \pm 0.003$	100	0
	1	$0.814 \pm 0.002$	72.9	27.06%
	2	$0.317 \pm 0.0008$	28.4	61.05%
	3	$0.169 \pm 0.0005$	15.2	46.7%
13	0	$0.939 \pm 0.002$	100	0
	1	$0.635 \pm 0.001$	67.7	32.3%
	2	$0.214 \pm 0.0004$	22.8	66.2%
	3	$0.126 \pm 0.0003$	13.5	41.2%

The data in the last column of this table are the percentage of fluorine exchanged following an aliquot of HF and relative to the previous aliquot.

**Figure 4.21**

Room temperature fluorine exchange reaction between  $^{18}\text{F}$ -radiolabelled diamond powder and anhydrous HF vapour



It was apparent from the data given in this table that room temperature fluorine exchange can occur between an  $^{18}\text{F}$ -labelled diamond surface, hydrogenated or oxygenated and non-labelled HF in the vapour phase. In every case less than 20% of the original activity remained on the diamond surface following successive exposure to three aliquots of non-labelled HF. This means that a pool of labile fluorine was present on the diamond surface, which has major implications as to the nature of the HF interaction with diamond surfaces. This feature will be discussed further later.

Closer examination of the data revealed a pattern; in three out of the four cases (samples 4, 12 and 13) the greatest relative exchange occurred following the second aliquot of HF. At the start of the experiment the quantity of fluorine present on the surface and that in the vapour phase (1 mmol) were similar, this was particularly true for samples 12 and 13. Consider these samples only. In the first instance, the statistical maximum for exchange was 50%, the observed exchange for samples 12 and 13 following the first aliquot was 27.06 and 33.3% respectively. It should be born in mind that exchange is a random process and the statistical maximum may not be observed. In the second instance, there was an excess of fluorine atoms present in the gas phase which means greater than 50% exchange was theoretically possible. For samples 12 and 13 the relative proportion of fluorine exchanged following the second aliquot was 61% and 66%. However, following the third aliquot the relative exchange has decreased to 46.7 and 41.2% respectively despite an increase in the  $^{19}\text{F}/^{18}\text{F}$  ratio compared with the previous experiment. It followed logically, that for some reason the labelled species present on the diamond surface at this stage was less easily

exchanged. This could be interpreted as being due to the presence of non-labile or chemically bound fluorine. Alternatively, if the remaining surface fluorine was less accessible by HF molecules from the vapour phase, the level of exchange would be decreased.

#### **4.2.5.6 Fluorine exchange reactions between anhydrous $H^{18}F$ vapour and diamond powder surfaces pre-treated with non-labelled HF vapour and determination of the f-factor**

The extent to which an exchange reaction, such as that described by scheme 1 right to left, occurs can be determined by measurement of an exchange factor  $f$ . The  $f$ -factor ranges from zero for no exchange to one for complete exchange.

If exchange occurs, the  $H^{18}F$  vapour specific activity will be decreased as a result of isotopic dilution. If the amount of fluorine present on the surface before the exchange reaction can be well estimated and the specific activity following reaction measured accurately, it is possible to determine the level of exchange or  $f$ -factor. The latter was accomplished easily; the former was achieved by using data obtained in the fluorine uptake studies. As outlined earlier in this section of the work, the uptake of fluorine-18 on diamond surfaces (Tables 4.12 and 4.13), following reaction with  $H^{18}F$  was subject to variation. In order to minimise the uncertainty associated with this, two identical diamond samples were used. One sample was reacted with  $H^{18}F$  and the fluorine uptake determined, at the same time another sample was prepared by reaction with non-labelled HF for use in the  $f$ -factor determination. In this way it was possible to

have some confidence in the magnitude of the estimated surface fluorine before exchange.

The fluorine exchange was studied for a total of eight diamond samples, four hydrogenated and four oxygenated. Two of each were reacted with non-labelled HF (3.52 mmol) at room temperature and the other two at 573 K, before reaction with  $H^{18}F$  under identical conditions. The uptake data used was given previously in tables 4.12 and 4.13 (hydrogenated samples: 4,5,9 and 10 oxygenated samples 12,13,15 and 16). The procedure for measurement of specific activity was discussed in section 2.1.10. The f-factor was calculated using the relation given by equation 4.1 which is followed by a typical example.

$$f = S_0 - S_t / S_0 - S_\infty \dots\dots\dots 4.1$$

In equation 4.1,

$S_0$  (count  $sec^{-1} mmol^{-1}$ ) is the specific activity before the exchange experiment,  $S_t$  is the specific activity after the exchange experiment and  $S_\infty$  is the specific activity in the event of 100% exchange which is given by equation 4.2.

$$S_\infty = S_0 \times nH^{18}F_{(g)} / nH^{18}F_{(g)} + nHF_{surf.} \dots\dots\dots 4.2$$

In equation 4.2,

$nH^{18}F_{(g)}$  is the amount of  $H^{18}F$  present in the gas phase i.e 3.5 mmol and  $nHF_{surf.}$  is the amount of unlabelled HF present on the diamond surface. It can be

seen that the accuracy of  $S_{\infty}$  depends on the estimated quantity,  $nHF_{surf}$ . hence the importance of a simultaneous uptake measurement.

This method has the great merit that it allows exchange to be studied at the higher reaction temperature, which was not possible in the FEP tube.

Measurement of the f-factor, example:

The fluorine uptake data used in this example was that obtained for the reaction of a hydrogenated diamond surface with  $H^{18}F$  at ambient temperature. (Table 4.12 sample 4:  $0.739 \text{ mmol g}^{-1}$ )

$$S_0 = 653.75 \text{ count sec}^{-1} \text{ mmol}^{-1}$$

$S_t$  is determined experimentally as follows:

Experimental count obtained for 1mmol of the gas phase adsorbed on CsF = 13585 in 60 seconds after a decay time of 140 minutes.

Decay corrected count = 32820 in 60 seconds, so  $S_t = 32820/60 = 547 \text{ count sec}^{-1} \text{ mmol}^{-1}$

$$S_{\infty} = 653.75 \times 3.52/3.52 + 0.739 = 2301.2/4.259 = 540.31 \text{ count sec}^{-1} \text{ mmol}^{-1}$$

$$f = 653.75 - 547 / 653.75 - 540.31 = 106.75/113.44 = \underline{0.94}$$

An f-factor of 0.94 is equivalent to 94% exchange. Within experimental error this means that essentially all the fluorine present on the diamond surface is exchangeable or labile. The f factors that were obtained, rounded to two decimal places, for all the diamond samples are given in table 4.17.

**Table 4.17** Reaction of  $\text{H}^{18}\text{F}$  with HF-pre-treated diamond samples, determination of the f-factor

Sample	f-factor	Fluorine uptake ( $\text{mmol g}^{-1}$ )
33 (c.f. sample 4)	0.94	
34 (c.f. sample 5)	0.85	$0.651 \pm 0.004$
35 (c.f. sample 9)	1.03	
36 (c.f. sample 10)	0.90	$0.413 \pm 0.003$
37 (c.f. sample 12)	0.88	$0.788 \pm 0.003$
38 (c.f. sample 13)	0.96	
39 (c.f. sample 15)	0.93	$0.583 \pm 0.004$
40 (c.f. sample 16)	1.08	

The f-factor values were consistently high which infers that a high level of labile fluorine was present on the diamond surface. The levels of exchange varied from 85% to 103% and 88% to 108% for the hydrogenated and oxygenated surfaces respectively. High levels of exchange were observed under all reaction conditions. Obviously, an exchange level of greater than 100% is impossible, there was an error associated with this method, for reasons explained earlier but, in general, the values were believed to be a good indication as to the extent of fluorine exchange that was occurring.

Also shown in table 4.17 are some fluorine uptakes that were measured on the diamond surface following the exchange experiment. These values could also be used to calculate an exchange factor for comparison with that calculated on the basis of changes in specific activity only. The relation used to do this is given by equation 4.3, which is followed by a typical example.

$$f = (A_1/A_1 + A_2)/(m_1n_1/m_1n_1 + m_2n_2) \dots\dots\dots 4.3$$

In equation 4.3,

$A_1$  (count  $\text{sec}^{-1}$ ) is the activity of the previously unlabelled phase following the exchange reaction, in this case the diamond sample.

$A_2$  (count  $\text{sec}^{-1}$ ) is the total activity of the labelled phase following the exchange reaction, in this case the gas phase given by:  $3.52 \times$  Specific activity following exchange.

$m_1$  and  $m_2$  are the amounts of fluorine present (mmol) on the diamond surface and in the gas phase respectively, before the exchange experiment.  $m_1$  is the fluorine uptake on the solid and  $m_2 = 3.52$  mmol.

$n_1$  and  $n_2$  are the number of exchangeable atoms present in both solid and gas phase respectively, in this case  $n_1=n_2=1$ .

Example:

The results quoted here were obtained for sample 34. (Table 4.17)

$A_1 = 425.5$  count  $\text{sec}^{-1}$  (Decay corrected count 25535 in 60s,  $\text{H}^{18}\text{F}$  specific activity  $653.75$  count  $\text{sec}^{-1}$   $\text{mmol}^{-1}$ )

$A_2 = 3.52 \text{ mmol} \times 539.7 \text{ count sec}^{-1} \text{ mmol}^{-1}$  the specific activity measured following the exchange experiment and corrected for decay.

$$= 1899.7 \text{ count sec}^{-1}$$

$m_1 = 0.909 \text{ mmol}$  the estimated amount of fluorine present on the diamond surface before the exchange experiment, obtained from previous uptake studies.

$$m_2 = 3.52 \text{ mmol}$$

So,

$$f = (425.5 \text{ count sec}^{-1} / 2325.2 \text{ count sec}^{-1}) / (0.909 \text{ mmol} / 4.429 \text{ mmol})$$

$$= 0.183 / 0.205$$

$$= \underline{0.89}$$

It can be seen that this value was in good agreement with that obtained previously, which implies that for this reaction the uptake measured on the diamond surface was a result of exchange only.

The accuracy of these calculations could be determined by calculating the radiochemical balance using equation 4.4.

$$A_1 + A_2 / A_3 \times 100\% \dots\dots\dots 4.4$$

In equation 4.4,

$A_3$  is the total gas phase activity before the exchange experiment i.e.  $3.52 \times \text{H}^{18}\text{F}$  specific activity.

For the above example:

$$2325 / 2301 \times 100\% = \underline{101\%}$$

This means that the entire radioactivity was accounted for and the results were meaningful.

The f-factor values calculated for the remainder of samples using this method are given in table 4.18, which also shows the radiochemical balance.

**Table 4.18** f-factor values calculated using measured fluorine uptake values on HF-pre-treated diamond samples following exchange with  $H^{18}F$

Sample	f-factor	Radiochemical balance
34	0.89	101%
36	1.08	101%
37	0.92	101%
39	1.04	101%

In every case the f-factor value was higher using this method but the increase was only significant for samples 36 and 39. In general, if an increased f-factor value is obtained using this method it implies that fluorine uptake without exchange has occurred; in addition to that which is due to exchange. Whilst this could not be ruled out completely in the cases of samples 34 and 37 it seemed unlikely given the good agreement between the f-factor values. However, using this method, values greater than 1 are only possible if there was activity present on the diamond surface which was not accounted for by fluorine exchange. This

has occurred following reaction at 573 K in both cases suggesting that, under these conditions, there are surface sites available for further fluorine uptake. It would then follow that this was not the case at ambient reaction temperatures and an argument for surface saturation under these conditions may be valid. Before pursuing this argument it would be necessary to perform a much more detailed study.

The picture that emerged from the uptake and exchange studies detailed was that the reaction of anhydrous HF with hydrogenated or oxygenated diamond powder resulted in a surface where all adsorbed fluorine was labile. In addition, there appeared to be a greater interaction at ambient temperatures compared with reaction at 573 K. Both of these observations are inconsistent with the profile of a reaction to form C-F bonds, which certainly occurred with F<sub>2</sub>. The C-F bond is not exchangeable and C-F formation was more extensive at higher reaction temperatures. Whilst exchange studies on highly fluorinated surfaces were not possible due to the low levels of activity, it was possible to determine if the uptake observed on these surfaces was a result of fluorine exchange between C-F and HF. This was achieved by measuring the H<sup>18</sup>F specific activity following reaction. It was also necessary to obtain some information on the nature of the diamond surface following reaction with HF and DRIFTS analysis was used to do this.

#### 4.2.5.7 Specific activity determination following the reaction between highly fluorinated diamond surfaces and anhydrous $\text{H}^{18}\text{F}$ vapour

Four highly fluorinated diamond samples were prepared by reaction of hydrogenated diamond powder and  $\text{F}_2$  at ambient temperature and at 673 K for 24 h. The reaction with  $\text{H}^{18}\text{F}$  was studied twice at ambient temperature and twice at room temperature with the specific activity following reaction being measured in every case. The results obtained are presented in table 4.19.

**Table 4.19** Measurement of specific activity following reaction between  $\text{H}^{18}\text{F}$  and highly fluorinated diamond powder surfaces, under various conditions

Sample history	$^{18}\text{F}$ Specific Activity (count $\text{sec}^{-1}$ $\text{mmol}^{-1}$ )	
	Before	After
Fluorinated at ambient	642	636
	1025	1009
Fluorinated at 673 K	642	640
	1025	1015

These results indicated that there was no observable fluorine exchange between  $\text{H}^{18}\text{F}$  and F-terminated diamond under the conditions employed.

The difference between the specific activity measurements before and after reaction was within experimental error.

This was confirmation of the expected result since, for example, a C-F bond in a fluoroalkane is known to be inert to exchange with HF. In this work, it has been shown that essentially all of the surface fluorine which exists on the diamond surface following exposure to HF is labile. It follows that C-F formation is not a feature of the reaction between diamond and HF. To investigate this further, DRIFTS analysis of some diamond powder surfaces following exposure to HF was performed.

#### **4.2.5.8 DRIFTS analysis of diamond powder surfaces following exposure to HF vapour**

DRIFTS analysis of diamond powder following reaction with HF, under similar conditions to those described earlier, has been performed immediately following reaction, several days and several weeks after reaction. In every case the sample was handled in the laboratory atmosphere where exposure to moist air had occurred. Typical results are shown in table 4.20.

**Table 4.20** DRIFTS analysis of a hydrogen-terminated diamond surface before and immediately after reaction with anhydrous HF vapour

Sample	$\nu_{\max}$ (cm <sup>-1</sup> )	Assignment
Before exposure to HF	2937	$\nu_1(\text{CH asym str}) \text{CH}_2$
	2860	$\nu_2(\text{CH sym str}) \text{CH}_3$
	2837	$\nu_3(\text{CH sym str}) \text{CH}_2$
After exposure to HF	3547 (weak, broad)	$\nu(\text{O-H}) \text{H}_2\text{O}$

The experimental spectra obtained are shown in figure 4.22. The absorptions observed below 1200 cm<sup>-1</sup> on the sample before reaction with HF have been omitted from the above table for clarity. These have not been assigned precisely but are thought to be due to C-H bending and diamond lattice phonons. The important observation was that following reaction with HF, the C-H bands were absent and there was no evidence for C-F formation. Except for a weak band in the O-H stretching region the spectrum was featureless.

Figure 4.22 also shows a spectrum recorded several days after the reaction between hydrogen-terminated diamond and HF. The strong band at 3843 cm<sup>-1</sup> was immediately obvious and accompanied by a band at 1656cm<sup>-1</sup>. These are the stretching and bending modes respectively, for the OH grouping of surface water. Weak bands at 2937 and 2837 cm<sup>-1</sup> were evident and assigned to C-H stretching. Interestingly, there was a band at 1897 cm<sup>-1</sup> which could be assigned to the C=O stretching mode. This band was of interest for two reasons; firstly it

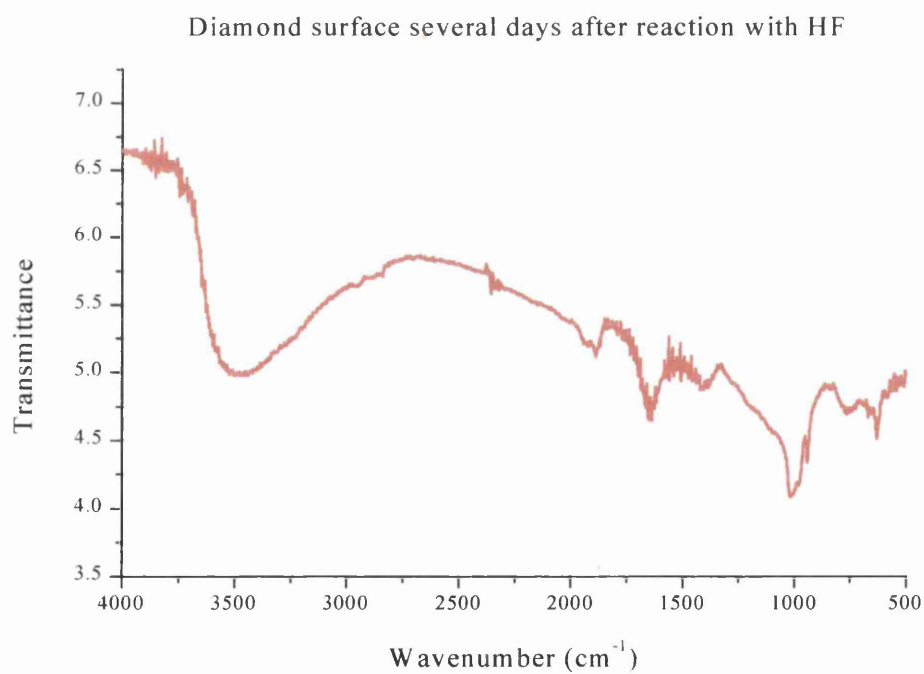
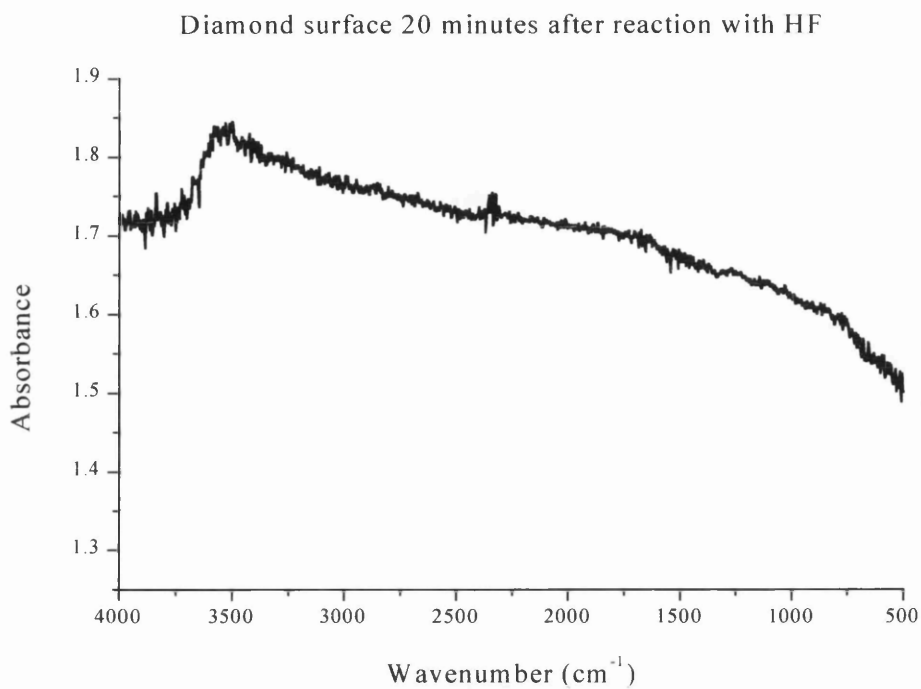


**Figure 4.22** DRIFTS analysis of diamond powder following exposure to anhydrous HF vapour

appeared at a high wavenumber, suggesting that the bond was in some way weakened compared with a normal C=O bond. Secondly, it was not a simple matter to account for the presence of C=O bonds on this surface. A band at  $1016\text{ cm}^{-1}$  was present and assigned to diamond lattice phonons. However, the major feature of the DRIFTS analysis was the presence of surface hydroxyl which was thought to be attributable to surface water.

These results imply that hydrolysis, of the adsorbed fluorine laid down on the surface in the reaction with HF, to form surface OH can occur. In agreement with the fluorine exchange studies this is not consistent with the formation of C-F, which is known to possess hydrophobic character, but rather reminiscent of the hydrophilic behaviour of a solid binary covalent fluoride.

## CHAPTER 5 DISCUSSION

### 5.0 Introduction

The key features that have emerged from this work are now discussed. These relate to the reactions of a number of fluorine-containing molecules with diamond powder and film surfaces. In this regard the study has been focussed on the reaction of  $F_2$  and HF with diamond surfaces, which have been found to have very different characteristics. A model for each reaction is proposed; these are based on the experimental evidence obtained in this work and comparisons made with existing knowledge in this field of research, such as the fluorination of graphite. To this end our understanding of the types of fluorine chemistry possible on diamond surfaces has been improved.

Fluorine chemistry on diamond is also relevant in the context of polishing polycrystalline film surfaces by chemomechanical methods and this is discussed further. It has been possible to explain the outcome of attempts to develop such methods on the basis of the fluorine chemistry observed, which was one of the aims of this work.

Finally, successful polishing experiments and their implication for the future, in terms of the developing science surrounding CVD diamond film and its industrial applications, are discussed.

## 5.1 The reaction of F<sub>2</sub> or ClF<sub>3</sub> with polycrystalline diamond powder and film surfaces

This reaction has been investigated, largely on hydrogen-terminated diamond surfaces, using a range of analytical methods. The replacement of hydrogen for fluorine at the diamond surface occurs easily, even at ambient temperature. A simple consideration of the bond energies for C-H, C-F, F-F and H-F (table 5.1) reveals that the fluorination of C-H, to form C-F and H-F, is favourable from a thermodynamic standpoint. The reaction is exothermic by  $-386 \text{ kJ mol}^{-1}$ , which is enough energy to cause the breakage of C-C bonds. For this reason combustion of carbon materials in F<sub>2</sub> can occur, this is normally avoided by careful control of the reaction conditions and often involves dilution of F<sub>2</sub> with an inert gas such as N<sub>2</sub>.

**Table 5.1** Useful bond energy data (128)

Bond	Bond energy (kJ mol <sup>-1</sup> )
C-H	414
C-F	486
H-F	569
F-F	155
C-C	337

DRIFTS analysis of hydrogen-terminated powder indicated the presence of surface CH, CH<sub>2</sub> and CH<sub>3</sub> groupings. Gas phase infrared spectroscopy showed the presence of hydrogen fluoride as a reaction product under all conditions. This is formed when C-H is replaced by C-F as shown in figure 5.1 and was observed following reaction with powder and film surfaces. Laser raman spectroscopy of dihydrogen treated film showed only a sharp diamond peak at 1332 cm<sup>-1</sup> with no indication of sp<sup>2</sup> carbon, the presence of considerable surface hydrogen was therefore expected.

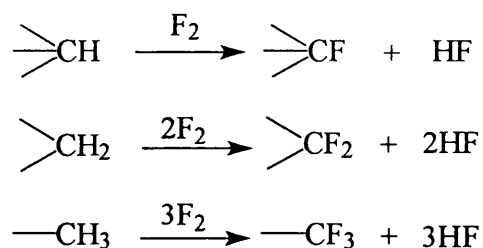


**Figure 5.1** Fluorination of (CH)<sub>n</sub> (n=1-3) groups on a diamond surface

The extent to which the reaction of F<sub>2</sub> with carbon-based materials occurs is a function of the experimental conditions, such as the reaction temperature and F<sub>2</sub> pressure. From this standpoint the reaction at 673 K was characterised by the formation of fluorocarbon species which were not evident following reaction at ambient temperature. In both cases DRIFTS analysis of the F<sub>2</sub> treated powder surface revealed that complete replacement of hydrogen for fluorine had occurred. However the peaks attributable to (CF)<sub>n</sub> (n=1-3) were more intense and better resolved into distinct signals for CF, CF<sub>2</sub> and CF<sub>3</sub> groupings in the analysis of powder fluorinated at 673 K. This can be explained as being a result

of further fluorination of surface CF or CF<sub>2</sub> to form CF<sub>2</sub> and CF<sub>3</sub> respectively. Breakage of C-C bonds must accompany this process as shown in figure 5.2.

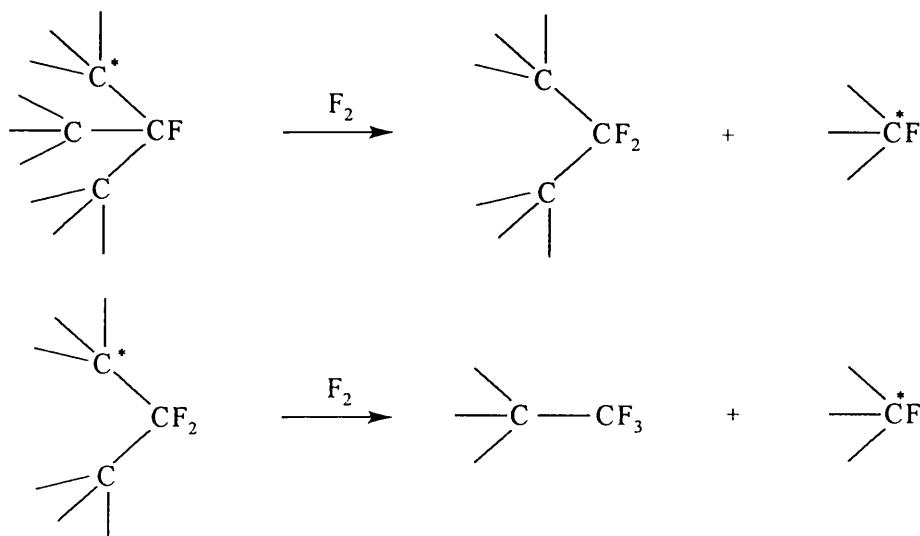


**Figure 5.2** Further fluorination of surface CF and CF<sub>2</sub> groups

The occurrence a mixture of fluorocarbons in the gas phase means that in addition to the process described by figure 5.2, gasification or etching of surface species is possible. The simplest etch products are difluorocarbene, :CF<sub>2</sub> and the trifluoromethyl radical, •CF<sub>3</sub>. If it is assumed that :CF<sub>2</sub> is the major etch product, with •CF<sub>3</sub> less likely on steric grounds, then formation of the fluorocarbon mixture observed (table 4.2) can be accounted for by the scheme of reactions shown in figure 5.3. These type of reactions are well known in the polymerisation of tetrafluoroethylene, C<sub>2</sub>F<sub>4</sub> (127) and in the analogous reaction between silicon and atomic fluorine, etching of SiF<sub>2</sub> and further reaction in the gas phase to form SiF<sub>3</sub> and SiF<sub>4</sub> is known to occur (117, 129). In this system an equilibrium concentration of atomic fluorine will be present, but this is expected to be small and the formation fluorocarbon species can be explained sufficiently well by the reactions of the etch product, :CF<sub>2</sub>, with molecular fluorine.

The presence of etch products was initially promising for the use of the  $F_2$  reaction as a precursor to polishing of polycrystalline diamond film. In this respect inducing surface damage was the desired effect.

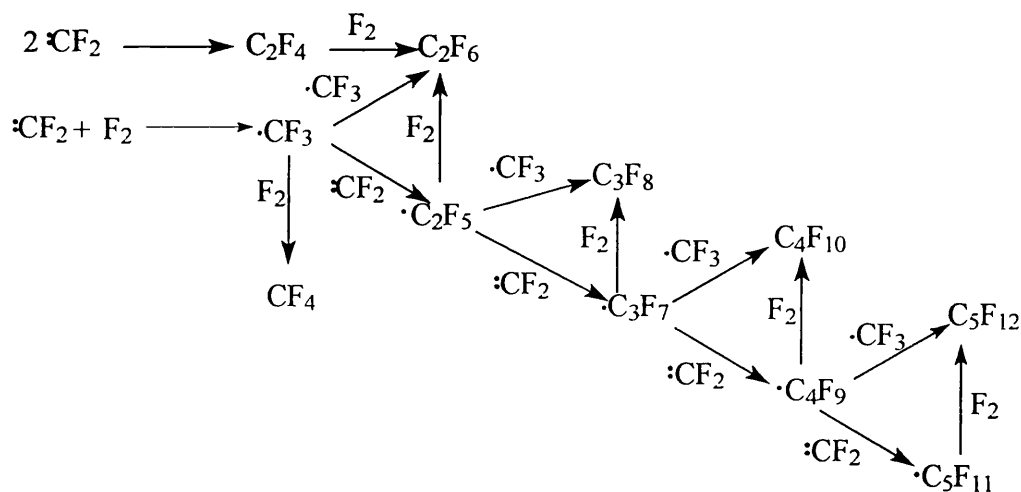


**Figure 5.3** Possible pathway to the formation of fluorocarbons in the gas phase during the reaction of  $\cdot CF_2$ , etched from a diamond surface, and  $F_2$  at 673 K

Therefore it was important to establish the extent to which the etching reaction was occurring, this was not possible using FTIR, which provided qualitative information only. Scanning electron microscopy (SEM) was used to study the morphology of diamond powder and film surfaces before and after reaction with  $F_2$  under various conditions. As a result it was shown that little or no change in the surface morphology of polycrystalline diamond film, in particular, had occurred after treatment with  $F_2$  at 673 K. There was no evidence for etch-pit formation, which might have been expected from the observation of volatile fluorocarbons. Instead the surface was characterised by randomly oriented

crystallites on which a number of crystal faces could be identified. However, unlike a polished monocrystalline surface, these materials also contained many different crystal edges and grain boundaries. Although disappointing from a polishing standpoint the absence of significant surface damage had implications for the reactivity of polycrystalline diamond film surfaces towards  $F_2$ .

Clearly a massive etching reaction was not a feature, as would be predicted from studies of fluorine on single crystal diamond (86, 87), however the nature of the reaction at edge sites, surface defects and grain boundaries is not accounted for in single crystal studies. In this sense the surface of a polycrystalline film has more in common with a powder than a single crystal. Surface area analysis of hydrogenated diamond powder had suggested an irregular surface and there was some evidence for increased irregularity following reaction with  $F_2$  at 673 K. These irregularities were not large enough to be pores, but could be considered as being due to grain boundaries or surface defects.

Energy-filtered TEM imaging at the 20 nm scale confirmed the involvement of grain boundaries or crystal edges in the reaction of fluorine-containing molecules with a diamond film surface. In this case  $ClF_3$  was the reagent used but as already outlined the behaviour of  $ClF_3$  and  $F_2$  in this system is similar. In the absence of a hydrogenation treatment, regions of  $sp^2$  carbon at crystallite grain boundaries and edges were detected. Following reaction with  $ClF_3$  at 623 K these were removed and only  $sp^3$  carbon was present, consistent with the expected termination of the surface with fluorine. The quantity of  $sp^2$  carbon on CVD diamond film is a function of the growth conditions (section 1.2), but this

will be removed upon hydrogenation, which was deliberately avoided in the EFTEM study to assess the role of fluorine in preserving the  $sp^3$  structure.

The presence of surface hydrogen on the diamond sample is one of the key differences between this work and previous studies on annealed single crystals, which are characterised by the absence of surface hydrogen and the existence of a  $\pi$ -bonded surface structure. In our system the formation of HF is likely to have an important role, acting as a thermodynamic sink, and may influence the extent to which fluorination occurs, this will be considered further later in the chapter.

DRIFTS, FTIR, SEM and EFTEM analyses had proved useful in the characterisation of the products formed when a diamond surface is exposed to a highly oxidising reagent such as  $F_2$  and the effect this has on the surface morphology and density of  $sp^2/sp^3$  carbon. However, these techniques did not offer any quantitative information about the amount of fluorine left on the diamond surface as a result of reaction.

XPS analysis of  $F_2$  treated diamond film was useful in this regard. The binding energy of a carbon-1s core electron is very sensitive to chemical environment of the carbon atom. This means that changes in C(1s) binding energy as a result of bonding to fluorine are easily detected. These changes are manifested as peaks that are shifted to higher binding energy when compared with that attributable to unaffected carbon. In addition, the information obtained in the XPS experiment can provide an indication of the quantity of fluorine present on the sample

surface. The methods used in the analysis of XPS data obtained in this work have already been outlined in some detail (sections 2.1.11 & 4.2.4).

Following exposure of hydrogenated diamond film to  $F_2$  at ambient temperature and 523 K the XPS data indicated the presence of surface bound fluorine. The binding energy of the F(1s) electrons, 689.7 and 690.2 eV respectively, confirmed, unambiguously, that the bonding to the fluorine atom was covalent. As explained in section 4.2.4 the binding energy of F(1s) electrons in ionic species, such as LiF, is about 684 eV.

In the C(1s) binding energy envelopes, peaks attributable to CF,  $CF_2$  and  $CF_3$  moieties were identified (table 4.10). Due to the presence of oxygen on the surface the peaks representing the CF moiety were not completely unambiguous. However, the contribution from CO to the C(1s) signal was expected to be negligible in light of the observed intensity of the O(1s) signal, which was small when, compared with the F(1s) signal. For this reason the presence of oxygen on the diamond surface will not be considered any further in this discussion.

In previous studies involving the chemisorption of F on monocrystalline diamond surfaces (72, 86, 87) and a polycrystalline diamond surface (94), only a CF moiety was assigned. The new signal occurred at a binding energy shift of + 1.8 eV from the main component in the C(1s) binding energy envelope. In the present study the range and size of the binding energy shifts observed was much greater. In agreement with DRIFTS analysis of  $F_2$  treated diamond powder, this indicated that further fluorination of CF to give  $CF_2$  and  $CF_3$  was possible in our

system. Also in agreement with DRIFTS analysis, the extent to which this occurs appears to be a function of the reaction temperature. The calculated F/C ratio, in the XPS sampling region ( $\approx$  7-21 angstroms), was 0.31 following reaction at room temperature and 1.13 following reaction at 523 K. These values compare to a value of 0.13, obtained following the reaction of a {100} single crystal with  $F_2$  at 300 K. The C(1s) binding energy envelope observed following  $F_2$  treatment of the diamond surface at 523 K was remarkable due to the absence of a bulk carbon signal. In this study the expected sampling depth for XPS was between 7 and 21 angstroms, which equates to 2.5-7.7 layers of carbon atoms. According to the XPS data for the sample treated with  $F_2$  at 523 K a subsurface fluorination reaction has occurred, resulting in fluorinated layer, which is homogeneous and has a minimum thickness of 7-21 angstroms. The actual thickness of the fluorinated layer is expected to fall within this range.

It is useful at this stage to consider the well-known reaction of  $F_2$  with graphite to form graphite fluoride, whilst graphite and diamond have different chemical and physical properties, the comparison could be useful in the development of a model for the  $F_2$ /diamond system. The pioneering work in this field was performed by Watanabe *et al.*(108) who identified two forms of graphite fluoride,  $(CF)_n$  and  $(C_2F)_n$ . For the purposes of this discussion it is sufficient to consider only one of these forms,  $(CF)_n$  was discovered first and as a result has been better characterised, which makes it a suitable model compound. The formation of  $(CF)_n$  in the reaction of graphite with  $F_2$  occurs at 673-873 K, it has a layered structure in which every carbon atom is covalently bonded to a fluorine atom (figure 5.4), note the structural similarities between a layer of graphite

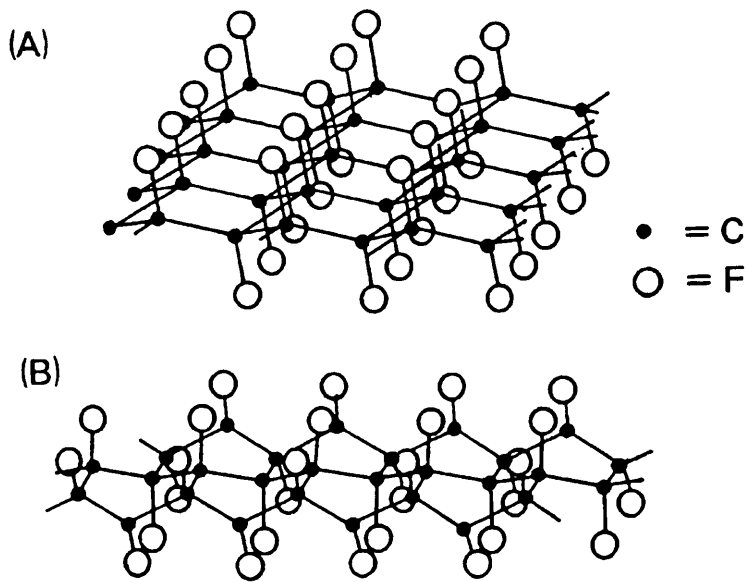
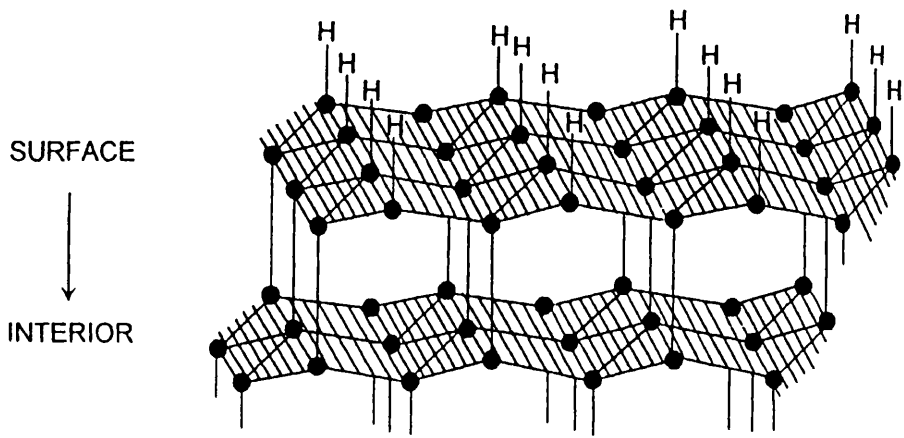


**Figure 5.4** The structure of CVD diamond and possible structures for  $(CF)_n$   
 (A) Chair (B) Boat

fluoride and a layer of CVD diamond. In addition,  $\text{CF}_2$  and  $\text{CF}_3$  groups can exist at the edge of these layers or at surface defects, the evidence for this was the presence of peaks in the C(1s) XPS spectrum (table 4.8) which were further shifted when compared with CF. A DRIFTS spectrum for the material showed several peaks in the CF stretching region ( $\text{CF}$  ( $1075\text{ cm}^{-1}$ )  $1354\text{ cm}^{-1}$  ( $\text{CF}_2$ ,  $\text{CF}_3$ )). The F/C ratio for  $(\text{CF})_n$  can exceed the theoretical value of 1, which is further evidence for the occurrence of  $\text{CF}_2$  and  $\text{CF}_3$  moieties. The fluorination mechanism is believed to involve the diffusion of fluorine into the graphite structure via surface defects or at the edges of the graphene layers.

Two models for the reaction of  $\text{F}_2$  and polycrystalline diamond surfaces in this work have been developed. In addition to the data obtained in the present study, these are based on previous studies involving monocrystalline diamond surfaces and the well-characterised reaction of  $\text{F}_2$  with graphite to form  $(\text{CF})_n$ . The proposed models are now discussed.

### **Model for the reaction of $\text{F}_2$ with hydrogenated polycrystalline diamond surfaces - 1**

On polycrystalline surfaces there exists a range of sites for reaction with  $\text{F}_2$ , these are crystallite faces, crystallite edges and the boundaries between crystallites. Various degrees of fluorination, involving the replacement of hydrogen for fluorine occurs at each of these sites, CF,  $\text{CF}_2$  and  $\text{CF}_3$  moieties have been identified on the surface. Crystallite edges and the boundaries between crystallites are the sites where  $\text{CF}_2$  and  $\text{CF}_3$  are most likely, with the

crystal faces restricted to CF for steric reasons. Etching of  $\text{CF}_2$  from the surface, which subsequently forms fluorocarbons in the gas phase, can occur during reaction at 523-673 K, once again the crystal edges, surface defects or grain boundaries are the most likely sites for etching. As a result of the etching reaction, there is enough room to allow access of  $\text{F}_2$  to the subsurface structure, where fluorination proceeds to form a layer of fluorinated material, which has a greater than monolayer thickness. It is also known, from the XPS data obtained, that the fluorinated layer is homogenous, there was no evidence for non-fluorinated carbon.

The formation of a homogeneous layer is only possible if transport of F or  $\text{F}_2$  through the diamond lattice is permitted. In previous studies involving the fluorination of single crystal diamond surfaces (86, 87), this has been dismissed as highly unlikely on the grounds that an enormous and energetically unfavourable lattice distortion would be required to allow fluorine penetration. If the F atom cannot penetrate the diamond lattice it is even more unlikely that the  $\text{F}_2$  molecule, believed to be the reactive species in the current work, will be able to do so.

However it should be born in mind that the fluorination conditions employed in the current work were more vigourous than those used in single crystal experiments. In our system 100 %  $\text{F}_2$  at atmospheric pressure could be used, compared with a 5 %  $\text{F}_2/\text{Ar}$  mixture at 2 torr to produce atomic F, which was the typical condition for the single crystal work (87).

The transport of  $F_2$  into the subsurface region may be further assisted by trace amounts of HF, which is a by-product of the reaction. Hydrogen fluoride can act as a catalyst in fluorination reactions and has been shown to have a role in the formation of graphite intercalation compounds (108) or in the fluorination of carbon fibers (109). However, this normally results in C-F bonds that exhibit ionic character, this was not our observation.

### **Model for the reaction of $F_2$ with hydrogenated polycrystalline diamond surfaces – 2**

In this model an alternative explanation for the formation of fluorocarbons and the resulting fluorinated layer formation during reaction at 523-673 K is proposed.

Fluorination reactions are highly exothermic and careful control of the reaction conditions is often required to prevent combustion, which results in the formation fluorocarbon decomposition products and amorphous carbon. In the fluorination of graphite Watanabe (108) avoided this problem by first filling the reaction vessel with an inert gas and then gradually replacing this with  $F_2$ . In this work no such measure was taken, since inducing surface damage was the desired effect from polishing perspective. It is possible that a thin layer of amorphous carbon is formed and fluorinated in the early stages of the reaction at 523-673 K. The attraction of this model is that it does not require diffusion of  $F_2$  into the diamond lattice, to account for the formation of a homogeneous layer.

Laser raman spectroscopy of fluorinated diamond surfaces showed only a sharp peak at  $1332\text{ cm}^{-1}$  which could be assigned to the  $\text{sp}^3$  carbon of diamond. There was no evidence of  $\text{sp}^2$  carbon, common in amorphous forms, which is not surprising given the weight of evidence for termination of each carbon atom with fluorine to form an  $\text{sp}^3$  hybridised structure.

Irrespective of the model used to account for the results obtained in this work, it is clear that the reaction of  $\text{F}_2$  with polycrystalline diamond surface is subject to kinetic limitations. Further reaction of already fluorine treated surfaces did not result in the formation of fluorocarbon species (table 4.3), even when a room temperature reaction was followed by reaction at 673 K. In addition, there was no evidence of a massive etching reaction in the SEM analysis of fluorinated surfaces.

This behaviour is well known for graphite fluoride and fluorinated silicon surfaces. In the former, graphite fluorides synthesised at 673 K do not show an increased reaction upon further exposure to  $\text{F}_2$  at 873 K. In the latter case as the layer of fluorinated material on the surface thickens, access to unreacted silicon becomes limited (113-115).

### **Some conclusions**

This work has shown that replacement for hydrogen for fluorine on a polycrystalline diamond surface occurs easily to form covalent C-F bonds. The extent of fluorination, which occurred, was dependent upon the reaction conditions and the nature of the reactive site. Under certain conditions a layer of

greater than monolayer thickness can be formed and this appeared to be closely related to the observation of fluorocarbon species in the gas phase. The reaction is subject to kinetic limitations and does not affect the gross morphology of the diamond surface. In the case of diamond film this had implications for the polishing of fluorinated diamond surfaces using traditional abrasive methods (section 3.1). These films behaved in a similar manner to non-fluorinated films, the fluorinated layer was presumably removed during the polishing procedure, however since its thickness was only tens of angstroms at the most, the effect on the overall roughness of the surface was negligible.

## **5.2 The reaction of hydrogen fluoride, HF, with polycrystalline diamond powder surfaces**

The interaction of anhydrous hydrogen fluoride with polycrystalline diamond powder surfaces, which have been terminated in hydrogen, oxygen or fluorine, has been studied.

Interestingly, an interaction was found to occur in all cases, the extent of which was primarily a function of the chemical species present on the diamond surface prior to reaction. The exact reaction conditions also had an effect, although this was less significant. Uptake of the radiotracer, [ $^{18}\text{F}$ ], which had been incorporated into the HF molecule, allowed quantitative analysis of the reaction. In addition a series of isotopic exchange reactions allowed the stability of adsorbed HF to be studied.

The fluorine uptake on a diamond powder surface, following 45 min exposure to  $H^{18}F$ , according to the chemical nature of the powder surface is summarised in figure 5.5.

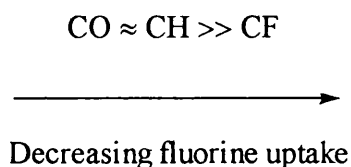


**Figure 5.5** Trends in fluorine uptake following exposure of a number of diamond surface to anhydrous  $H^{18}F$

Where,

CO denotes carbon-oxygen moieties of various types (table 4.6) on the diamond surface

CH denotes carbon-hydrogen moieties of various types (table 4.5) on the diamond surface

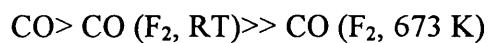
CF denotes carbon-fluorine moieties of various types (table 4.7) on the diamond surface

As shown in figure 5.5 the behaviour of  $H^{18}F$  vapour towards hydrogenated, oxygenated and fluorinated surfaces enabled a clear distinction to be made. A similar interaction was observed on O- and H- terminated surfaces (tables 4.12 and 4.13) and this was much greater than observed on the F- terminated surface (tables 4.14 and 4.13). It should be noted that the uptake on the F- terminated surface was by no means insignificant.

Interestingly, in addition to variations in fluorine uptake due to the chemical nature of the surface, a lower uptake was found to occur on all surface types following exposure to HF at 573 K when compared with exposure at ambient temperature. Although the effect was much less marked for the F-terminated surface when compared with the H- or O-terminated surfaces. This was a very different reactivity when compared with the reaction of F<sub>2</sub> and diamond surfaces which, as outlined in section 5.1, became more extensive as the reaction temperature was increased.

The observed interaction between HF and diamond powder is not simply a result of weak physical adsorption at the surface, since the [<sup>18</sup>F] counts after H<sup>18</sup>F treatment did not change materially with time, even after removal of volatile materials.

Comparing the fluorine uptakes on partially and almost completely fluorinated surfaces established the important role of surface atoms in determining the interaction with HF. Diamond surfaces exhibiting varying degrees of F-termination could be prepared from O-terminated diamond by reaction with F<sub>2</sub> at ambient temperature or 673 K. The trend that emerged is summarised in figure 5.6.



—————→  
Decreasing fluorine uptake

**Figure 5.6** Variation in fluorine uptake in the reaction of  $\text{H}^{18}\text{F}$  with O-terminated surfaces containing different amounts of CF

The reaction of O-terminated diamond powder with  $\text{F}_2$  at ambient temperature produces a surface, which contains more oxygen than fluorine, this condition is reversed following reaction at 673 K, where most, but not all, of the oxygen has been replaced by fluorine. The nature of these surfaces was established in a DRIFTS study by Ando *et al.* (90, 91). The greater fluorine uptake that was observed on the former surface type proves the existence of a direct interaction between molecules of HF from the gas phase and atoms of oxygen on the surface.

It can also be concluded that a similar interaction between molecules of HF from the gas phase and F atoms on the surface is much less favourable.

It was not possible, using similar methods, to establish a direct interaction between HF from the gas phase and hydrogen atoms on the diamond surface, since complete removal of hydrogen for fluorine in the reaction with  $\text{F}_2$  occurs at ambient temperature.

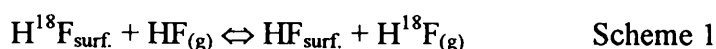
The fluorine uptake studies had established that an interaction between diamond powder and anhydrous HF was possible and for O- and F- terminated a direct correlation, between the relative concentration of O and F atoms present and the size of the fluorine uptake, had been observed.

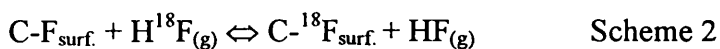
However the exact nature of the reaction was not known, the relevant questions were:

1. Did the reaction involve the replacement of surface -H or -O for -F to form C-F, i.e. was chemisorption occurring?
2. Alternatively, was a strong physisorption or a weak chemisorption occurring?
3. Was the interaction observed on F-terminated a result of a fluorine exchange reaction between surface C-F and gas phase H-F?

These questions were addressed using DRIFTS analysis of the HF-treated surfaces and by investigating the lability of the surface bound fluorine.

The isotope exchange reaction described by scheme 1 was used to investigate the lability of the fluorine laid down on H- and O-terminated diamond surfaces following exposure to  $\text{H}^{18}\text{F}$  (tables 4.16 and 4.17). Scheme 2 describes the exchange reaction used to study the interaction of  $\text{H}^{18}\text{F}$  with F-terminated surfaces (table 4.19).





A reduction in the activity of [ $^{18}\text{F}$ ] labelled diamond surfaces upon successive exposure to aliquots of HF indicated the presence of labile fluorine.

It was also found that H- or O-terminated surfaces which had been treated with HF before exposure to  $\text{H}^{18}\text{F}$  had a marked effect on the specific activity of the latter following exposure. The implication of this effect, which was manifested as a significant decrease in the specific count rate of the vapour, is that the surface-bound fluorine is labile with respect to exchange with  $\text{H}^{18}\text{F}$  vapour. Furthermore calculation of the fraction exchanged, or f-factor, by the methods described in section 4.2.5.6, indicated that the statistical maximum exchange had occurred. Values near to 100 %, expected from random distribution of [ $^{18}\text{F}$ ] between the surface and the vapour, were observed in all cases. Whilst the presence of non-labile fluorine on the surface cannot be ruled out completely, the exchange data obtained here suggested it was highly unlikely.

In contrast, exposure of F-terminated diamond powder, prepared by reaction of H-terminated samples with  $\text{F}_2$  at either ambient or 673 K, to  $\text{H}^{18}\text{F}$  has no effect on the specific count rate of the latter. It is apparent that the exchange reaction described by scheme 2 does not occur, which was the expected result since C-F is known to be inert with regard to exchange with HF.

Clearly the reaction of HF with H- or O-terminated diamond powder does not involve the formation of C-F bonds at the surface. Further evidence for this was

obtained in a DRIFTS study of the reaction, DRIFTS has already been shown in this work to be sensitive in the detection surface CF. The DRIFTS spectra of diamond powder, which has been exposed to HF are interesting in that they are featureless, with no evidence for the presence of surface C-H, C-O or C-F groups. However, after prolonged exposure to moist air, bands attributable to H<sub>2</sub>O (figure 4.22) are observed, with the implication that the HF-treated surface has hydrophilic character. Once again, this behaviour is not consistent with the presence of C-F bonds.

A model for the observed interaction between O-, H- and F- terminated diamond surfaces, based on the available evidence is now proposed.

It has been demonstrated conclusively that in the case of the O-terminated surface an interaction between surface oxygen and molecules of HF in the gas phase exists. Furthermore, it has been shown that this interaction does involve the formation of C-F, instead a labile species which can be hydrolysed occurs. Hydrogen bonding between the oxygen atoms of surface carbonyl, ether or alcohol groups is feasible to give the surface species shown in figure 5.7. The differences in the amount of HF adsorbed at ambient temperature and 573 K can be accounted for by variations in the physical form of HF vapour. At ambient temperature the hydrogen-bonded oligomer (HF)<sub>n</sub>, with n believed to equal 6 (130), exists, whilst at 573 K the oligomer is decomposed into 6 equivalents of HF monomer.

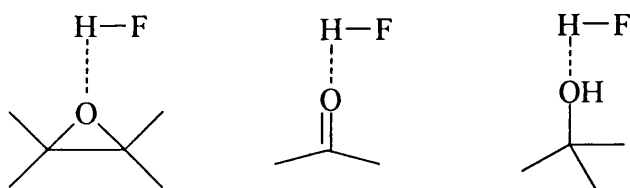


**Figure 5.7** Hydrogen bonded surface species formed in the reaction of O-terminated diamond and anhydrous HF vapour

A similar interaction is much less likely in the cases of the H-terminated and F-terminated surfaces. Hydrogen bonding to C-H can occur, but only when the hydrogen atom is sufficiently acidic (131), hydrogen bonding to C-F is even less likely (132). A lack of hydrogen bonding can be used to explain the small interaction between HF and F-terminated surfaces, however the significant uptake observed on H-terminated surfaces is less easy to rationalise.

One possibility is that HF or  $(\text{HF})_n$  oligomers are adsorbed at surface defects or grain boundaries, for which an affinity for  $\text{F}_2$  has been demonstrated in this work. Further hydrogen-bonding between such adsorbed HF and that from the vapour phase may account of the large uptake observed, a quasi-liquid layer may be formed. Indeed this could also be the case on the oxygen-terminated surfaces, but is less likely on the F-terminated surface where the adsorption of HF is kinetically hindered. A possible model for this surface and its interaction with the vapour phase is shown in figure 5.8. Exchange can occur via diffusion into the layer from the vapour phase, exchange and subsequent desorption back into the vapour phase.

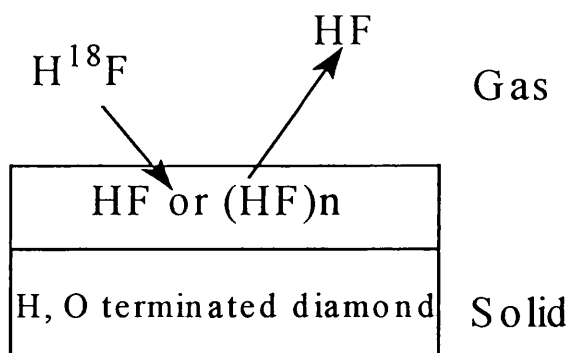
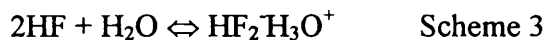


**Figure 5.8** Possible model for the interaction of HF or (HF)<sub>n</sub> with H- or O-terminated diamond surfaces

The adsorption of HF at grain boundaries may explain the slow hydrolysis of the material, which can occur according to scheme 3, since access for the H<sub>2</sub>O molecule to the adsorbed HF molecules may be restricted.



The smaller uptake observed on the F-terminated surfaces may be due to reaction with a remnant of surface oxygen or by limited transport of HF to grain boundaries.

These results can be used to account of the behaviour of bifluoride-based polishing reagents, which were ineffective in the polishing of polycrystalline diamond film, as outlined in section 3.2. Aqueous conditions were a requirement of all polishing experiments performed in this work. There is a significant interaction between diamond surfaces and HF which can be

considered a precursor to  $\text{HF}_2^-$ , however under aqueous polishing conditions the surface species would be washed away. It's not clear that  $\text{HF}_2^-$  would have had a positive effect, in a polishing sense, but its chances of doing so were slim in our polishing systems. Exposing diamond film to an aqueous solution of  $[\text{}^{18}\text{F}]\text{-CsHF}_2$  allowed this hypothesis to be readily tested. In table 5.2 the measured activity on a range of diamond film surfaces following exposure to  $[\text{}^{18}\text{F}]\text{-CsHF}_2$  at ambient temperature for 60 minutes.

**Table 5.2** Diamond film surface activity following exposure to  $[\text{}^{18}\text{F}]\text{-CsHF}_2$

Sample	Activity (count $\text{sec}^{-1}$ )
Virgin film	0.23
Hydrogen treated film	0.18
Oxygen treated film	0.25
Fluorine treated film	0.20

As shown in this table there was negligible interaction between diamond film  $[\text{}^{18}\text{F}]\text{-CsHF}_2$ , which agreed with our expectations for the system.

Studies in the reactions of  $\text{F}_2$  and  $\text{HF}$  with polycrystalline diamond surfaces have shown that chemisorption and strong physisorption of fluorine atoms or fluorine containing molecules are possible. In addition to broadening our understanding of diamond surface chemistry, which is emerging as a vital part of diamond film technologies, these studies provided direction in the attempt to develop a novel process for polishing CVD-grown diamond film. In this regard some success

has been obtained in this work, as described in sections 3.2.2 and 3.3.3, the main features of those results are discussed now.

### 5.3 Polishing success

In the absence of a useful polishing process, involving either chemical pretreatment of the surface or the use of nucleophilic species such as  $[\text{HF}_2]^-$  as polishing reagents, alternative methods had to be sought.

The process which, has been pursued in this work was initiated on the basis of a Japanese study (124) which, showed that diamond film could be polished in the presence of an electrical potential and superoxide ions. The  $\text{O}^{2-}$  ions travelled to the diamond film surface, which had been made the +ve electrode or the anode, where etching of carbon to produce CO and  $\text{CO}_2$  occurred.

In the present study initial tests using a similar method were unsuccessful. Following an empirical change in the experimental conditions, a positive effect was observed. The precise experimental conditions involved are described in detail in section 3.3.2, briefly these consisted of a brass polishing plate, an aqueous solution of  $[\text{OH}]^-$  and an electrical potential which made the diamond sample the -ve electrode.

The positive effect was manifested as the appearance of shiny crystallites in the early stages of the experiment. As the experiment progressed a semi-polished developed on the sample surface. This kind of effect had not been observed in

any of the previous polishing experiments up to this point. The result was repeated in further experiments, which established the important parameters. It was possible to produce diamond samples, semi polished to an average surface roughness of 17-40 nm  $R_a$  over a sample area of up to 4cm<sup>2</sup>, with a stock removal rate of 15-80  $\mu\text{m h}^{-1}$  under optimum conditions. This compares very favourably with traditional diamond lapping and polishing processes. In addition, throughout this phase of the work a number of key themes emerged, these were:

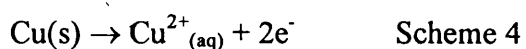
1. Deposition of copper on the diamond surface occurs, this can be correlated with a thinning of the polishing plate
2. Sparks, accompanied by the evolution of explosive gases, were apparent
3. A green colour develops on the polishing plate and during prolonged processing this becomes black
4. In the initial stages, the polishing-type effect is most marked at the high parts of the sample surface. These correspond to the regions closest to the polishing plate surface
5. The polishing-type effect is subject to some form of limitation and always falls off to zero, the 'effective' process time has been extended with development in the method but a limitation is still observed
6. Material can be removed in the absence of added abrasive but the stock removal rate is greatest in the presence of diamond grit

A possible model for the polishing effect observed using these methods and accounting for the general themes described above is proposed now.

In the early stages of the process, investigation of the diamond surface showed that erosion had occurred. Areas where material appeared to have been blasted off the surface were present (figure 3.8). This feature was a key indication as to the type of processes that were occurring. Spark erosion or arcing is the basis for electrochemical machining processes for machining industrial tool bits, for example. These processes take advantage of the enormous heat that is generated in the sparking region, which can exceed 50 000 K.

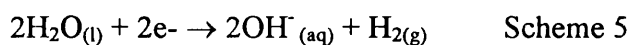
Sparks were observed in the current work and it is likely that the erosion observed on the diamond surface was a result of an interaction with a high energy spark produced between the sample and the plate. The only way that this can occur is by the deposition of metal on the diamond surface. Clean diamond is an insulator. The deposition of copper on the diamond surface did occur and is clearly an important feature. Its occurrence can be accounted for by the following sequence of events.

1. Anodic oxidation occurs on the plate surface which produces a concentration of copper ion in solution according to scheme 4

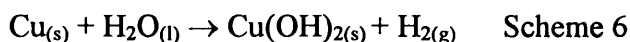


2. Deposition of copper metal at the cathode, which is the diamond sample, can then occur

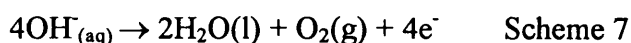
Anodic oxidation is also important in the explanation of the insoluble green compound, which was consistently present on the polishing plate. This was almost certainly copper hydroxide,  $\text{Cu}(\text{OH})_2$  and/or  $\text{CuCl}_2$ . When a solution of  $[\text{OH}]^-$  is used as an electrolyte the formation of copper hydroxide can be explained easily. Green compounds were also observed when using a solution of  $\text{NaCl}$  as an electrolyte,  $\text{CuCl}_2$  is soluble in aqueous solution and would not be expected to precipitate out of solution. The hydrolysis of water at the cathode, according to scheme 5, results in the formation of aqueous hydroxide and dihydrogen gas.



The redox reaction shown in scheme 6, which is a combination of schemes 4 and 5, accounts for the formation of  $\text{Cu}(\text{OH})_2$  and also suggests that dihydrogen gas can be formed. This is entirely consistent with the observations made in this work which suggested the formation of explosive gas. Even the classical sound of  $\text{H}_2$  igniting with a pop could be detected.



The evolution of oxygen gas via the oxidation of hydroxide ion at the anode, according to scheme 7 was also a possibility.



Therefore a cycle involving the electrolysis and reformation of H<sub>2</sub>O with the evolution of H<sub>2</sub> and O<sub>2</sub> gases can be envisaged. This produces a very reactive environment, especially when high energy sparking is also present. These sparks will not travel far; hence the sample must be in close locality with the plate.

It is proposed that, a combination of local high energy sparking and the formation of a reactive gas mixture, is responsible for the observed improvement in the rate at which material was removed from the diamond surface, as described for sample number 10 (section 3.3.3). Following exposure of the sample surface to the sparking environment for several hours and the addition of diamond grit, material was removed at rates as high as 80 μm h<sup>-1</sup>. However, this initially high rate dropped off as the experiment progressed and when the affected area of the sample had reached 4 cm<sup>2</sup> the stock removal rate was comparable with that observed for traditional lapping and polishing processes.

It is likely that the diamond surface was in some way weakened as a result of exposure to the sparking environment and reactive gas mixture for several hours. At present it is only possible to speculate as to the nature of this 'weakening' process, graphitisation of diamond in the local sparking region is one possibility. Since graphite is the thermodynamically favoured form of carbon, the transformation of diamond to graphite is relatively easy if the large activation energy barrier can be overcome. The transformation can be accomplished at temperatures exceeding 1173 K, given that the local temperature during sparking is thought to exceed 50 000 K, graphitisation is conceivable. Removal of

graphite formed on the surface by abrasive action, or even by the reaction with  $H_2$  or  $O_2$  would be a facile process.

Identification of such processes must await further development of the method, which is ongoing at Logitech, and is addressing the limitations of the method.

For the purposes of this thesis it is sufficient to conclude that a promising method for producing a CVD diamond film with a good quality surface finish albeit over a limited sample area, has been developed. This was possible by making a number of simple modifications to current technology and does not require the use of molten metal solutions or lasers.

From an economic standpoint, with some further development, the method could take its place in the emerging market surrounding CVD diamond film technology.

In terms of the aims of this project, the development of process ready for the commercial market was of limited importance. It was more relevant to broaden our knowledge of the types of chemistry possible on diamond surfaces and to apply the knowledge gained in our investigations of diamond polishing. In this the project has been a success.

## REFERENCES

1. H. T. Hall, Proceedings of the Third Conference on Carbon, Pergamon Press, London (1959)
2. C.R.C. Handbook of Chemistry and Physics, 47<sup>th</sup> Edn., F126
3. A. R. West, 'Basic Solid State Chemistry', 2<sup>nd</sup> Edn., John Wiley & Sons, (1999)
4. A. F. Wells, 'Structural Inorganic Chemistry', 5<sup>th</sup> Edn., Clarendon Press, (1984)
5. S. M. Owen, A. T. Brooker, 'A Guide to Modern Inorganic Chemistry', Longman, (1991)
6. F. P. Bundy, J. Chem. Phys., 46 (1967) 3437
7. K. Baba, Y. Aikawa, N. Shohata, J. Appl. Phys., 69(10) (1991) 7313
8. M. W. Geis, IEEE Elec. Dev. Lett., 8 (1987) 341
9. N. N. Efremau, J. Vac. Sci. Technol., B3 (1985) 416
10. J. Glinski, X. J. Gu, R. F. Code, Appl. Phys. Lett., 45 (1984) 26
11. M. Rothschild, C. Arnone, J. Vac. Sci. Technol., B4 (1986) 310
12. S. Praver, R. Kalish, M. Adel, Appl. Phys. Lett., 48 (1986) 1585
13. 'The Hutchinson Concise Encyclopedia', Guild Publishing, (1989)
14. J. McMurry, R. Fay, 'Chemistry', Appendix B, Prentice Hall, (1995)
15. F. P. Bundy, Science, 137 (1962) 1057
16. J. E. Field, 'The Properties of Diamond', Academic Press, (1979)
17. G. Davies, 'Diamond', Adam Hilger, (1984)

18. 'Crystals, Growth, Properties and Applications' Vol 2, Springer-Verlag, (1980)
19. P. S. DeCarli, F. C. Jamieson, *Science*, 133 (1961) 1821
20. 'Crystals, Growth, Properties and Applications' Vol 11, Springer-Verlag, (1988)
21. W. G. Eversole, U.S. Patents 3030187 and 3030188
22. B. V. Deryagin, D. B. Fedoseev, *Scientific American*, 233 (1975) 102
23. B. V. Deryagin, B. V. Spitsyn, A. E. Gordetcky, A. P. Zakharov, L. L. Builov, A. E. Aleksenko, *J. Cryst. Growth*, 31 (1975) 44
24. J. C. Angus, C. C. Hayman, *Science*, 241 (1988) 913
25. R. F. Davis, *J. Cryst. Growth*, 137 (1994) 231
26. M. N. R. Ashfold, P. W. May, C. A. Rego, N. M. Everitt, *Chem. Soc. Rev.*, 23 (1994) 21
27. Y. Hirose, Y. Terasawa, *Jpn. J. Appl. Phys.*, 6 (1986) L519
28. P. W. May, N. M. Everitt, C. G. Trevor, M. N. R. Ashfold, K. N. Rosser, *Appl. Surf. Sci.*, 68 (1993) 299
29. P. K. Bachmann, D. Leers, H. Lydtin, *Diamond and Related Materials*, 1 (1991) 1
30. J. C. Angus, H. A. Hill, W. S. Stanko, *J. Appl. Phys.*, 39 (1968) 2915
31. M. Tsuda, N. Nakajima, S. Oikawa, *J. Am. Chem. Soc.*, 108 (1986) 5780
32. M. Tsuda, N. Nakajima, S. Oikawa *Jpn. J. Appl. Chem. Phys.*, 26 (1987) 1527
33. W. D. Partlow, K. E. Kline, *Mater. Res. Soc. Symp.*, 68 (1986) 309

34. C. Chu, J. Margrave, *J. Appl. Phys.*, 70(3) (1991) 1695
35. S. Verpek, *J. Cryst. Growth*, 17 (1972) 1010
36. Y. Han, Y. Kim, J. Lee, *Thin Solid Films*, 310 (1997) 39
37. S. Kapoor, M. Kelly, S. Hagstrom, *J. Appl. Phys.*, 77(12) (1995) 6267
38. A. Sawabe, T. Inuzuka, *Thin Solid Films*, 137 (1986) 89
39. C. Wild, P. Koidl, W. Muller-Sebert, H. Walcher, R. Kohl, N. Hennes, R. Locher, R. Samlenski, R. Brenn, *Diamond and Related Materials*, 2 (1993) 158
40. S. D. Wolter, *Appl. Phys. Lett.*, 62 (1993) 1215
41. M. W. Geis, H. I. Smith, A. Argoitia, J. Angus, G. Ma, J. T. Glass, J. E. Butler, C. J. Robinson, R. Pryor, *Appl. Phys. Lett.*, 58 (1991) 2485
42. Twyman, F., 'Prism and Lens making', Adam Hilger, (1957)
43. D. S. Boyle, J. M. Winfield, *J. Mater. Chem.*, 6(2) (1991) 227
44. I. Nicol, PhD Thesis, University of Glasgow (1996)
45. L. McGhee, I. Nicol, R. D. Peacock, M. I. Robertson, P. R. Stevenson, J. M. Winfield, *J. Mater. Chem.*, 7(12) (1997) 2421
46. *Binary Alloy Phase Diagrams*, 2<sup>nd</sup> Edn., 834 (1990)
47. S. Jin, J. E. Graebner, G. W. Kamlott, T. H. Tiefel, S. G. Kosinski, L. H. Chen, R. A. Fastnacht, *Appl. Phys. Lett.*, 60(16) 1992
48. S. K. Choi, D. Y. Jung, S. Y. Kweon, S. K. Jung, *Thin Solid Films*, 279 (1996) 110
49. H. Tokura, M. Yoshikawa, C. F. Yang, *Thin Solid Films*, 212 (1992) 49
50. C. E. Johnson, *Surface Coatings and Technology*, 68/69 (1994) 374

51. S. Jin, J. E. Graebner, M. McCormack, T. H. Tiefel, A. Katz, W. C. Dautremont-Smith, *Nature*, 362 (1993) 822
52. J. Ullmann, A. Delan, G. Schmidt, *Diamond and Related Materials*, 2 (1993) 266
53. H. Shiomi, *Jpn. J. Appl. Phys.*, 36 (1997) 7745
54. A. Hirata, H. Tokura, M. Yoshikawa, *Thin Solid Films*, 212 (1992) 43
55. R. Ramesham, W. Welch, W. C. Neely, M. F. Rose, R. F. Askew, *Thin Solid Films*, 304 (1997) 245
56. I. Watanabe, K. Haruta, Y. Shimamura, *Jpn. J. Appl. Phys.*, 33 (1994) 2035
57. B. R. Stoner, G. J. Tessmer, D. L. Dreifus, *Appl. Phys. Lett.*, 62(15) (1993) 1803
58. V. G. Ralchenko, S. M. Pimenov, *Diamond Films and Technology*, 7(1) (1997) 15
59. M. Yoshikawa, *Diamond Films and Technology*, 1 (1991) 1
60. P. Tosin, W. Luthy, H. P. Weber, 3<sup>rd</sup> Int. Conf. On Applications of Diamond Films and Related Materials, 885 (1995) 271
61. V. P. Ageev, L. L. Bouilov, V. I. Konov, A. V. Kuzmichov, S. M. Pimenov, A. M. Prokhorov, V. G. Ralchenko, B. V. Spitsyn, N. I. Chapliev, *Soviet Physics- Doklady*, 33 (1988) 840
62. B. Bhushan, V. V. Subramaniam, B. K. Gupta, *Diamond Films and Technology*, 4 (1994) 71

63. D. E. Patterson, B. J. Bai, C. J. Chu, R. H. Hauge, J. L. Margrave, Second International Conference on the New Diamond Science and Technology, Washington D.C, paper 3.5, September (1990)
64. R. A. Rudder, J. B. Posthill, R. J. Markunas, *Electron Lett.*, 25 (1989) 1220
65. P. A. Molian, B. Januvin, *Wear*, 165 (1993) 133
66. S. Miyake, *Appl. Phys. Lett.*, 65(9) (1994) 1109
67. J. Wei, J. T. Yates, 'Critical Reviews in Surface Chemistry', 5(1-3) (1995) 1
68. J. F. Morar, F. J. Himpsel, G. Hollinger, J. L. Jordan, G. Hughes, F. R. McFeely, *Phys. Rev.*, B33 (1986) 1346
69. J. C. Vickerman, 'Surface Analysis- The Principal Techniques', John Wiley & Sons, (1997)
70. S. Brennan, J. Stohr, R. Jaeger, J. E. Rowe, *Phys. Rev. Lett.*, 45 (1980) 1414
71. B. B. Pate, *Surf. Sci.*, 165 (1986) 83
72. T. Yamada, T. J. Chuang, H. Seki, Y. Mitsuda, *Mol. Phys.*, 76(4) (1991) 887
73. S. T. Lee, G. Apai, *Phys. Rev.*, B48 (1993) 2684
74. A. V. Hamza, G. D. Kubiak, R. H. Stulen, *Surf. Sci.*, 206 (1988) L833
75. X. M. Zheng, P. V. Smith, *Surf. Sci.*, 261 (1992) 394
76. Y. L. Yang, M. P. D'Evelyn, *J. Vac. Sci. Technol.*, A10 (1992) 978
77. A. V. Hamza, G. D. Kubiak, R. H. Stulen, *Surf. Sci.*, 237 (1990) 35
78. R. Sappok, H. P. Boehm, *Carbon*, 6 (1968) 283
79. R. Sappok, H. P. Boehm, *Carbon*, 6 (1968) 573
80. T. Ando, M. Ishii, M. Kamo, Y. Sato, *J. Chem. Soc., Faraday Trans.*, 89(11) (1993) 1783

81. T. Ando, M. Ishii, M. Kamo, Y. Sato, K. Yamamoto, *J. Chem. Soc., Faraday Trans.*, 89(19) (1993) 3635
82. S. Matsumoto, H. Kanda, Y. Sato, N. Setaka, *Carbon*, 15 (1977) 299
83. R. E. Thomas, R. A. Rudder, R. J. Markunas, *J. Vac. Sci. Technol.*, A10 (1992) 2451
84. X. M. Zheng, P. V. Smith, *Surf. Sci.*, 262 (1992) 219
85. Q. Sun, M. Alum, *J. Mater. Sci.*, 27 (1992) 5857
86. A. Freedman, C. D. Stinespring, *Appl.Phys.Lett.*, 57(12) (1990) 1194
87. A. Freedman, C. D. Stinespring, *J.Appl.Phys.*, 75(6) (1994) 3112
88. J. F. Morar, F. J. Himpsel, G. Hollinger, J. L. Jordan, F. R. McFeely, *Phys.Rev.*, B33 (1986) 1340
89. T. Ando, J. Tanaka, M. Ishii, M. Kamo, Y. Sato, N. Ohashi, S. Shimosaki, *J.Chem.Soc., Faraday Trans.*, 89(16) (1993) 3105
90. T. Ando, K. Yamamoto, M. Kamo, Y. Sato, Y. Takamatsu, S. Kawasaki, F. Okino, H. Touhara, *J.Chem.Soc., Faraday Trans.*, 91(18) (1995) 3209
91. F. Okino, M. Matsuzawa, H. Touhara, T. Ando, Y. Sato, 15<sup>th</sup> International Symposium on Fluorine Chemistry, Vancouver, paper C6 1997
92. R. A. Rudder, G. C. Hudson, J. B. Posthill, R. E. Thomas, R. J. Markunas, *Appl.Phys.Lett.*, 59 (1991) 791
93. M. Kadano, T. Inoue, A. Miyanaga, S. Yamazaki, *Appl.Phys.Lett.*, 61 (1992) 772
94. C. Vivensang, G. Turban, E. Anger, A. Gicquel, *Diamond and Related Materials*, 3 (1994) 645

95. K. Nakamoto, 'Infrared and Raman spectra of inorganic and coordination compounds', 4<sup>th</sup> Edn., John Wiley & Sons, (1986)
96. V. Gutmann, 'Halogen Chemistry' Vol 1., Academic Press, (1967)
97. S. Brunauer, P. H. Emmett, E. Teller, J. Am. Chem. Soc., 60 (1938) 309
98. J. Kelvin, Phil. Mag., 42 (1871) 448
99. E. P. Barrett, L. S. Joyner, P. P. Halenda, J. Am. Chem. Soc., 73 (1951) 373
100. J. W. S. Hearle, J. T. Sparrow, P. M. Cross, 'The Use of the Scanning Electron Microscope', Pergamon Press, (1972)
101. R. F. Egerton, 'Electron Energy Loss Spectroscopy in the Electron Microscope', Plenum Press, (1986)
102. L. Ponsonnet, C. Donnet, K. Varlot, J. M. Martin, A. Grill, V. Patel, Thin Solid Films, 319 (1998) 97
103. D. A. Muller, Y. Tzou, R. Raj, J. Silcox, Nature, 366 (1993) 725
104. M. P. Seah, W. A. Dench, Surf. Interface. Anal., 1 (1997) 2
105. G. Nanse, A. Papirer, P. Fioux, F. Moguet, A. Tressaud, Carbon 35(2) (1997) 175 and references therein
106. G. Nanse, A. Papirer, P. Fioux, F. Moguet, A. Tressaud, Carbon 35(3) (1997) 371
107. G. Nanse, A. Papirer, P. Fioux, F. Moguet, A. Tressaud, Carbon 35(4) (1997) 515
108. N. Watanabe, T. Nakajima, H. Touhara, 'Graphite Fluorides', Elsevier, (1988)

109. A. Bismarck, R. Tahhan, J. Springer, A. Schultz, T. M. Klapotke, H. Zell, W. Michaeli, J. Fluorine. Chem., 84 (1997) 127
110. J. H. Scofield, J. Elect. Spectrosc. Rel. Phenom., 8 (1976) 129
111. D. Briggs, M. P. Seah, 'Practical Surface Analysis' 2<sup>nd</sup> Edn., John Wiley & Sons, (1994)
112. R. Flitsch, S. I. Raider, J. Vac. Sci. Technol., 12 (1975) 305
113. F. R. McFeely, J. F. Morar, N. D. Shinn, G. Landgren, F. J. Himpsel, Phys. Rev., B30 (1984) 764
114. F. R. McFeely, J. F. Morar, F. J. Himpsel, Surf. Sci., 165 (1986) 277
115. B. Roop, S. Joyce, J. C. Schultz, J. I. Steinfield, Surf. Sci., 173 (1986) 455
116. A. S. Barriere, B. Desbat, H. Guegan, L. Lozano, T. Seguelong, A. Tressaud, P. Alnot, Thin Solid Films, 170 (1989) 259
117. A. Freedman, C. D. Stinespring, J. Phys. Chem., 96 (1992) 2253
118. F. A. McMonagle, PhD Thesis, University of Glasgow (1995)
119. W. D. S. Scott, PhD Thesis, University of Glasgow (1997)
120. C. R. C. Handbook of Chemistry and Physics, 75<sup>th</sup> Edn., 11-37
121. C. Keller, 'Radiochemistry', John Wiley & Sons, (1988)
122. K. A. Brownlee, 'Statistical Theory and Methodology in Science and Engineering', John Wiley, (1960)
123. J. H. Dancy, Appl. Opt., 20 (1981) 1785
124. J. E. Yehoda, J. J. Cuomo, Appl. Phys. Lett., 66(14) (1995) 1751
125. C. J. Pouchert, 'The Aldrich Library of FT-IR Spectra- Vapour Phase' Edn.1

126. American Petroleum Institute Research Project Vol. 44, Catalogue of Infrared Spectral Data
127. J. H. Simons, 'Fluorine Chemistry' Vol. 2, Academic Press, (1954)
128. Scottish Examination Board, Science Data Booklet, (1982)
129. M. J. Vasile, F. A. Stevie, J. Appl. Phys., 53(5) (1982) 3799
130. J. H. Simons, 'Fluorine Chemistry' Vol. 1, Academic Press, (1950)
131. D. J. Teff, C. Huffman, K. G. Caulton, Inorg. Chem., 36 (1997) 4372
132. J. D. Dunitz, R. Taylor, Chem. Eur. J., 3(1) (1997) 89

